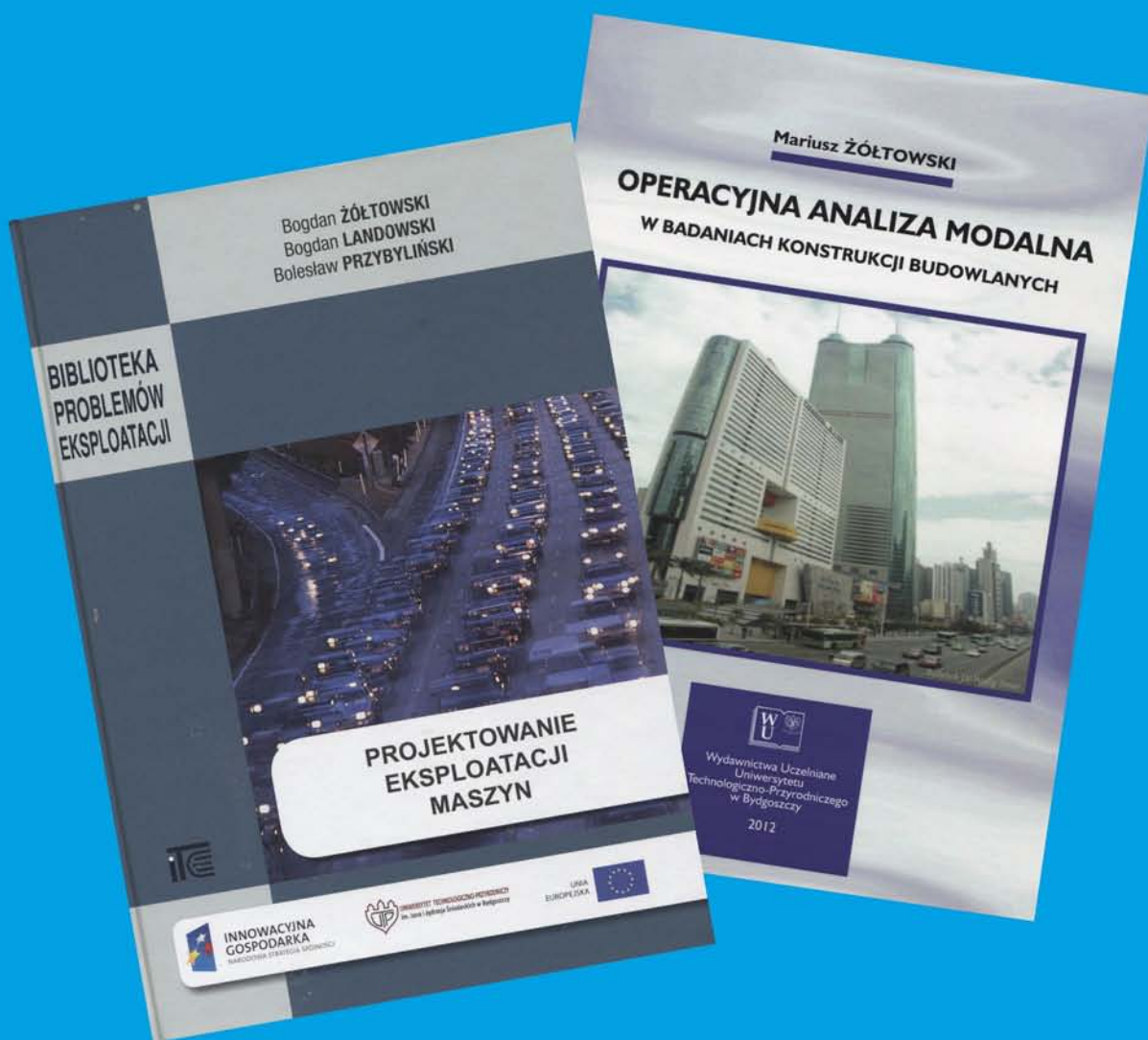


Diagnostyka

Applied Structural Health, Usage and Condition Monitoring

Rok założenia 1990

ISSN 1641-6414



Nr 3(63)/2012

RADA NAUKOWA / EDITORIAL BOARD

PRZEWODNICZĄCY / EDITOR IN CHIEF:

prof. dr hab. dr h.c. mult. **Czesław CEMPEL** – *Politechnika Poznańska*

REDAKTOR NACZELNY / SCIENTIFIC EDITOR:

prof. dr hab. inż. **Wiesław STASZEWSKI** – *AGH w Krakowie*

CZŁONKOWIE / MEMBERS:

prof. dr hab. inż. **Jan ADAMCZYK**
AGH w Krakowie

prof. **Francesco AYMERICH**
University of Cagliari – Italy

prof. **Jérôme ANTONI**
University of Technology of Compiègne – France

prof. dr. **Ioannis ANTONIADIS**
National Technical University Of Athens – Greece

dr inż. **Roman BARCZEWSKI**
Politechnika Poznańska

prof. dr hab. inż. **Walter BARTELMUS**
Politechnika Wroclawska

prof. dr hab. inż. **Wojciech BATKO**
AGH w Krakowie

prof. dr hab. inż. **Adam CHARCHALIS**
Akademia Morska w Gdyni

prof. **Li CHENG**
The Hong Kong Polytechnic University – China

prof. dr hab. inż. **Wojciech CHOLEWA**
Politechnika Śląska

prof. dr hab. inż. **Zbigniew DĄBROWSKI**
Politechnika Warszawska

Prof. **Charles FARRAR**
Los Alamos National Laboratory – USA

prof. **Wiktor FRID**
Royal Institute of Technology in Stockholm – Sweden

dr inż. **Tomasz GAŁKA**
Instytut Energetyki w Warszawie

prof. **Len GELMAN**
Cranfield University – England

prof. **Mohamed HADDAR**
National School of Engineers of Sfax – Tunisia

prof. dr hab. inż. **Jan KICIŃSKI**
IMP w Gdańsku

prof. dr hab. inż. **Daniel KUJAWSKI**
Western Michigan University – USA

prof. **Graeme MANSON**
University of Sheffield – UK

prof. dr hab. **Wojciech MOCZULSKI**
Politechnika Śląska

prof. dr hab. inż. **Stanisław RADKOWSKI**
Politechnika Warszawska

prof. **Bob RANDALL**
University of South Wales – Australia

prof. dr **Raj B. K. N. RAO**
President COMADEM International – England

prof. **Massimo RUZZENE**
Georgia Institute of Technology – USA

prof. **Vasily S. SHEVCHENKO**
BSSR Academy of Sciences Mińsk – Belarus

prof. **Menad SIDAHMED**
University of Technology Compiègne – France

Prof. **Tadeusz STEPINSKI**
Uppsala University - Sweden

prof. **Wiesław TRĄMPCZYŃSKI**
Politechnika Świętokrzyska

prof. dr hab. inż. **Tadeusz UHL**
AGH w Krakowie

prof. **Vitalijus VOLKOVAS**
Kaunas University of Technology – Lithuania

prof. **Keith WORDEN**
University of Sheffield – UK

prof. dr hab. inż. **Andrzej WILK**
Politechnika Śląska

dr **Gajraj Singh YADAVA**
Indian Institute of Technology – India

prof. dr hab. inż. **Bogdan ŻÓLTOWSKI**
UTP w Bydgoszczy

WYDAWCA:

Polskie Towarzystwo Diagnostyki Technicznej
ul. Narbutta 84
02-524 Warszawa

REDAKTOR NACZELNY:

prof. dr hab. inż. **Wiesław STASZEWSKI**

SEKRETARZ REDAKCJI:

dr inż. **Sławomir WIERZBICKI**

CZŁONKOWIE KOMITETU REDAKCYJNEGO:

dr inż. **Krzysztof LIGIER**

dr inż. **Paweł MIKOŁAJCZAK**

ADRES REDAKCJI:

Redakcja Diagnostyki
Katedra Budowy, Eksploatacji Pojazdów i Maszyn
UWM w Olsztynie
ul. Oczapowskiego 11, 10-736 Olsztyn, Poland
tel.: 89-523-48-11, fax: 89-523-34-63
www.diagnostyka.net.pl
e-mail: redakcja@diagnostyka.net.pl

KONTO PTD:

Bank PEKAO SA O/Warszawa
nr konta: 33 1240 5963 1111 0000 4796 8376

NAKLAD: 500 egzemplarzy

Spis treści / Contents

Wojciech CHOLEWA, Marcin AMAROWICZ – Silesian University of Technology	3
Management of requirements for developed diagnostic systems <i>Zarządzanie wymaganiami dla projektowanych systemów diagnostycznych</i>	
Michał CISZEWSKI, Tomasz BURATOWSKI, Mariusz GIERGIEL, Krzysztof KURC, Piotr MAŁKA – AGH University of Science and Technology	9
The pipes mobile inspection robots <i>Mobilne roboty do inspekcji rurociągów</i>	
Adam CHARCHALIS, Mirosław DERESZEWSKI – Gdynia Maritime University	17
Experimental method of evaluation of diagnostic value of the angular speed discrete signal from free end of the crankshaft <i>Eksperymentalna metoda oceny przydatności diagnostycznej dyskretnego sygnału prędkości kątowej z wolnego końca wału korbowego</i>	
Marcin ŁUKASIEWICZ, Tomasz KAŁACZYŃSKI, Bogdan ŻÓŁTOWSKI – University of Technology and Life Sciences in Bydgoszcz	23
Application of the operational modal analysis in transmission gearbox technical state identification <i>Zastosowanie eksploatacyjnej analizy modalnej w badaniach stanu technicznego skrzynki przekładniowej</i>	
Jan DERĘGOWSKI, Krzysztof MENDROK – AGH University of Science and Technology.....	27
Comparison of selected algorithms for force identification in time domain <i>Porównanie wybranych algorytmów identyfikacji wymuszeń działających w dziedzinie czasu</i>	
Piotr KOHUT, Krzysztof HOLAK, Ziemowit DWORAKOWSKI, Tadeusz UHL – AGH University of Science and Technology	35
Vision data employed for crack detection and localization	
Miłosz MEUS – Uniwersytet Warmińsko-Mazurski w Olsztynie	43
Issues of diagnosis for a hybrid electric vehicle with independent four-wheel power transmission system <i>Problematyka diagnostyki pojazdu hybrydowego z autonomicznym czterokołowym układem napędowym</i>	
Tomasz LUS – Polish Naval Academy.....	49
Marine diesel engines turbochargers diagnostic methods <i>Metody diagnozowania turbosprężarek silników okrętowych</i>	
Paweł SZCZEPAŃSKI	55
Dynamic programming of full conditional program for diagnosing <i>Programowanie dynamiczne pełnego warunkowego programu diagnozowania</i>	
Kazimierz WITKOWSKI – Polish Naval Academy	59
The possibility of using multivalued evaluation of residuals in the diagnostics of marine diesel engine <i>Możliwość wykorzystania w diagnostyce okrętowych silników wysokoprężnych wielowartościowej oceny residuów</i>	
Janusz ZACHWIEJA – University of Technology and Life Sciences in Bydgoszcz	63
Application of numerical analysis in dynamic state diagnosis of the machine with a shock character of operation <i>Analiza numeryczna w diagnozowaniu stanu dynamicznego maszyn o udarowym charakterze pracy</i>	
Wspomnienie o prof. Januszu GARDULSKIM.....	69

MANAGEMENT OF REQUIREMENTS FOR DEVELOPED DIAGNOSTIC SYSTEMS

Wojciech CHOLEWA, Marcin AMAROWICZ

Silesian University of Technology, Department of Fundamentals of Machinery Design
Konarskiego 18a, 44-100 Gliwice, tel. 32 2371660
wojciech.cholewa@polsl.pl, marcin.amarowicz@polsl.pl

Summary

This study presents results of a research on the development of methods for supporting design processes of diagnostic systems. One major challenge during the process is the precise description of goals or, in other words, determining the planned functionality of the developed diagnostic system given financial as well as technology constraints. The goals can be presented in the form of a set of requirements that the developed system should meet. Also, one critical task that occurs during the process of requirement acquisition is an appropriate management of the process. Nowadays, methods for requirement management are under intensive development in the field of software engineering in particular. However, their application in the process of diagnostic system design requires an additional treatment in order to account for the domain knowledge on technical diagnostics as well as diagnosed objects. As a solution the authors propose multimodal statement networks.

Keywords: requirement management, diagnostic systems, multimodal statement network.

ZARZĄDZANIE WYMAGANIAMI DLA PROJEKTOWANYCH SYSTEMÓW DIAGNOSTYCZNYCH

Streszczenie

W artykule przedstawiono wyniki badań związanych z poszukiwaniem metod wspomagania procesu projektowania systemów diagnostycznych. Zwrócono w nim uwagę na fakt, że trudnym etapem tego procesu jest dokładne opisanie potrzeb czyli określenie oczekiwanej funkcjonalności projektowanego systemu diagnostycznego przy uwzględnieniu istniejących ograniczeń np. kosztowych czy też technologicznych. Potrzeby te mogą być przedstawiane w postaci zbioru wymagań stawianych projektowanemu systemowi. Ważnym zadaniem występującym w procesie gromadzenia takich wymagań jest odpowiednie zarządzanie tym procesem. Metody zarządzania wymaganiami są intensywnie rozwijane w inżynierii oprogramowania. Ich zastosowanie w procesie projektowania systemów diagnostycznych wymaga jednak dodatkowych działań pozwalających na uwzględnienie wiedzy dziedzinowej dotyczącej diagnostyki technicznej oraz diagnozowanego obiektu. W celu rozwiązania tego zadania autorzy zaproponowali wykorzystanie wielomodalnych sieci stwierdzeń.

Słowa kluczowe: zarządzanie wymaganiami, systemy diagnostyczne, wielomodalne sieci stwierdzeń.

1. INTRODUCTION

Modern state-of-the-art diagnostic systems are sophisticated systems that register and analyze multiple signals (process variables, residual processes). The signal analysis is carried out by means of advanced tools and techniques, e.g. artificial intelligence methods, and the result of that process is then transferred to appropriate systems of an object as control inputs as well as to end-users in the form of sound signals, light signals and the like.

Designing such systems is often a challenging task. The process incorporates the following: need (goal) recognition (definition of a function that a specific diagnostic system should realize), generation of a set of solutions capable of meeting the specified goals, definition of existing or potential constraints, definition of selection criteria for an

optimum solution, designation of an ultimate solution meeting established criteria. The set of likely solutions can be presented in the form of a morphological table (see Fig. 1) in which specific rows correspond to particular goals (diagnostic system functionalities), and row elements describe possible solutions capable of meeting particular goals. The process of determining the contents of specific rows as well as their elements in the table is not an easy task. Simply, it is required to account for the domain knowledge on an object, diagnostic knowledge, as well as existing constraints, for example, engineering constraints, financial restrictions, etc. Therefore, in order to support the table development it is recommended to use a set of requirements describing the diagnostic system under development.

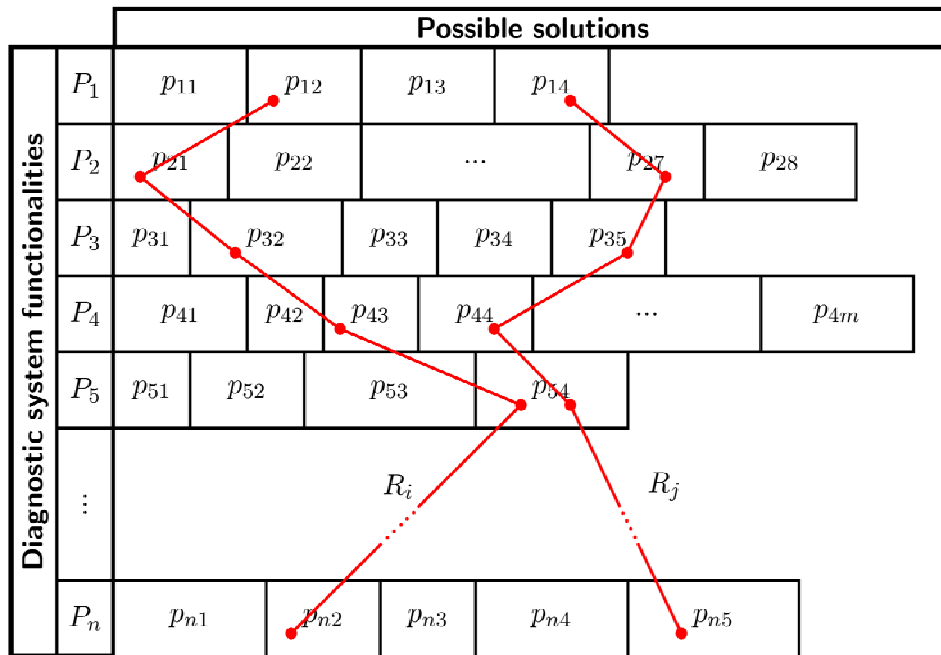


Fig. 1. Morphological table as a set of possible solutions

The size of a designed table depends on characteristics of an object that the system is developed for (number of rows) as well as diagnostic methods and techniques (row elements).

As shown in Fig. 1, specific solutions (R_i, R_j) are developed in the form of a combination of selected solutions for meeting particular goals. In a generic case, it is then possible to develop a set of

$$\prod_i \text{card}([P_i]) \quad (1)$$

diagnostic system solutions, where $\text{card}(P_i)$ is the number of solutions capable of meeting the goal i (i.e. the number of elements in the row i). Initially, the set of solutions may comprise inefficient solutions as well unrealizable solutions. They will be eliminated in subsequent steps of the development process. The application of a morphological table guarantees the considering of all solutions. The process of selecting an ultimate solution out of the solution set is an optimization task and that of a multicriterial optimization in particular.

2. REQUIREMENT ENGINEERING

Requirement based procedures are often used in the area of software engineering. For example, various literature sources [10,13,15,16] have proposed definitions of the term „requirement” in the software engineering aspect. In general, it is assumed that a requirement is a statement describing functions that a specific solution should meet. One

example of a requirement for a condition monitoring (diagnostic) system project can be the following statement: „relative displacement amplitude measurement in the bearing node no. 4 in the range from XX to YY at the accuracy of ZZ”.

One field of science to consider and examine all requirement related aspects is requirement engineering, and its fundamental tasks are revealed in Fig. 2.

2.1. Defining requirements

Defining requirements comprises four fundamental processes, i.e., acquisition, analysis, specification, and verification.

The purpose of the acquisition process is to discover or reveal, emphasize, and to present system requirements. In existing literature sources the process is also called a requirement collection or acquisition, identification, formulation, etc. Each term reflects process-related specific activities depending on object characteristics.

The purpose of the analysis process is to evaluate the set of collected requirements. The requirements are clustered into subject-related groups, pending the removal of possible contradictions, and prioritized.

Also, requirement specification is a process that allows for a translation of a requirement into the form that can be understood by system designers. Possible formats include natural languages, symbolic languages and graphics.

Finally, verification is a process that allows requirements to be tested for correctness, integrity,

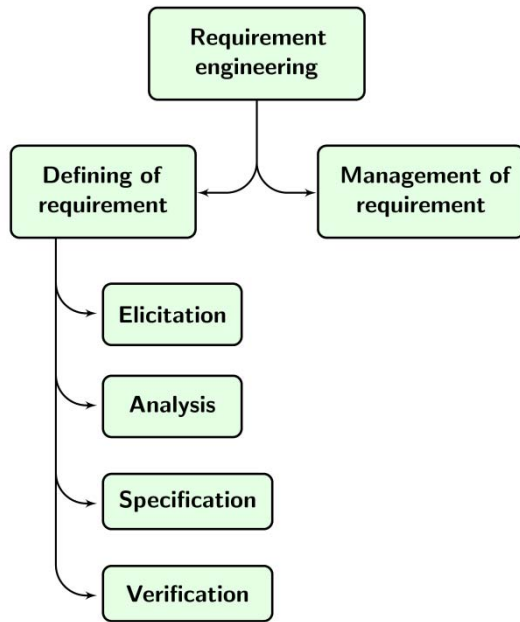


Fig. 2. Requirement engineering tasks

completeness, and importance (ranking). Also, note that the above processes are mutually dependent and often performed simultaneously, and their outputs influence one another.

In a majority of cases there exist three fundamental categories of requirements, i.e., structural requirements, functional requirements and non-functional requirements. The structural requirements describe the structure of designed technical means. The functional requirements report services that a specific solution should deliver.

Moreover, the non-functional requirements allow one to determine the level of compliance of structural and functional requirements with respect to the project goals. They are the result of the technology used, timing constraints, standards and regulations, quality policies, etc. This category of requirements can be then split into appropriate sub-categories, e.g. usability requirements, organizational requirements, performance requirements, operating requirements, safety requirements, legal requirements, design and the like. This sectioning depends on specific features of a project for which requirements should be defined.

In general requirements can be acquired from various sources, e.g.:

- principal customer,
- end-users,
- existing solutions,
- domain experts,
- standards, recommendations,
- knowledge and experience of the project developers,
- prototypes, etc.

Availability of particular sources depends on project specifics. While defining requirements it is recommended to apply multiple sources.

Unfortunately the resulting requirements can be inconsistent or contradictory. The number of requirements to be defined within a projects varies from as low as few hundreds for small projects to well over 300 thousand requirements while designing passenger aircrafts for example [10].

2.2. Requirement specification

As a result of requirement evaluation using appropriate methods and techniques, a subset of fundamental requirements is extracted from the initial set of requirements. The subset ensures that both planned functionality and constraints are met. The requirement set is then recorded in a document – requirement specification. According to the standard IEEE 830 [6] that defines requirement specification for IT (Information Technology) projects, the document should be as follows:

- correct – each requirement is a requirement to be met by a designed system,
- unambiguous – each requirement must be interpreted in only one possible manner,
- complete – the document contains a set of all possible and essential requirements,
- consistent – the set of requirements cannot contain contradictory elements,
- ranked for importance and/or stability – each requirement should have a granted priority (importance level) for a better management of the requirement set,
- verifiable – there must exist a (funded) process to determine whether specific requirements can be accomplished in a timely and cost-effective manner,
- modifiable – the specification document structures should allow for changes in the requirement set,
- traceable – the origin of each requirement as well as their mutual relationships should be identifiable.

The process of defining requirements is a challenging and time-consuming task. In general, numerous requirements are collected – they come from different sources and are defined by various individuals. Therefore, the answer to two basic questions may become difficult. Is the developed set of requirements complete? Is it free of contradictions? It becomes clear then that the application of appropriate methods for the process management is necessary and a key to a successful project.

3. MANAGEMENT OF THE PROCESS FOR REQUIREMENT ACQUISITION

The process of requirement management can be supported with dedicated IT systems [7, 14]. Their support capability depends on project specific characteristics. Also, they allow for an assignment of various attributes (author, priority, status, version,

etc.) to defined requirements. They have filtering as well as search capability. Moreover, they incorporate mechanisms for tracking changes in a requirement set and collaborating with external applications, e.g. database systems, MS Office documents and the like. In addition to that, they allow for team collaboration during the requirement development process, establishing various levels of access to the requirement set, developing mechanisms of automated messaging on any potential modifications in the requirement set and the like.

Analyzing the description of numerous projects and IT projects in particular implies that in many circumstances the requirement development process relies on negotiations between a client and a project's engineer. One common methodology is the so-called EasyWinWin whose origin can be tracked to the negotiation model Win-Win, in which the primary objective is a mutual satisfaction of a client and an engineer of formulated requirements [1]. Throughout the course of a negotiation participants formulate requirements, prioritize and evaluate them in order to extract principal requirements describing the designed system.

However, such approach cannot be used directly when designing a diagnostic system. It is indeed rather difficult to define a customer for negotiations in such projects. By a fashion, the so-called customer can be the object end-user. In many scenarios such approach is not optimal – mainly because end-users do not usually have the right domain knowledge and the diagnostic knowledge that allows them to define appropriate requirements.

The essence of the proposed approach for requirement acquisition is the hypothesis that this problem can be solved by assuming that any analyzed technical object is a virtual client in a negotiation process. The object (virtual customer) can be represented by an expert system that is capable of establishing object-oriented requirements to be met by a diagnostic system.

4. STATEMENTS, STATEMENT NETWORKS

An expert system for use as a virtual client in a negotiation process should be capable of operating based on the knowledge it has access to. A knowledge database of the expert system may occur in the form of a multimodal statement network [2, 3, 4, 5].

It is assumed that a statement concerns a sentence (or an expression) on an observed fact or an opinion. The expression (statement contents) can be assigned the value v , in order to inform of its logical value or a belief that the statement is true. In the case of definite statements the value is one element out of the set $\{yes, no\}$. The statement s is an ordered pair

$$s = \langle c, v \rangle, \quad (2)$$

where c is a statement contents, and v refers to the statement value. Relationships occurring among statements can be described by developing a statement network (see Fig. 3) in which statements appear in the form of network nodes. The network is a directed graph

$$G = \langle N, E \rangle, \quad (3)$$

in which N is a finite and non-empty set of vertices of this graph, and E is a finite and non-empty set of directed edges linking selected vertices.

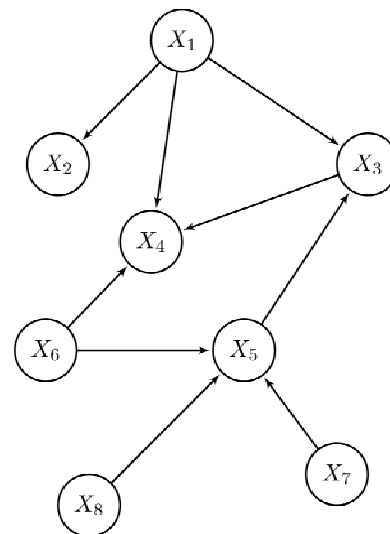


Fig. 3. Multimodal statement network

All statements used for developing such networks should be collected in a set of statements – thesaurus.

Statements that are gathered in a thesaurus include both descriptive statements (on the object's structure, possible failure modes of object's selected components, failure mode probabilities, repair and servicing costs, etc.) and statements (requirements) reporting the expected or demanded functionality of a designed diagnostic system. Both knowledge and requirements that are represented by statements are developed and collected based on available literature incl. object's maintenance manual and documentation, description of similar objects, data from domain experts, designers and end-users, as well as similar existing solutions.

Statements that are selected out of a thesaurus can appear as nodes in various developed statement networks. Particular statement networks can be formulated based on various aspects of an available knowledge on the object's structure, functionality, object characteristics, etc., thus forming a set of statement networks over a common set of nodes. Such a set of statement networks is called a multimodal statement network.

Well designed and developed statement networks reflect relationships between the knowledge on

objects and requirements describing the diagnostic system of interest. Statement networks utilize various methods for representing node-to-node relationships. One widely used statement network type is a Bayesian network (belief network) [8, 9, 11], in which the relationships are expressed with conditional probability tables assigned to specific nodes. Also, it is possible to utilize approximate networks in which node-to-node relationships are described with necessary and sufficient conditions [3, 4].

Statement networks allow then to realize reasoning processes in which unknown values of certain nodes (conclusions) are determined based on known values of other nodes (reasons and premises). One advantage of a statement network is its ability for carrying out a reasoning process based on incomplete, uncertain, and partially inconsistent knowledge.

5. REQUIREMENT MANAGEMENT USING MULTIMODAL STATEMENT NETWORKS

The morphological table that is described in Section 1 allows for representing a set of likely solutions of a diagnostic system. The process of defining such tables incorporates two stages. In the first stage table row captions (titles) are assumed. In other words, this stage determines functionalities referring to subsequent rows of the table. The second stage goal (that should be established independently for each row) is to identify row elements. It becomes apparent that a clear distinction of both stages emphasizes that in order to accomplish the first stage a detailed knowledge on both the structure and substance of object operation principles as well as a generic diagnostic knowledge are needed. At the same time it is clear that the second stage goals can be accomplished with a detailed in-depth diagnostic knowledge as well as a generic high-level knowledge on a particular object.

One component of a morphological table that is particularly important is a set of table rows for determining various approaches to ensure required functionalities of a designed diagnostic system are met. The functionalities should reflect the knowledge on a given object, and the object structure, specific sub-systems and components in particular. The domain knowledge should be incorporated there as well.

By acquiring a certain amount of knowledge on a given object and recording it in the form of a set of statements, it is then possible to develop a multimodal statement network to define captions (titles) of morphological table rows. In this network statements describing an object and object operation conditions are input nodes, whereas requirements (for determining the proposed functionality of a diagnostic system – morphological table rows) are output nodes.

As a result of a reasoning process specific requirements are given so-called belief levels (assuming the examined multimodal statement network is a Bayesian network) to describe their capability of meeting a goal function by a designed diagnostic system. It is also possible to extract a subset of requirements out of a requirement set for which a belief level is greater than a specified threshold level. The subset will contain the assumed description of a diagnostic system functionality.

Next, it is required to determine elements of specific rows of a morphological table. In this case a diagnostics-related knowledge is accounted for. Statement networks are developed at this state in order to reflect relationships among functionalities (morphological table rows) and diagnostic methods. The outcome of the reasoning process is a set of diagnostic methods and techniques to ensure specific functionality is met for an assumed functionality and existing constraints.

Note that the result of a process of collecting requirements to describe a diagnostic system is a numerous set of requirements. It incorporates all requirements that can be formulated during the development process. However, some of the formulated requirements can be contradictory or incapable of meeting assumed goals. As such, with multimodal statement networks the requirement set is limited to a rational subset of requirements to describe the required functionality of a diagnostic system (morphological table rows) and related diagnostic techniques and methods (table row elements).

Multimodal statement networks can be formulated e.g. with the dedicated software platform REx [5, 12]. The package was developed based on the well-known language R. An installation package is available as well [12]. It allows for formulating statement sets, grouping of selected statements into thematic subsets with assigned keywords, and using them for the development of multimodal statement networks. Finally, it allows one to carry out reasoning processes assuming that dependencies between particular statement networks are expressed with conditional probability tables (Bayesian networks) and/or with sufficient and necessary conditions (approximate networks).

6. SUMMARY

In this paper the authors described issues concerning requirement management in the development of diagnostic systems. Specifically, the needs for representing a set of possible solutions of a diagnostic system project with a morphological table were analyzed and emphasized. The process of determining particular rows of such a table (representing assumed functionalities of a diagnostic system) and row elements (describing possible variants of diagnostic methods and techniques) may be supported by an expert system delivering

appropriate requirements. Simply, the essence of this requirement acquisition approach is the assumption that the problem can be solved by claiming the examined diagnosed system is a virtual client in a requirement negotiation process. Here, the client is represented with an expert system whose knowledge base is written down as multimodal statement network.

Finally, determining morphological table elements with multimodal statement networks is reduced to a reasoning process in which requirements describing a developed diagnostic system are resolved based on known facts on a technical object and a domain in which the diagnostic system is applied.

ACKNOWLEDGEMENTS

Described herein are selected results of study, supported partly from the budget of Research Task No. 4 implemented under the strategic program of The National Centre for Research and Development in Poland entitled "Advanced technologies of generating energy".

BIBLIOGRAPHY

- [1] Boehm B., Grunbacher P. and Briggs R. O.: EasyWinWin: *A Groupware-Supported Methodology for Requirement Negotiation*, 8th European Software Engineering Conference (ESEC), 9th ACM SIGSOFT Symposium on The Foundations of Software.
- [2] Cholewa W. (Ed): *Szkieletowy system doradczy MMNET*, Politechnika Śląska, Katedra Podstaw Konstrukcji Maszyn, Gliwice, 2010.
- [3] Cholewa W.: *Mechanical analogy of statement networks*, International Journal of Applied Mathematics and Computer Science, 18(4), pp. 477-486, 2008.
- [4] Cholewa W.: *Multimodal statement networks for diagnostic applications*, in: Sas P., Bergen B. (Eds): Proceedings of the International Conference on Noise and Vibration Engineering ISMA 2010, Leuven, Belgium, Katholieke Universiteit Leuven, September 20-22, pp.817-830.
- [5] Cholewa W., Rogala T., Chrzanowski P. and Amarowicz M.: *Statement networks development environment Rex*, in: Jędrzejowicz et al. (Eds): Proceedings of the Third International Conference on Computational Collective Intelligence: Technologies and Applications – Volume part II (ICCCI'11), LNCS 6923, Heidelberg, Springer-Verlag, pp. 30-39.
- [6] IEEE Recommended Practice for Software Requirements Specifications, IEEE Std 830, IEEE Press, 1998.

- [7] *INCOSE Requirements Management Tools Survey*, available online <http://www.incose.org/ProductsPubs/products/rmsurvey.aspx>, February 2012.
- [8] Jensen F. V.: *Introduction to Bayesian Networks*, Springer, 1997.
- [9] Koski T. and Noble J. M.: *Bayesian Networks. An Introduction*, John Wiley and Sons, 2011.
- [10] Lefingwell D. and Widrig D.: *Zarządzanie wymaganiami*, Warszawa, WNT, 2003.
- [11] Neapolitan R. E.: *Learning Bayesian Networks*, Prentice Hall, 2003.
- [12] Platform REx (Home Page): <http://kpkm.polsl.pl/index.php?n=ProjREx.HomePage>.
- [13] Sommerville I. and Sawyer P.: *Requirement Engineering: A Good Practice Guide*, Chichester, John Wiley & Sons, 1997.
- [14] *Software Requirements Management Tools – Business Analysis, UML Case, Agile User Stories*, available online <http://requirementsmanagementtools.com>, February 2012.
- [15] Young R.R.: *The requirement engineering handbook*, Boston, Artech House, 2003.
- [16] Westfall L.: *Software Requirements Engineering: What, Why, Who, When and How*, The Westfall Team, 2005-2006.



Wojciech CHOLEWA, head of the Department of Fundamentals of Machinery Design, Silesian University of Technology, has developed artificial intelligence methods and techniques due to fuzzy and approximate knowledge representation for technical diagnostics applications as

well as supporting processes of machine design and engineering. He has advanced the theory of expert systems based on statement networks and object inverse models.



Marcin AMAROWICZ, PhD student, Department of Fundamentals of Machinery Design, Silesian University of Technology, has focused on artificial intelligence methods and techniques and their applications in technical diagnostics. Moreover, his research

interests include requirements acquisition and estimation due to risk analysis for technical diagnostic system design.

THE PIPES MOBILE INSPECTION ROBOTS

Michał CISZEWSKI*, Tomasz BURATOWSKI, Mariusz GIERGIEL, Krzysztof KURC, Piotr MAŁKA

*AGH University of Science and Technology, Faculty of Mechanical Engineering and Robotics
Mickiewicza 30 Avenue, 30-059 Kraków, Poland, e-mail: mcisz@agh.edu.pl

Summary

In this paper, the design of a tracked in-pipe inspection mobile robot with a flexible drive positioning system is presented. The robot would be able to operate in circular and rectangular pipes and ducts, oriented horizontally and vertically with cross section greater than 200 mm. The paper presents a complete design process of a virtual prototype, with usage of CAD/CAE software. Mathematical descriptions of the robot kinematics and dynamics that aim on development of a control system are presented. Laboratory tests of the utilized tracks are included. Performed tests proved conformity of the design with stated requirements, therefore a prototype will be manufactured basing on the project.

Keywords: mobile robot, pipe and duct inspection, kinematic model, dynamic model, vision system

MOBILNE ROBOTY DO INSPKCIJI RUROCIĄGÓW

Streszczenie

W artykule opisano projekt gąsienicowego robota inspekcyjnego do rurociągów z elastycznym systemem pozycjonowania gąsienic. Opisany robot przeznaczony jest do pracy w rurociągach o przekroju prostokątnym i kołowym i średnicy ponad 200 mm. W artykule przedstawiono kompletny proces projektowy, mający na celu utworzenie modelu trójwymiarowego w środowisku CAD/CAE. Opisane zostały również modele matematyczne robota w zakresie kinematyki i dynamiki ruchu, niezbędne do utworzenia algorytmów sterowania. Dołączono również opis badań laboratoryjnych gąsienic. Przeprowadzone testy potwierdzają poprawność projektu, który będzie służył do stworzenia prototypu robota.

Słowa kluczowe: robot mobilny, inspekcja rurociągów, kinematyka, dynamika, system wizyjny.

INTRODUCTION

Pipeline inspection is a popular application field of mobile robots. Since the access to a particular segment of a pipeline is usually limited, various in-pipe inspection mobile robots are utilized. This paper presents a design of a tracked mobile robot, that can adapt to various working environments. The robot platform is based on two track modules with integrated motors, mounted on a positioning structure, consisting of three drives per track. The robot can adapt to operate in pipes and ducts with round and rectangular cross-section, oriented horizontally and vertically or work on flat surfaces. Operation in liquid environment was also taken into consideration.

There already exist many other designs of mobile pipe inspection robots, but the majority of them possess low level of adaptivity to the operating environment, mainly due to geometric limitations. Choi and Roh [4] focus on design of wheeled inspection robots suitable for $\varnothing 200$ and $\varnothing 85-109$ mm round pipes, that are based on modular structure that

feature segments with wheeled legs on pantograph mechanisms for diameter. Another concept is presented by Horodnica et al. [8]. They designed four robot architectures, utilizing rotor, equipped with three pairs of tilted wheels that move on helical trajectories, propelling the robot forwards in axial direction. The robots have different sizes for 170, 70 and 40 mm round pipes and allow only small changes of diameter. A snake-like 13-segment robot designed by Kuwada et al. [12] may operate in 40-170 mm pipes. The structure equipped with camera propels by clinging to pipe walls and is able to pass bends, T-shapes and changes of diameter. However, maintaining steady camera position for proper inspection may be problematic. Tadakuma et al. [14] proposed a platform with cylindrical track drive: Omni-Track that increases the contact area with pipes of different diameters and allows forward and backward motion along with side motion, realized by roll mechanism. A three-track vertical configuration for constant pipe diameter was described by the authors.

Robots for operation in ventilation ducts are mainly designed with focus on cleaning tasks. Wang and Zhang [16] propose a tracked platform with guiding wheel that can host interchangeable brushes, intended for cleaning of horizontal ducts.

Market research for inspection robots revealed several solutions. Inuktun produces a wide range of tracked inspection robots. Versatrax models are available in three different sizes for minimal pipe diameters: 100, 150 and 300 mm [10]. Their main components are individually operated tracks of different sizes. Manually adjustable chassis allows adapting of the robot to sewer and storm drains, air ducts, tanks, oil and gas pipelines, pulp and paper industry. Versatrax Vertical is a three-track version for vertical, dry pipe inspection [9]. iPEK produces wheeled inspection vehicles, ROVVER for pipes with diameter 100-300, 150-760 and 230-1520 mm [11]. These robots have modular design, with replaceable wheels, suitable for horizontal pipes and operation up to 10 m underwater. Solo robot by RedZone is a tracked, wireless, autonomous robot that can be used in horizontal pipes ranging from 200-300 mm diameter [13]. CUES offer tracked inspection robots for pipes with diameter from 150 to 760 mm. Their main feature is narrow track made of large segments. [5].

As we may observe, numerous solutions for inspection robots are available. Wheels provide the least rolling resistance and are energy efficient, however small contact surface may not be sufficient for some uneven surfaces. Crawling motion has speed limitations and especially upper limit of pipe or duct dimension is a major drawback. As presented by the market research, numerous solutions utilizing track drive have been developed. Tracks provide proper obstacle passing capabilities and considerably large contact is advantageous in terms of friction. The presented tracked robots, do not possess online track positioning and are designed for specific purposes. This paper presents a design of a versatile tracked mobile robot with an adaptive track positioning system intended for video inspection.

1. MECHANICAL STRUCTURE

Similarly to most of the analyzed robot structures, it was decided to utilize two tracks. That configuration will ensure proper robot stability and maneuverability, assuming that the robot will consist of one segment. For this project, Inuktun Microtrac track modules with dimensions 60x50x170 mm will be utilized. They are designed specifically for pipe inspection, with focus on small inspection platforms.

For creating the virtual prototype of the inspection robot, Autodesk Inventor Professional 2012 was used.

Track positioning system consists of two independently rotating rings, with a centre of rotation in the axis of the robot body. To each of these rings, an arm is attached on a rotary joint. These arms are similarly mounted to both sides of each track. This configuration allows various orientations of track with respect to the robot body. Each track unit is adjusted by three drives. Two drives allow rotation of rings in the robot body axis and the third drive positions one arm with respect to the track. Drives selected for the rotating rings are digital servomotors Hitec HS-7950TH that possess high holding torque, compact size and integrated position controller. The rotating rings are connected with robot outer and inner arms. The general view of the robot is presented in the Fig. 1. Drive controllers and power electronics are located inside the robot body as depicted in Fig. 2.

In total, the robot has 8 drives: 2 tracks and 6 track positioning servomotors and consists of over 230 components, among which over 60 have to be manufactured. The total weight of the robot is 6.9 kg, where the weight of one stainless steel track is 2 kg. The total weight does not include camera, lighting and cables. Components such as robot body, arms, ring spacers, cups and track mounts. The robot is capable of operation in liquid environment such as water, sewage or oil. In order to meet this requirement, connections are sealed and cables are routed with usage of waterproof connectors.

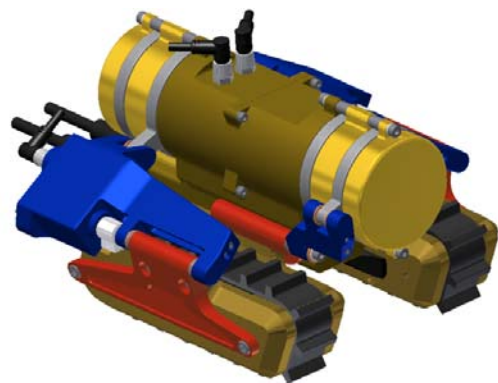


Fig. 1. Robot model - general view

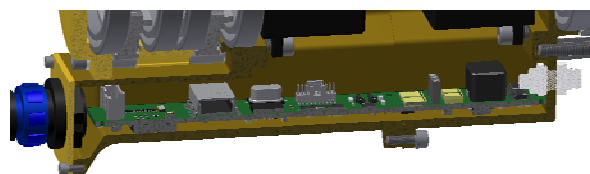


Fig. 2. Controller compartment

2. KINEMATIC MODEL OF THE ROBOT

Description of a crawler track motion in real conditions with uneven ground and changeable parameters is very complex. The detailed mathematical description of the movement of individual crawler track points is so compound that it is necessary to apply simplified models. It is possible to model elastomer tracks with treads (Fig. 3 a) as a non-stretch tape wound about determined shape by the drive wheel, tensioning wheel and undeformable ground (Fig. 3 b) [1, 6, 15, 17]. For the kinematic model, a horizontal orientation of two tracks was utilized, basing on formulation used for tank robot presented in [7].

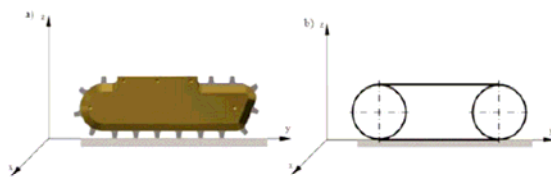


Fig. 3. a) CAD Model, b) Simplified Model

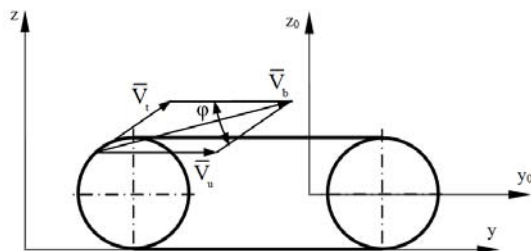


Fig. 4. Simplified model of the crawler track

For the description of motion points on the crawler track circumference (Fig. 4) two systems of coordinates were selected. Axes y and z form a reference frame associated with the ground, whereas axes y_0, z_0 are attached to a movable coordinate system associated with the vehicle [1, 2, 3, 6]. The motion of any crawler track point is a composition of two motions: relative motion of the moving frame y_0, z_0 and transportation motion relative to the reference frame y, z . The absolute velocity of any point on the crawler track circumference is equal to the resultant of transportation velocity and relative velocity.

$$V_{by} = V_u + V_t \cos \varphi \quad (1)$$

$$V_{bz} = V_t \sin \varphi \quad (2)$$

$$V_b = \sqrt{V_{by}^2 + V_{bz}^2} = \sqrt{V_u^2 + V_t^2 + 2V_u V_t \cos \varphi} \quad (3)$$

where: V_u – transportation velocity

V_t – relative velocity of any point on the crawler track circumference

V_b – absolute velocity of the point on crawler track circumference

φ – angle between vectors V_t and V_u

In case when $\varphi = \pi$, that is when points on the crawler track circumference contact the ground, the absolute velocity is a sum of transportation and relative velocities.

When the track load-bearing segment is in contact with the ground, then the effect of slip occurs [1, 2, 3]. The slip phenomenon is affected by properties of the ground, driving force, type and placement of track treads. The driving force appearing in the robot track driving modules, exerts shear stresses on the ground. It is possible to determine the relationship between the driving force and factors that influence the slip by:

$$P_n = 10^3 b \int_0^L \tau_x dx \quad (4)$$

where: P_n – driving force

b – width of the crawler track

L – length of the load-bearing segment of the crawler track

τ_x – shear stresses in the soft ground

Assuming that the course of parallel deformations to the ground is linear, it is possible to express these deformations by:

$$\Delta l_x = x s_b \quad (5)$$

where: s_b – slip

x – distance of the point, for which the slip is calculated from the point of crawler track contact with the ground; the greatest slip appears for $x = L$.

Therefore, it is possible to express the slip by:

$$s_b = \frac{\Delta l_x}{x} = \frac{\Delta l_{\max}}{L} \quad (6)$$

The velocity of point C, placed in the axis of symmetry of the crawler, assumed to be the center of gravity, [1, 2, 3, 6, 17] may be expressed as:

$$V_c = \frac{rd_1(1-s_1) + rd_2(1-s_2)}{2} \quad (7)$$

When slip is neglected:

$$V_C = \frac{rd_1 + rd_2}{2}, \quad (8)$$

Velocity components of the point C:

$$\dot{x}_C = V_C \cos \beta, \quad (9)$$

$$\dot{y}_C = V_C \sin \beta. \quad (10)$$

After taking into account the relation (7) the equation of simple kinematic task was obtained:

$$\dot{x}_C = \frac{rd_1(1-s_1) + rd_2(1-s_2)}{2} \cos \beta, \quad (11)$$

$$\dot{x}_C = \frac{rd_1(1-s_1) + rd_2(1-s_2)}{2} \cos \beta, \quad (12)$$

$$\beta = \frac{rd_2(1-s_1) - rd_1(1-s_2)}{R}, \quad (13)$$

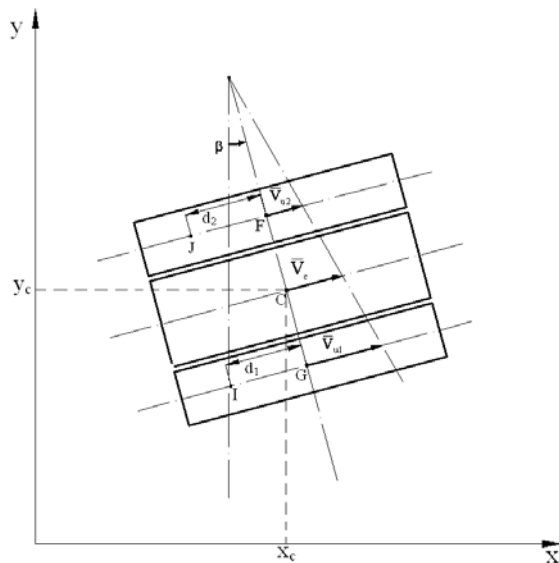


Fig. 5. Diagram of the robot frame turn for the angle

3. DYNAMICS OF THE INSPECTION ROBOT

In the dynamic model of the robot, the kinematic description is expanded, but still considering the same characteristic points on the structure (Fig. 6).

The dynamic description of the robot [1, 2, 3, 6, 15, 17] is based on energetic method based on Lagrange equations. In order to avoid modeling problems connected with decoupling Lagrange multipliers, Maggi equations were used. The final

form of the dynamic motion equations based on Maggi formalism have been presented as follows:

$$\begin{aligned} & \left(\frac{r}{2} [d_1(1-s_1) + d_2(1-s_2)] \cos \gamma \right) (m_R + \\ & 2m) \frac{1}{2} r(1-s_1) \cos \gamma + \\ & \left(\frac{r}{2} [d_1(1-s_1) + d_2(1-s_2)] \sin \gamma \right) (m_R + \\ & 2m) \frac{1}{2} r(1-s_1) \sin \gamma + I_y \ddot{\alpha}_1 = \\ & M_{21} \eta l + (-0.5F_u - 0.5F_D - 0.5G \sin \gamma + \\ & 0.5F_W \sin \gamma - 0.5W_{T1}) r(1-s_1), \end{aligned}$$

$$\begin{aligned} & \left(\frac{r}{2} [d_1(1-s_1) + d_2(1-s_2)] \cos \gamma \right) (m_R + \\ & 2m) \frac{1}{2} r(1-s_2) \cos \gamma + \\ & \left(\frac{r}{2} [d_1(1-s_1) + d_2(1-s_2)] \sin \gamma \right) (m_R + \\ & 2m) \frac{1}{2} r(1-s_2) \sin \gamma + I_y \ddot{\alpha}_2 = \\ & M_{22} \eta l + (-0.5F_u - 0.5F_D - 0.5G \sin \gamma + \\ & 0.5F_W \sin \gamma - 0.5W_{T2}) r(1-s_2). \end{aligned}$$

where: α_1 - angle of rotation of wheel 1, α_2 - angle of rotation of wheel 2, m_R - frame mass, m - track mass, W_T - the force of resistance of the rolling track, F_u - pulling force, F_W - hydrostatic force, F_D - hydrostatic resistance force, I_y - inertia moment for the robot frame, s_1 - slip for wheel 1, s_2 - slip for wheel 2, G - gravity force, η - efficiency.

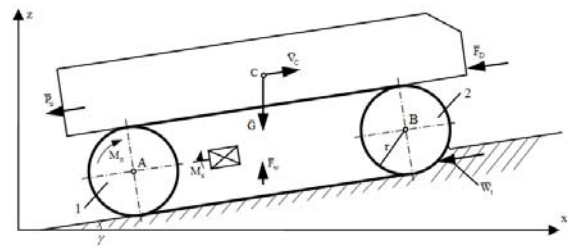


Fig. 6. The Dynamic model of the robot

The dynamic motion equations correspond to the robot moving on the horizontal surface. In case of operation with other track alignments, it is necessary to take into consideration the projections of forces and moments acting on a particular track.

4. OPERATION ENVIRONMENTS

According to project requirements, the robot is capable of positioning its driving mechanism in various ways, to accommodate to working environment. For the most compact alignment, the robot will be able to operate in pipes with diameter above 210 mm (Fig. 7. a). In the Fig. 7. b), we may observe the robot with alignment for operation in a 330 mm diameter pipe. The upper limit of pipe

diameter is determined by the capabilities of the vision system.

For pipes and ducts with rectangular cross-section, there are two different configurations. The first one, presented in the Fig. 8. a) is the configuration, when tracks are horizontally aligned, giving the robot the highest stability and lowest height, whereas in the Fig. 8. b) tracks positioned the closest to each other are depicted, making the robot capable of operation in narrower and higher ducts, or positioning the camera higher above the ground for greater field of view.

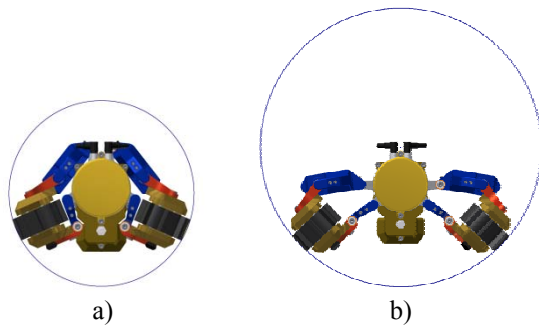


Fig. 7. Operation in round pipes:
 a) $\varnothing 206$ mm, b) $\varnothing 330$ mm

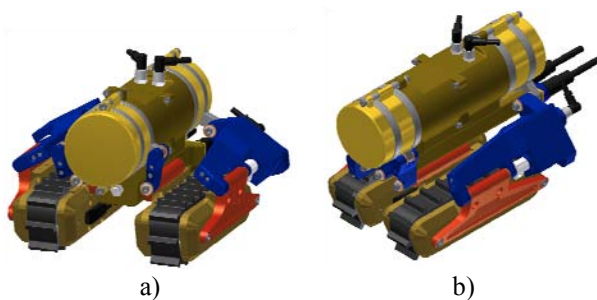


Fig. 8. Operation in rectangular ducts:
 a) wide,
 b) narrow

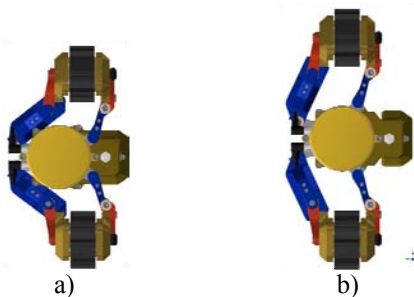


Fig. 9. Track parallel extension:
 a) minimum,
 b) maximum

Parallel extension of tracks is also possible for the robot structure. It may be utilized to operate in pipes or ducts with rectangular or circular cross

section that are oriented in any direction, basing on friction force with respect to the walls. Possible minimum and maximum extensions (230 mm to 270 mm) are presented in Fig. 9.

5. TESTING OF INUKTUN MICROTRACS IN REAL ENVIRONMENT

In case of motion of such mobile platforms as the described robot, there appear problems with precise determination of position and orientation due to deformations of track treads and working surface. In order to reduce this unwanted influence, a previously described mathematical model was proposed. In the model it was assumed that the track treads deform and the surface is undeformable.

The testing procedure was conducted in a laboratory with usage of horizontal pneumatic table with vibration isolation, Phantom v9.1 camera with 2 megapixel resolution. The vision system was equipped with TEMA Automotive software, dedicated to motion analysis, that feature automatic tracking and processing tools. The object of investigation consisted of two Inuktun Microtrac units mounted to a test frame with dimensions and weight corresponding to designed robot. Markers were placed on each track tread and on the track body. During motion, displacements in axes x and y were obtained for particular treads with respect to the marker situated in the lower left corner of the table (Fig. 10). In the we may observe plots of tread marker position in Y axis. Basing on the region of plot when the investigated tread is in contact with the table (lower plot), deformation that will be introduced in the was calculated to be $\Delta l = 0.02$ mm for this kind of motion.

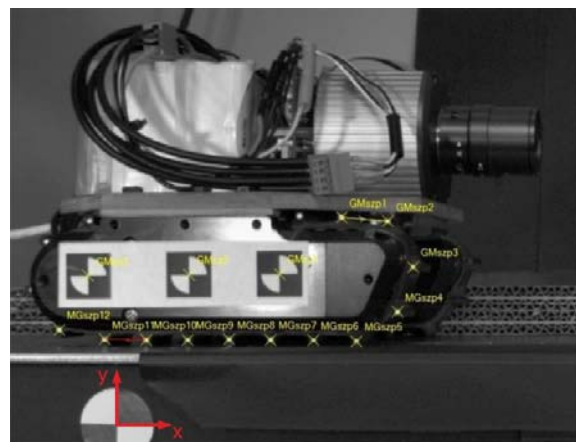


Fig. 10. Track deformation test - markers

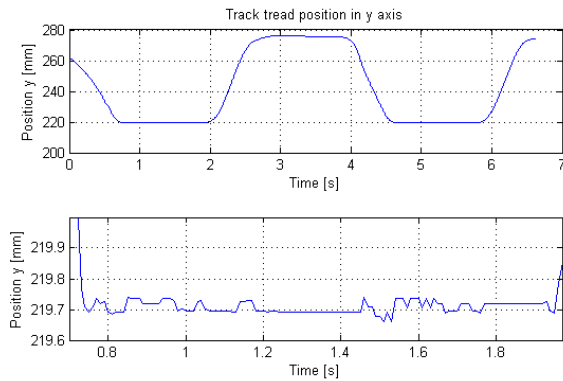


Fig. 11. Track tread position in y axis

6. CONCLUSIONS

This project covers a design process of a pipe inspection robot, using CAD/CAE tools. By reviewing over 20 solutions, market need for a tracked inspection robot with flexible positioning mechanism was identified. A 3D model of a versatile mobile inspection robotic platform was created and simulated. Basing on the conducted laboratory tests, determination of track tread deformation was crucial to correctly formulate the dynamic equations of motion, used for precise estimation of position and orientation of the robot.

7. FURTHER WORK

Experiments with track modules should be performed on different pipe and duct surfaces to provide values of coefficient of friction that will allow estimation of proper loading for positioning drives.

An efficient control system that would allow easy positioning and utilization of all opportunities of the structure must be created. A prototype should be created and equipped with a CCTV camera and lighting to conduct further tests in real operating environment. An algorithmic determination of track treads deformation need to be developed, basing on particular operating surfaces to optimize positioning in work environment.

REFERENCES

- [1] Burdziński, Z., *Teoria ruchu pojazdu gąsienicowego*, Wydawnictwa Komunikacji i Łączności, Warszawa, 1972.
- [2] Chodkowski A. W., *Badania modelowe pojazdów gąsienicowych i kołowych*, Wydawnictwa Komunikacji i Łączności, Warszawa, 1982.
- [3] Chodkowski A. W., *Konstrukcja i obliczanie szybkojeźnych pojazdów gąsienicowych*,

Wydawnictwa Komunikacji i Łączności, Warszawa, 1990.

- [4] Choi, H. R., Roh, S., *In-pipe Robot with Active Steering Capability for Moving Inside of Pipelines*. Bioinspiration and Robotics Walking and Climbing Robots, Maki K. Habib (Ed.), InTech, 2007.
- [5] CUES, 2012. *Ultra Shorty III*. <http://www.cuesinc.com/UltraShortyIII.html> [Accessed 24.04.2012]
- [6] Dajniak H. *Ciągniki teoria ruchu i konstruowanie*, Wydawnictwa Komunikacji i Łączności, Warszawa, 1985.
- [7] Giergiel M., Buratowski T., Małka P., Kurc K., Kohut P., Majkut K. *The Project of Tank Inspection Robot*, Key Engineering Materials, vol. 518, pp.375-383, 2012
- [8] Horodnica, M. H., Doroftei, I., Mignon, E., Preumont A., 2002. *A simple architecture for in-pipe inspection robots*. Int. Colloquium on Mobile and Autonomous Systems, 10 Years of the Fraunhofer IFF, 2012.
- [9] *Vertical Crawler Specification Sheet, Hydropulsion*, 2012. http://www.hydropulsion.com/robotic-crawler-systems/vertical-crawler/vertical_crawler.pdf [Accessed 24.04.2012]
- [10] *Inuktun crawler vehicles*, Inuktun, 2012. <http://www.inuktun.com/crawler-vehicles> [Accessed 24.04.2012]
- [11] ROVVER Brochure, iPEK, 2011. http://www.ipek.at/fileadmin/FILES/downloads/brochures/iPEK_rovver_web_en.pdf [Accessed 08.03.2012]
- [12] Kuwada, A., Tsujino, K., Suzumori, K., Kanda, T. *Intelligent Actuators Realizing Snake-like Small Robot for Pipe Inspection*, International Symposium on Micro-NanoMechatronics and Human Science, 2006, pp.1-6.
- [13] *SOLO Unmanned Inspection Robot*, RedZone, 2012. <http://www.redzone.com/products/solo%C2%AE> [Accessed: 24.04.2012]
- [14] Tadakuma, K., Tadakuma, R., Nagatani, K., Yoshida, K., Aigo Ming, Shimojo, M., Iagnemma, K., *Basic running test of the cylindrical tracked vehicle with sideways mobility*. IROS 2009 IEEE/RSJ International Conference on Intelligent Robots and Systems, vol., no., pp.1679-1684, 10-15 Oct. 2009
- [15] Trojnecki M., *Modelowanie i symulacja ruchu mobilnego robota trzykołowego z napędem na przednie koła z uwzględnieniem poślizgu kół*

jezdnych, Modelowanie Inżynierskie Tom 10, Nr 41, Gliwice, 2011, pp. 411-420.

- [16] Wang, Y., Zhang, J. *Autonomous Air Duct Cleaning Robot System*, MWSCAS '06. 49th IEEE International Midwest Symposium on Circuits and Systems, vol.1, 2006, pp.510-513.
- [17] Żylski W., *Kinematyka i dynamika mobilnych robotów kołowych*, Oficyna Wydawnicza Politechniki Rzeszowskiej, Rzeszów, 1996.



Michał CISZEWSKI

received a M.Sc. degree in Mechatronics from the Faculty of Mechanical Engineering and Robotics, AGH University of Science and Technology in 2012. He is currently a Ph.D. student at AGH University.

His main research area is mechatronics, mobile robots, virtual modelling, analyses and design.



Tomasz BURATOWSKI

received a M.Sc. degree in Robotics and Automatics from the Faculty of Mechanical Engineering and Robotics, AGH University of Science and Technology in 1999, the Ph.D. degree in 2003 also at AGH

University. He is currently employed at AGH University as an assistant professor. His main research area is connected with industrial and mobile robots and also human-robot interaction, fuzzy logic applications, modelling and identification of mechatronic systems.

Mariusz GIERGIEL received a M.Sc. degree in Electronics, from the Faculty of Electrotechnics, Automatics and Electronics, AGH University of Science and Technology in 1985. In 1992 earned a Ph.D. degree in the field of mechanics at AGH University. Since 2005



he is professor at AGH UST at Faculty of Mechanical Engineering and Robotics. He works in the field of automatics and robotics, applied mechanics and mechatronics. Currently, he is the research manager of a group working on a

project of underwater tank inspection robots. He is a member of local and international scientific societies, author of many publications, patents, developed researches and applied solutions.



Krzysztof KURC received a M.Sc. degree from the Faculty of Mechanical Engineering and Aeronautics, Rzeszow University of Technology in 1999. He is currently employed in department of Applied Mechanics and Robotics as

an assistant professor. His main research area is connected with mechatronics, robotics, mechanical engineering and design.



Piotr MAŁKA received a M.Sc. degree in Robotics and Automatics from the Faculty of Mechanical Engineering and Robotics, AGH University of Science and Technology in 2001, the Ph.D. degree in 2008 also at AGH University. He is

currently employed at Municipal Waterworks and Sewer Enterprise, holds the position of manager for the automation. His main research area is connected with industrial and mobile robots, fuzzy logic applications, modelling and identification of mechatronic systems.

EXPERIMENTAL METHOD OF EVALUATION OF DIAGNOSTIC VALUE OF THE ANGULAR SPEED DISCRETE SIGNAL FROM FREE END OF THE CRANKSHAFT

Adam CHARCHALIS, Mirosław DERESZEWSKI

Gdynia Maritime University, Faculty of Marine Engineering
Akademia Morska w Gdyni, Wydział Mechaniczny
ul. Morska 83, 81-225 Gdynia, tel.: +48 58 6901398, e-mail: achar@am.gdynia.pl

Summary

The paper presents the method of the experimental way of finding the answer whether IAS (Instantaneous Angular Speed) of the crankshaft is carrying information about quality of combustion in cylinder of the diesel engine. The experiment was carried out at laboratory stand in Gdynia Maritime University, equipped with diesel engine Sulzer 3AL 25/30 driving the electro-generator. Sulzer 3AL 25/30 is three cylinder, medium speed, four stroke marine diesel engine, with maximum output 400 kW at 750 rpm. In order to evaluate of IAS utility for diagnosis of the engine, the healthy engine run was recorded and malfunction of engine's fuel system were simulated. The malfunction was fuel leakage from high pressure line and bad condition of the injector. The IAS was measured and recorded by perforated disc mounted at the shaft and photo-optic sensor.

Keywords: diagnostics, marine diesel engine, combustion control, angular speed variation.

EKSPERYMENTALNA METODA OCENY PRZYDATNOŚCI DIAGNOSTYCZNEJ DYSKRETNEGO SYGNAŁU PRĘDKOŚCI KĄTOWEJ Z WOLNEGO KOŃCA WAŁU KORBOWEGO

Streszczenie

W artykule zaprezentowano eksperymentalną metodę sprawdzenia czy chwilowa prędkość kątowa wału korbowego jest nośnikiem informacji o jakości procesu spalania w cylindrze silnika z zapłonem samoczynnym. Eksperyment przeprowadzono na stanowisku testowym w Akademii morskiej w Gdyni, wyposażonym w silnik wysokoprężny Sulzer A1. 25/30, napędzający prądnicę. Sulzer 3A1 25/30 jest trzycylindrowym, średnioobrotowym, czterosuwowym silnikiem o mocy maksymalnej 400 kW, przy prędkości obrotowej 750 obr./min. W celu oceny przydatności sygnału prędkości kątowej do celów diagnostycznych przeprowadzono pomiary na silniku w stanie wzorcowym bez usterek, a następnie powtórzono pomiary symulując usterki systemu paliwowego. Symulowane usterki to przeciek na pompie wtryskowej oraz zły stan techniczny wtryskiwacza. Do pomiarów prędkości kątowej zastosowano laserowy czujnik fotooptyczny.

1. INTRODUCTION

Marine Diesel Engines are widely used on board of vessels as a main propulsion and auxiliary engines, mostly diesel generators. Majority of them are low or medium speed engines, within revolutionary speed span from 90 up to 800 rpm (revolutions per minute). Due to importance of such mechanisms for ships operation and safety, and obvious fact that reparation on board is complicated and limited by sea state and limited spare parts supply, to ensure reliability of these engines is primary importance. Engine's condition monitoring helps predict and avoid failures of equipment.

Many malfunctions of diesel engines are related to the combustion process. The process can be

disturbed because of wrong function of subsystem such as valves and camshaft, injection system (high pressure pumps and injectors), turbocharger, or piston and cylinder liner wear. The in-cylinder pressure contains many data about the combustion process. However, direct measurement of in-cylinder gas pressure is impractical and quite expensive. For every cylinder installation of a transducer is necessary, but these tend to have limited lifetime due to exposure at high temperature and pollutants.

Analysis of the crankshaft instantaneous angular speed (IAS) variation has been in focus of attention for several years. Convenience of that method is non-invasive measurement and relatively easy mounting of measurement system elements. According to some authors, analysis of the lowest

harmonics can even point the faulty cylinder, other methods are focused on indicated torque.

This work is dedicated to validation of IAS measurement as a diagnostic information source. As an object of experiment was selected 3-cylinder engine driving an electro-generator. The implemented measuring method uses photo-optical sensor emitting with high frequency a laser beam received by photodiode. The system counts number of signals passing through slots of perforated disc, mounted at free end of a crankshaft. In order to preliminary predict the engine behaviour under condition of different malfunction, the simplified dynamic model of the crankshaft rotation has been elaborated. Results of healthy engines run were a backup of model's correction.

As the method of evaluation of the IAS utility, has been undertaken comparison of records done under different but known malfunctions of fuel system with the model and subsequent approach to identification of source of troubles. Simulated malfunction was a leakage from injection pump. The value of leak was adjusted proportionally to of on-line measured pressure of fuel in injector pipe.

2. THE CHARACTERISTICS OF THE ENGINE AND TEST RIG

The experiment was carried out at the test bed with the electro – generator driven by the engine Sulzer AL 25/30. Short description of the engine and test equipment is presented below.

2.1. Description of the engine

The main engine particulars are reported in Tab.1. It is turbocharged medium speed diesel engine designed by Sulzer. This 3- cylinder in row engine develops 408 kW at rotational speed of 750 rpm. The engine drives alternate current generator, connected to the main electric board. The load of the engine can be fluently adjusted by changing of the load of generator. The high pressure fuel system has three injection pumps, one for each cylinder. General view of the engine is presented in Phot. 1.

Tab.1. Engine technical particulars

Manufacturer	HCP Cegielski/Sulzer
Type	3 AL 25/30
Rated power (kW)	408
Cylinder number	3
Cylinder swap capacity (cm ³)	4922
Rotational speed (rpm)	750
Compression ratio	13:1



Phot. 1. General view of the Sulzer 3 AL 25/30

2.2. Experimental rig description

The crankshaft angular speed variations were measured at the crankshaft free end. Measurements were carried out at different loads, i.e. 150, 200, 250 kW and idle run. IAS measurement was conducted under every load in healthy condition and with implemented malfunction of significant leakage of injection pump and with installed out of order injector. Simultaneously was recorded in-cylinder pressure of each cylinder using Diesel Engine Tester UNITEST 2008. This system is permanent equipment of the laboratory test bed and enables measurement of in-cylinder pressure and high pressure fuel pipe pressure in every cylinder in the same time.

For measurement of angular speed variation was used laser photo optical system ETNP-10 produced by ENAMOR Ltd. Gdynia. The system originally dedicated for torque measurement at ship's propulsion shaft, consist of laser sensor which emits laser beam with frequency of 16 MHz, and calculating module based on signal converter and programmable logic controller PLC SAIA. The speed variation signal transmitter is a perforated disc with proportional slots and teeth at disc's circumference. Number of impulses going through the slot or "blind" due to tooth, depends on instantaneous angular speed. The picture of the disc and the sensor is presented in Phot. 2.



Phot. 2. Measurement disc and laser sensor mounted at crankshaft free end

3. RESULTS OF EXPERIMENT

The aim of the experiment was to find the answer whether disturbances of combustion process caused by malfunction of high pressure fuel system and injector, would be reflected by the angular speed of the crankshaft. For diagnostic purposes, necessary is to obtain three objectives: detection of malfunction, localisation of malfunction, evaluation of severity of malfunction. Answers for all above questions shall come from one source – angular speed deviation analysis.

Results of the experiment are presented in parts according to introduced malfunction.

3.1. Running with leak from the injection pump of 2nd cylinder

The introduced malfunction was the leakage from injection pump number 2. The level of leakage was adjusted basing on observation of high pressure fuel decreasing, at UNITEST display, and was established at 30% max. pressure down. The angular speed is presented as “instant-to-mean” ratio. Very important factor for further detecting and identification of malfunctions is the shape and the magnitude of difference value of compared runs’ waveforms.

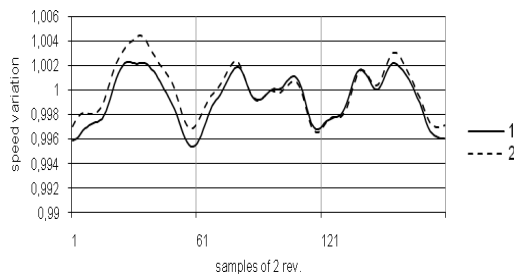


Fig. 1. Angular speed variations of healthy engine (1) and fuel leakage (2), load 250 kW

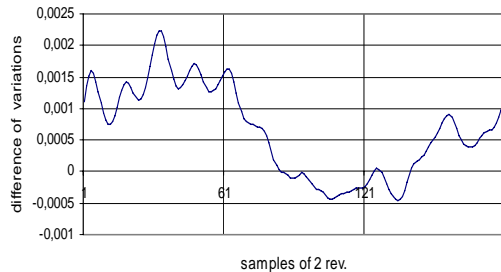


Fig. 2. Angular speed variations difference between healthy engine and fuel leakage, load 250 kW

3.2 Running with low injector pressure in 2nd cylinder

In order to get records of impact of an injector malfunction, specially prepared injector with lowered injection pressure from 250 to 150 bar was installed in 2nd cylinder’s head. The engine was working at load of 250 kW. Simultaneously with angular speed recording, in-cylinder pressure and injection pressure were measured. The waveform of disturbed combustion in comparison with healthy one is presented in Fig.3.

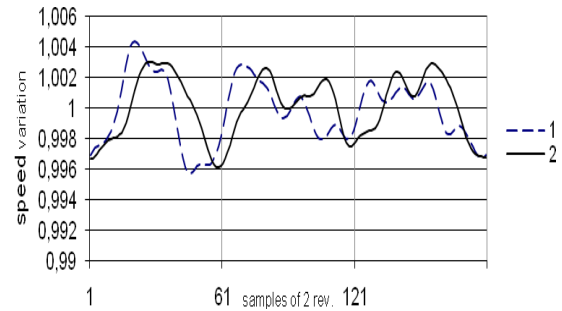


Fig.3. Comparison of healthy engine (1) and low injection pressure (2), load 250 kW

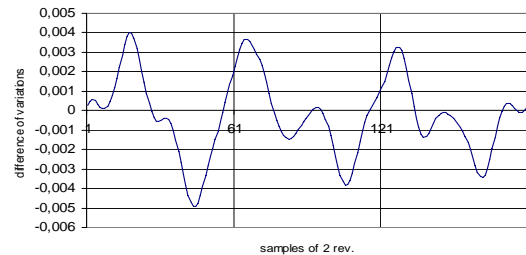


Fig.4. Angular speed variations difference between healthy engine and low injection pressure, load 250 kW

3.3 RUNNING WITH ENLARGED INJECTOR’S NOZZLE HOLES IN 2ND CYLINDER

In order to simulate above malfunction, special injector with enlarged holes of the injector nozzle was prepared. That situation can occur due to unprofessional repair of the injector and results with deviations of injection pressure and change of fuel spray drops. Results of measurement are presented in Fig.6. and 7.

4. MODELLING OF THE CRANKSHAFT SPEED VARIATIONS

The crankshaft was modelled as a simple system balanced dynamically. As the engine is large and masses of pistons and connection roads cannot be omitted, a model with flexible crankshaft has been developed. It takes under consideration the

torsional vibrations creating twisting of main journals of the crankshaft. The torsional vibrations creating torsional twisting of main journals of the crankshaft.

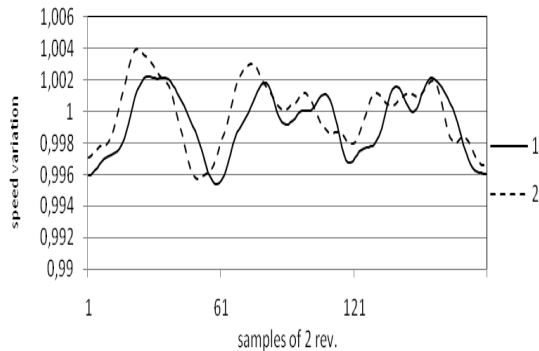


Fig. 5. Comparison of healthy engine (1) and enlarged injector nozzle holes (2), load 250 kW

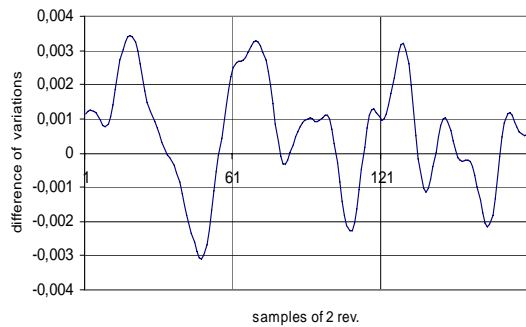


Fig. 6. Angular speed variations difference between healthy engine and enlarged injector nozzle holes, load 250 kW

The torsional vibrations were superimposed with the rotational motion of the rigid crankshaft. In-cylinder pressure consists of two elements, the combustion pressure and compression pressure. For modelling purposes, the results of in-cylinder pressure records of the run of healthy engine at 250 kW load, were taken as the basis. Inertia forces were calculated basing on masses and dimensions of crankshaft-connecting rod-piston system.

Finally the theoretical waveform of crankshaft angular speed oscillation was elaborated, and compared with results of healthy engine measurement (Fig. 7).

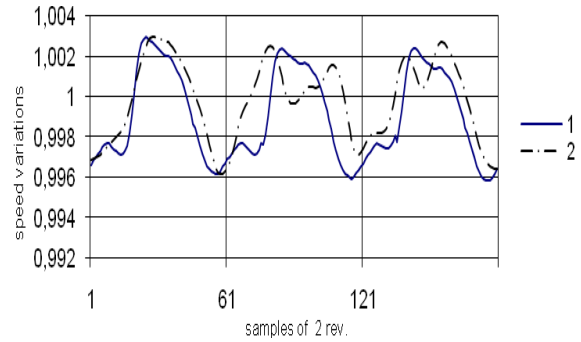


Fig. 7. Comparison of calculated (1) and measured (2) waveforms of speed variations

5. DETECTION OF MALFUNCTION PRESENCE, SOURCE AND MARKING OF THE AFFECTED CYLINDER

Analysis of healthy and disturbed waveforms of IAS leads to the conclusion that simple comparison of waveforms is not sufficient for definition of the malfunction. Better picture of disturbances is given by comparison of waveforms presenting difference between angular speed of healthy and faulty condition, at the same load value [6]. Analysis of tendencies and magnitudes can give the information about malfunction presence and its character. Samples of measured angular speed differences between: two healthy, healthy - leakage fault, and healthy - plugged injector are presented at Fig. 8. and Fig. 9.

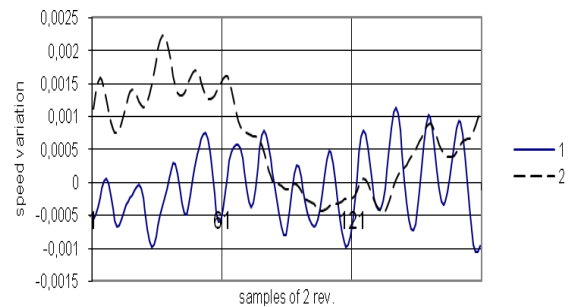


Fig. 8. Angular speed variation difference comparison: two runs healthy engine (1); healthy and fault of fuel leaking (2), domain of samples of 2 rev., 250 kW

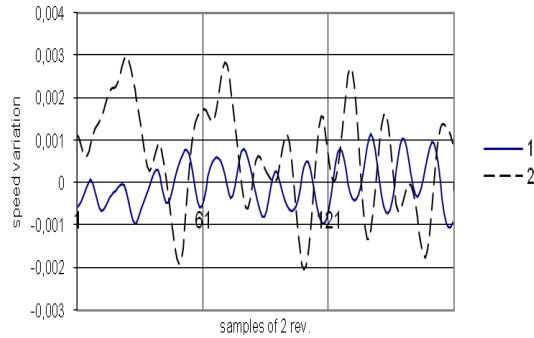


Fig. 9. Angular speed variation difference comparison: two runs healthy engine (1;) healthy and fault of plugged injector (2), domain of samples of 2rev., 250 kW

Occurring of the malfunction is shown due to magnitude amplification. Detection of faulty cylinder in the case of fuel leaking can be done in the way of span analysing, between maximum and minimum value of variation's difference, in every interval (240°) between TDC's of the work stroke of each cylinder (Fig. 8). In the case of partly plugged injector, simple analysis of amplitude span is insufficient (Fig. 9).

6. CONCLUSION

The results of conducted experiment showed that malfunctions of fuel system were the source of angular speed deviations. The level of deviations is strong enough to be detected by photo-optical measurement system. The signal obtained from the perforated disc after decomposing of noise, is a base for diagnostic analysis focused on identification and definition of reason of faulty condition. The way to receive diagnostic information is comparison of healthy and faulty condition IAS waveforms. The conclusion coming from above is that for detection and localisation of malfunction, necessary is having template measurements of a healthy engine. From diagnostic practice is known that collecting of healthy engine data can be difficult, especially for engines being in permanent exploitation. To avoid that inconvenient limitation, a template in a form of healthy engine measurements shall be replaced by very accurate mathematical dynamic model of a crankshaft movement. Construction of such model should enable easy adjustment to any type of diesel engine by setting changeable factors related to certain technical parameters of an engine.

REFERENCES

[1] Bonnier, J. S., Tromp, C. A. J., Klein Woud, J., *Decoding torsional vibration recordings for cylinder process monitoring*, CIMAC vol.3 1998.

- [2] Citron, S. J., O'Higgins, J. E., Chen, L. Y., *Cylinder-by Cylinder Engine Pressure and Pressure Torque Waveform Determination Utilizing Speed Fluctuation*. SAE Paper No 890486.
- [3] Dereszewski, M., Charchalis, A., Polanowski, S., *Analysis of diagnostic utility of instantaneous angular speed of a sea going vessel propulsion shaft*, Journal of KONES, vol. 18, No 1, 2011.
- [4] Geveci, M., Osburn, A. W., Franchek, M. A., *An investigation of crankshaft oscillations for cylinder health diagnostics*, Mechanical Systems and Signal Processing 19(2005).
- [5] Jianguo Yang, Lijun Pu, Zhihua Wang, Yichen Zhon, Xiping Yan., *Fault detection in a diesel engine by analyzing the instantaneous angular speed*, Mechanical Systems and Signal Processing 15(3) (2001).
- [6] Krzyżanowski, J., Witkowski, K., *Possibility of using visualization to present running point of marine diesel engine*. Journal of KONES 2010.
- [7] Margaronis, I. E., *The torsional vibration of marine diesel engines under fault operation of its cylinder*, Forsh. Ingenieurw., 1992, No 1-2.
- [8] Merkisz, J., Jakubczak, M., *System monitoringu silnika tłokowego z wykorzystaniem sensora optycznego*. Journal of KONES, 1999.
- [9] Piotrowski, I., Witkowski, K., *Okrętowe silniki spalinowe*. TRADEMAR, Gdynia 2003.
- [10] Polanowski, S., *Studium metod analizy wykresów indykatorowych w aspekcie diagnostyki silników okrętowych*, Zeszyty Naukowe AMW Nr 169 A (2007).



Adam CHARCHALIS, born in 1944 in Przemysł. In 1968 he accomplished engineering course in Polish Navy University and subsequently followed master studies in Gdansk University of Technology, in Faculty of Shipbuilding. Finally graduated to Msc. Eng. in 1971. In years 1968 - 1971 was appointed as a chief engineer on board a mine sweeper ORP „Krogulec”. Since 1971 had been working in Polish Navy Academy. In 1979 was appointed in substitution as a Commander of Institute of Ships Construction and Propulsion. From 1990 to 2003 was performing the duty of Institute Commander. From 1994 to 2003 was appointed as a Dean of Mechanical -Electrical Faculty of Polish Navy Academy. Since 1999 has been a professor in Maritime Academy in Gdynia. Promoted to Phd. of Engineering in 1978, professor since 1994. Zone of scientific interest is Marine Propulsion, Marine Power Plants, Gas Turbine Propulsion and Diagnostics of Marine Mechanisms.. Author of 3 monographs, 8 handbooks and more than 250 articles.



Mirosław DERESZEWSKI, born in 1961 in Puck. In 1987 had accomplished studies in Polish Navy University and was promoted to Msc. Eng degree. In years from 1987 to 2002 was appointed at various Navy positions, from chief engineer on

board a corvette up to squadron deputy commander. In years 2002 – 2005 was performing a duty in NATO Headquarters as Maritime Infrastructure Officer. From 2005 to 2007 was Logistics Section Officer in Polish navy Headquarters. From 2007 to 2010 was employed by company ENAMOR Ltd in Gdynia as Research and Development Engineer. From beginning of 2011 has been appointed in Maritime University in Gdynia as an assistant in Mechanical Faculty, Chair of Marine Power Plants. Area of scientific interest is Marine Diesel Engines, Gas turbines and Diagnostics of Marine Propulsion.

APPLICATION OF THE OPERATIONAL MODAL ANALYSIS IN TRANSMISSION GEARBOX TECHNICAL STATE IDENTIFICATION

Marcin ŁUKASIEWICZ, Tomasz KAŁACZYŃSKI, Bogdan ŻÓŁTOWSKI

Institute of Machine Engines Exploitation and Transportation,
University of Technology and Life Sciences in Bydgoszcz,
Kaliskiego 7, 85-796 Bydgoszcz, Poland, e-mail: mlukas@utp.edu.pl

Summary

The chosen results of the technical conditions identification investigations of the car transmission gearbox which was situated in the investigative laboratory of Department of Vehicles and Diagnostics in UTP Bydgoszcz by operational modal analysis methods were introduced in this paper. Conducted investigations of transmission gearbox depended on delimitations of vibroacoustics measures for chosen gear sets and accomplishment the assessment of received results influence on transmission gearbox state by operational modal analysis methods.

Keywords: operational modal analysis, diagnostic inference

ZASTOSOWANIE EKSPLOATACYJNEJ ANALIZY MODALNEJ W BADANIACH STANU TECHNICZNEGO SKRZYŃKI PRZEKŁADNIOWEJ

Streszczenie

W pracy przedstawiono wybrane wyniki badań identyfikacji stanów technicznych skrzynki przekładniowej, która znajduje się na stanowisku badawczym laboratorium Zakładu Pojazdów i Diagnostyki UTP w Bydgoszczy metodą eksploatacyjnej analizy modalnej. Przeprowadzone badania skrzynki przekładniowej polegały na pomiarze sygnałów drganiowych dla założonych stanów zdatności oraz badanie wpływu jej rozregulowań na zmianę sygnałów wibroakustycznych z wykorzystaniem metody eksploatacyjnej analizy modalnej.

Słowa kluczowe: eksploatacyjna analiza modalna, wnioskowanie diagnostyczne.

1. INTRODUCTION

The necessity of the technical state estimation is conditioned the possibility of making decisions connected with object exploitation and the procedure of next advance with object. The present development of automation and computer science in range of technical equipment and software creates new possibilities of realization of diagnosing systems and monitoring technical condition of more folded mechanical constructions.

These new possibilities are connected with the new constructions of intelligent sensors, module software and the modules of transport and data exchange [1, 2, 6].

The vibrodiagnostics is one of the machine condition description methods - understood as the organized set of methods and means to the technical state estimation (his causes, evolution and consequence) of technical systems, with utilization of vibration processes or the noise signal [4].

Looking synthetically in generally possible uses of the vibration diagnostics in the next phase of the object existence, it should distinguish the need of the acquaintance of knowledge about the object, about the signals, the syndromes and symptoms and the theory elements of decision in range of the

diagnostic inference, indispensable to the correct estimation of the technical object state. The investigations of vibroacoustics processes in many cases are very complicated, in peculiarity when vibration processes step out in real physical arrangements.

Modal analysis is the process of determining the modal parameters of a structure for all modes in the frequency range of interest. The ultimate aim is to use these parameters to construct a modal model of the response. Following the changes of modal model parameters as a result of engine maladjustment, waste, damages or its failure is the main idea of operational modal analysis. Modes of vibration which lie within the frequency range of the operational dynamic forces always represent potential problems [2, 3, 5, 7].

2. TRANSMISSION GEARBOX MODAL PARAMETERS ESTIMATION

For mechanical object analysis several types of function could be used – time or frequency signals: autopower spectrum, crosspower spectrum, coherence and others. Modal test could be divided into three phases. First phase of modal test is

measurement set-up (system calibration, force and response transducers attachment).

The second step of modal test is measurement of frequency response data – measured in time domain signal is transformed into the frequency domain functions.

The last step of test is modal parameters estimation where measured frequency functions are used for modal model estimation. As a result we received the stabilization diagram with natural frequencies and damping factors, the modal participation factors and estimated mode shapes.

Basis on these three steps of modal testing the investigations of transmission gearbox were conducted in the investigative laboratory in UTP Bydgoszcz. LMS SCADAS recorder with LMS Test.Lab software with Modal Analysis Lite module was used for modal analysis.

Figure no 1 presents LMS SCADAS recorder used for data acquisition during investigations.



Fig. 1. The LMS SCADAS recorder used for data acquisition and object of investigations – car gearbox transmission

3. THE MEASUREMENT POINTS

Measurements were realized with gearbox speed 930 min-1 on the various shifts. During measurement 90 seconds time periods of the signals were recorded with the frequency range 128 Hz.

Figure no 2 presents transmission gearbox model with signal acquisition points.

Figure no 3 presents LMS Data Collection module.

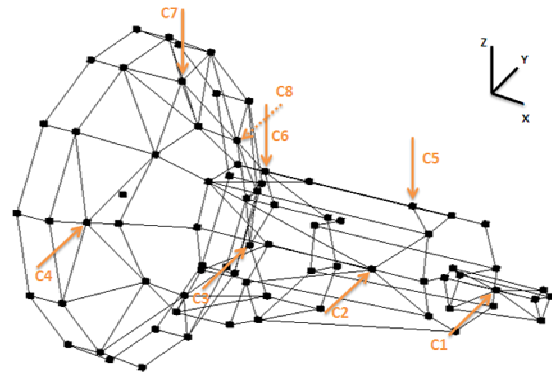


Fig. 2. Transmission gearbox model with signal acquisition points

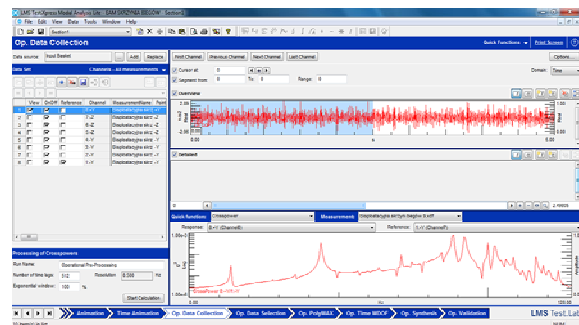


Fig. 3. The LMS Data Collection module

4. THE MODAL TEST

Basis on modal analysis theory the Time MDOF module with non-linear Least Square Frequency Domain (LSFD) method and Balanced Realisation (BR) was used for modal parameters estimation. LSFD is multiple degree of freedom method that applied for multiple inputs it generates global estimates for stabilisation diagram (system poles), modal participation factors and mode shapes.

In first step of Time MDOF method we should define the frequency range within modal test will be done. The geometrical model creation in “Geometry” module will enable the arrangement natural frequencies visualisation. Figure no 4 present “Geometry” module during investigations.

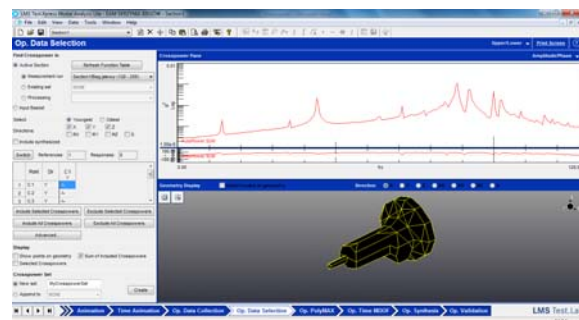


Fig.4. Data selection with “Geometry” module during investigations

In second step of Time MDOF the Balanced Realisation method was used. This is one of the "subspace" techniques which identifies natural frequency, damping and mode shapes. A subset of the response functions can be selected as references. These are used in the computation of the cross power functions from the original time domain data. This method is useful in identifying the most dominant modes occurring under operational conditions [8]. Figure no 5 presents sample of Time MDOF stabilisation diagram for investigated transmission gearbox.

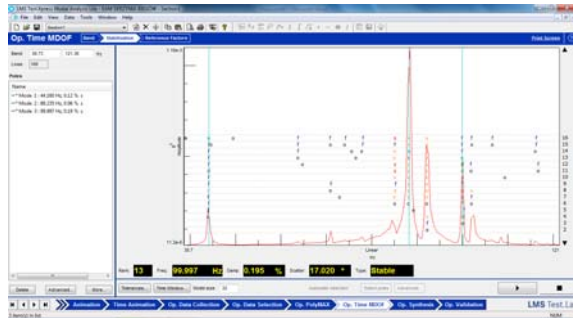


Fig. 5. Time MDOF stabilisation diagram

The result of investigations was a modal model of investigated transmission and mode shapes. The results of modal tests were introduced in table 1.

Table 1. Results of transmission gearbox modal tests

	Natural Frequency [Hz]	Damping factor [%]	Modal model Order
Idle run	44,160	0,12	16
	88,235	0,06	14
	99,997	0,19	13
First gear	44,080	0,20	8
	70,976	0,13	14
	88,504	0,13	12
Second gear	99,986	0,03	16
	44,444	0,15	12
Third gear	88,890	0,22	10
	43,844	0,28	7
Fourth gear	70,433	0,25	12
	124,216	0,46	9
	42,627	0,17	8
Fourth gear	81,967	1,01	8
	87,734	3,04	10

The last step of Time MDOF modal parameters estimation were mode shapes estimation with LSFD method introduced in figure no 6.

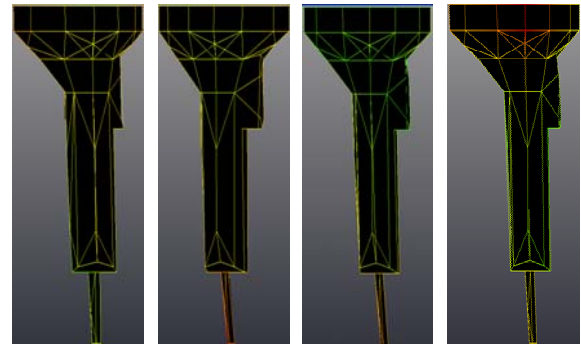


Fig. 6. Transmission gearbox sample mode shapes for frequencies: (from left) 44,16 Hz, 70,97 Hz, 88,23Hz, 99,99 Hz

5. RESULTS VALIDATION

As results validation was used LMS Synthesis module with Auto-MAC criteria estimation - introduced in figure 7, where we could calculate the error of estimation for all recognised mode shapes of object.

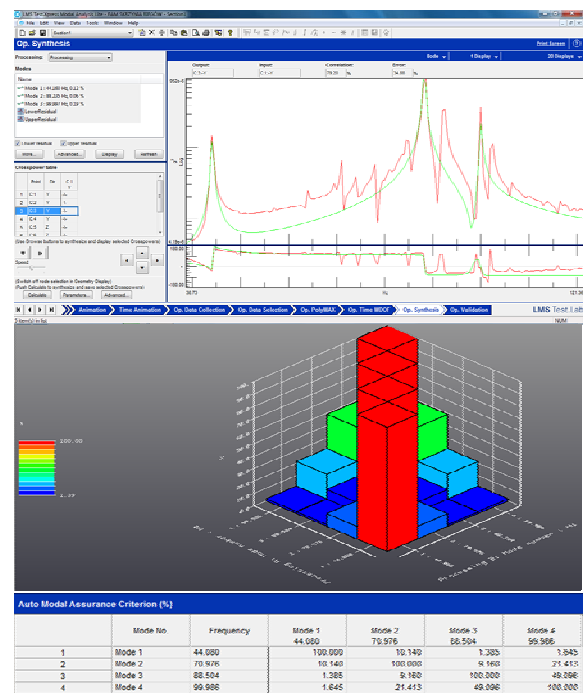


Fig. 7. LMS Synthesis module and Auto-MAC criteria estimation

6. CONCLUSION

Conducted investigations of gearbox depended on delimitations of vibroacoustics measures for chosen gear sets and accomplishment the assessment of received results influence on transmission gearbox state by operational modal analysis methods. As a results we received the stabilization diagram with natural frequencies with damping factors, the modal participation factors and estimated mode shapes. Analysing results of

investigations for idle run, the first identified natural frequency (44,160 Hz) describes the movement of shaft unbalances. The figure of this own vibrations is very well visible on the animation of modal model in the geometry model analysis as determined deformations of model. Second identified figure of natural frequency (88,235 Hz) is caused the differential mass schedule on the gearbox casing and also the unbalances shaft movement - that influences on whole gearbox stiffness. Third figure of natural frequency (99,997 Hz) results from the way of studied gearbox fasten and the kind of the supports on which the whole construction of gearbox leant. Changing gears we received changes of natural frequencies for given transmissions realised by gearbox.

Presented in this paper conducted investigations and modern engineering application allows to quick process of transmission gearbox identification including their own vibration and gearbox body mode shapes visualisation. The advantage of this method is fact that the studied object can be investigated during normal process of exploitation, the investigations don't generate additional costs and we got results basis of real signals that are generated through the exploitation process of studied object.

Introduced in this paper results of investigations are only the part of realized investigative project and they do not describe wholes of the investigative question, only chosen aspects. This paper is a part of investigative project WND-POIG.01.03.01-00-212/09.

REFERENCES

- [1] Cempel, Cz., *SVD Decomposition Of Symptom Observation Matrix As The Help In A Quality Assessment Of A Group Of Applications*, Diagnostyka v.35, PTDT Warszawa 2005.
- [2] Łukasiewicz, M., *Próba odwzorowania modelu modalnego stanu technicznego silnika spalinowego w zastosowaniu do badań diagnostycznych*, Diagnostyka v.33, PTDT, Warszawa 2005.
- [3] Łukasiewicz M. *Investigation of the operational modal analysis applicability in combustion engine diagnostics*, Journal of Polish CIMAC, vol.3 no.2 Gdańsk 2008.
- [4] Łukasiewicz M.: *Vibration measure as information on machine technical condition*, Studies & Proceedings of Polish Association for Knowledge Management 35, ISSN 1732-324X, Bydgoszcz 2010.
- [5] Łukasiewicz M.: *The multidimensional analysis of the combustion engine investigations results with SVD method*. 36th International Scientific Congress on Powertrain And Transport Means, Warszawa – Gdynia – Jurata, Vol. 17, No. 2, s. 285--292, Poland, 12 – 15 September 2010.
- [6] Łukasiewicz M., Żółtowski B.: *The SVD method applicability in combustion engine diagnostics investigation*, Journal of Polish CIMAC Diagnosis, Reliability and Safety Vol.5 No3 Gdańsk 2010, ISSN 1231 – 3998, ISBN 83 – 900666 – 2 – 9.
- [7] Żółtowski B., Cempel Cz.: *Inżynieria diagnostyki maszyn*, Polskie Towarzystwo Diagnostyki Technicznej, Warszawa, Bydgoszcz, Radom 2004.
- [8] The LMS Test.Lab *Operational Modal Analysis Lite manual* – LMS International 2010.



Prof. **Bogdan ŻÓLTOWSKI** is a chief of Department of Vehicle and Diagnostics at Bydgoszcz University of Technology and Life Science.

In the scientific work deal with machine engines dynamics problems, machine engine acoustics and vibration problems, technical diagnostics, metrology and vehicles exploitation. The main problems of this activity are: the physical aspects of damages, the identification in diagnostics, objects dynamics analysis, diagnostic experiments, the diagnostics technique and reliability, the diagnostics steering function, machine engines computer - aid analysis of dynamic exploitation.



Marcin ŁUKASIEWICZ PhD is an assistant in Department of Vehicle and Diagnostics at Bydgoszcz University of Technology and Life Science.

In the scientific work deal with the problems of the dynamics of machine engines, vibroacoustics problems, modal analysis theory and modal investigations, the technical diagnostics and the questions of building and the exploitation of mechanical vehicles.



Tomasz KAŁACZYŃSKI PhD is an assistant in Department of Vehicle and Diagnostics at Bydgoszcz University of Technology and Life Science.

In the scientific work deal with the problems of the dynamics of machine engines, vibroacoustics problems, cars construction and exploitation, the technical diagnostics and the questions of building and the exploitation of mechanical vehicles.

COMPARISON OF SELECTED ALGORITHMS FOR FORCE IDENTIFICATION IN TIME DOMAIN

Jan DERĘGOWSKI, Krzysztof MENDROK

AGH University of Science and Technology, Department of Robotics and Mechatronics,
al. Mickiewicza 30, 30-059 Krakow, Poland, e-mail: mendrok@agh.edu.pl

Summary

In recent years one can observe significant growth of the interest in the structural health monitoring (SHM) systems development and applications. However many authors focuses on the damage detection and all the activities related with diagnosis of failure. Meanwhile, classical, full SHM system should have in addition to a diagnostic module also module for excitation monitoring. Excitation can be measured, but easier and cheaper is to identify it by measuring the response of the object. Often it is the only practical possibility to monitor the excitation. The authors took this often overlooked problem of SHM systems, comparing the most commonly used algorithms for the identification of excitation acting in the time domain in terms of their usefulness in SHM systems. Showing a description of each of the algorithms and simulation results. The following features were compared: accuracy of the excitation reconstruction, simplicity of the algorithm, including the amount and type of data needed to build the model.

Keywords: force identification, inverse problems.

PORÓWNANIE WYBRANYCH ALGORYTMÓW IDENTYFIKACJI WYMUSZEŃ DZIAŁAJĄCYCH W DZIEDZINIE CZASU

Streszczenie

W ostatnich latach obserwuje się znaczny wzrost zainteresowania budową i zastosowaniami układów monitorowania stanu obiektów (ang. Structural Health Monitoring - SHM). Jednakże większość autorów skupia się na wykrywaniu uszkodzeń i innymi czynnościami związanymi z diagnostyką. Tymczasem, klasyczny, pełny układ monitoringu powinien posiadać poza modulem diagnostycznym również moduł odpowiedzialny za rejestrację wymuszeń. Wymuszenia te mogą być mierzone, lecz taniej i łatwiej niejednokrotnie jest identyfikować je na podstawie pomiaru odpowiedzi. Często jest to jedyna praktyczna możliwość monitorowania wymuszeń. Autorzy podjęli ten często pomijany problem, dokonując porównania najpopularniejszych algorytmów identyfikacji wymuszeń działających w dziedzinie czasu pod kątem ich przydatności w układach SHM. Pokazano zarówno opis metod jak i wyniki ich symulacyjnej weryfikacji. Porównywano następujące cechy algorytmów: dokładność odtwarzania wymuszenia, prostota algorytmu z uwzględnieniem implementacji, czasu działania i rodzaju danych koniecznych do przygotowania algorytmu.

Słowa kluczowe: identyfikacja wymuszeń, zagadnienie odwrotne.

1. INTRODUCTION

Structural health monitoring (SHM) is a relatively new appearance in science. The first references to this subject appeared in world literature in the 1980s. SHM is a natural development of technical diagnostics and is also very closely connected with non-destructive testing. According its definition SHM is: the interdisciplinary field of science leading to the provision of, at any moment of the working life of the object, a diagnosis of the material integrity of successive elements, as well as the state of all elements together creating the tested object as a whole. This state must stay in the range defined during design of the object, although it may

change as a result of normal usage, environmental effects or unexpected events. Thanks to the continuous monitoring, which allows an analysis of the complete history of the structural health, as well as the monitoring of operating conditions (loads), the SHM system should also provide a prognosis (damage development, remaining work time etc.) [1]. Many authors often forgets about the second part of the definition, which says about the excitation monitoring, and it is equally important as damage detection in the SHM systems. In Fig. 1. the classic, full SHM system block diagram is presented.

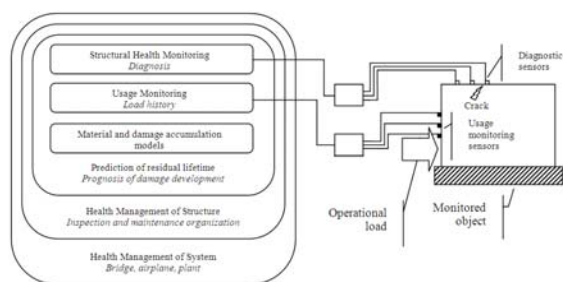


Fig. 1. Block diagram of SHM system

The presented block diagram depicts that each SHM system should be composed of three equally important modules:

- a diagnostics module,
- a module monitoring operating conditions,
- a database containing material models and damage accumulation models.

The first of these performs the basic task of SHM systems, in other words, it tests the integrity of particular sub-system elements. This allows (depending on the level that a given system represents – see the previous section) the detection, localisation and identification of damage developing in the object. When damage appears, the module automatically informs the operators about it, simultaneously sending information to higher management levels. The operators, helped by the diagnosis provided by the sub-system management level and system management level, take a decision regarding further actions. Possible actions include changing the work system parameters, turning off sub-systems or, as a last resort, turning off the whole system.

The second of the modules helps by monitoring exploitation conditions. Environmental conditions are measured, including temperature, humidity, pressure (depending on requirements), as well as the main forces present in the system. These are excitations or in the form of generalised forces or kinematic excitations, and can be measured directly or indirectly, or identified on the basis of response measurements. In cases where the recorded forces exceed the average due to inappropriate usage, or unfavourable external appearances, e.g. storms, hurricanes and earthquakes, this sub-system may send a warning to the operators, and administration of the object, which on this basis may or, in fact, should, conduct a more detailed analysis. This analysis aims at checking the influence of the exceeded force values on the object.

It is worth noting that the two modules discussed above use separate sensor networks. It sometimes occurs that both a change in force and structural changes occurring in the object as a result of damage cause a change in the system response. The independence of both measurement networks allows the differentiation of both sources of anomalies. Before placement of the sensors, an appropriate analysis is performed with the aim of finding the

best sensor localisation for both groups of sensors. In the case of sensor networks for force identification transfer path analysis (TPA) is very helpful, while sensitivity analysis can be applied during the placement of diagnostic sensors.

The third module of execution level contains a database of material models suitable for monitoring sub-systems as well as damage accumulation models. Together with information from the two previously described modules, a prognosis concerning damage development and the remaining work time of sub-systems is generated. It is worth adding that this module may be located on execution levels or on one of the management levels depending on where greater computing power is accessible.

Last two of the above modules required the excitation monitoring. Unfortunately measurement of operational excitations is sometimes very difficult or even impossible. That is why the excitations are often monitored on the basis of structure response measurement. The actual excitation value is reconstructed with use of the inverse problem solution.

2. CLASSIFICATION OF LOAD IDENTIFICATION ALGORITHMS

An overview of the literature concerning the problems of force identification on the basis of signal response measurements allows the formulation of a few divisions of these methods.

The first of these is a division due to the number of forces present in systems. The next factor differentiating methods of force identification is their ability to identify whole force vectors (direction, sense and value) or only the values of forces present at known locations and directions of its activities. The most-well-known division of force identification methods is based on differences in the type of estimation algorithms [2]. According to this division, one can distinguish:

- methods based on deterministic dependencies:
 - methods operating in the time domain:
 - iterative methods,
 - single-step methods,
 - methods operating in the frequency domain:
 - methods based on frequency characteristics,
 - methods based on the mutual energy theorem,
 - methods based on modal filtration,
 - methods operating in the amplitude domain.
- methods based on statistical dependencies.
- methods based on intelligent algorithms:
 - methods using neural networks,
 - methods using genetic algorithms,
 - methods based on fuzzy reasoning.

A separate problem connected with the identification of forces is the separation of many sources present in systems [3, 4], for example, for

the needs of transfer path analysis.

Since for the prognosis of remaining life of the system the time history of the excitations and loads are necessary, for the purposes of application in SHM the algorithms which operate in time domain were selected to the comparison.

3. COMPARISON DETAILS AND ASSUMPTIONS

As it was stated in the previous section the time domain algorithms were selected for further consideration. Among these methods the four most promising were chosen:

- quality function minimization method (QFM),
- method based on state and input observer (SO),
- method based on regressive parametric model inversion (PMI),
- method based on artificial neural network (ANN).

To test the method in the first step the simulation data were prepared. To do so the finite element model of the steel - aluminum frame was created. Next the model was imported to the Simulia Abaqus/CAE 6.10-1 software in order to simulate the dynamic responses in time domain. In Figure 2 the model of the object is presented.

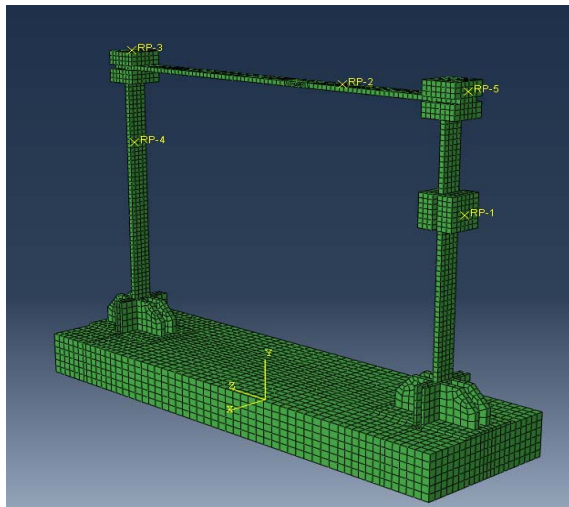


Fig. 2. Model of the simulated system

The excitation was placed in point RP1. The responses in form of vibration accelerations were virtually measured in points RP2 – RP5. Two simulations with two types of excitation signals were carried out:

- harmonic excitation with amplitude 50 N and frequency 5 Hz,
- random excitation with mean value 0.5, normal distribution and amplitude 1 N.

In the consecutive steps the data were used for verification of selected methods. Next each of the methods was classified and evaluated according to the following criteria:

- the accuracy of the signal reconstruction - which were taken into account two factors: Pearson's correlation coefficient and percentage fit of the signals expressed by the formula:

$$Fit = \left[\frac{1 - Norm(Y - \hat{Y})}{Norm(Y - \bar{Y})} \right] \cdot 100\% \quad (1)$$

where: Y, \hat{Y} - normalized vectors of measured and estimated force

- the level of complexity in software/hardware implementation and computational,
- time of calculations,
- type and number of required training data.

For every of the above criteria the ranking of methods was done – the algorithms were ordered from the worst to the best one.

4. FORCE IDENTIFICATION WITH USE OF QUALITY FUNCTION MINIMIZATION

This method belongs to the most often used iterative methods [5, 6, 7, 8]. It may be used for reconstructing the force time history on the basis of knowledge of responses. In particular, it is suitable for the identification of impulse force. It is based on the minimization of the objective function as a measure of the fit between the measured response signal and the calculated one.

Using a reduced vector of state variables q we define the objective function as a difference between the measured response y and the calculated response q .

$$J(c, f_j) = \sum_{j=1}^N (q_j - y_j) D (q_j - y_j)^T + f_j E f_j^T \quad (2)$$

where: c – vector of initial conditions of motion,
 f_j, q_j, y_j – force, calculated and measured state variables vectors at the time j ,
 D, E – weight matrices.

The introduction of the element $f_j E f_j^T$ to the objective function (1) is necessary due to the quality of the obtained force. This operation is the so-called regularisation. In order to obtain forces present in the system, J should now be minimised:

$$\min J \rightarrow f \quad (3)$$

With the objective function defined in this way, it is necessary to select the methods for its minimization. Here, methods based on dynamic programming [5], [6] or genetic algorithms [7] are applied. The advantage of these methods is their ability to be applied in non-linear systems, a drawback is the large calculation power and the long time required for calculations.

In the performed simulation the authors used the state space model identified for the system presented

in Fig. 2. As the optimization algorithm the dynamic programming was applied. As it was stated in Section 3 the method was tested with use of two type of signals – harmonic and random. In Figure 3 the results of comparison between applied and estimated harmonic excitation signal are presented. In Figure 4, appropriate comparison for random signal is shown.

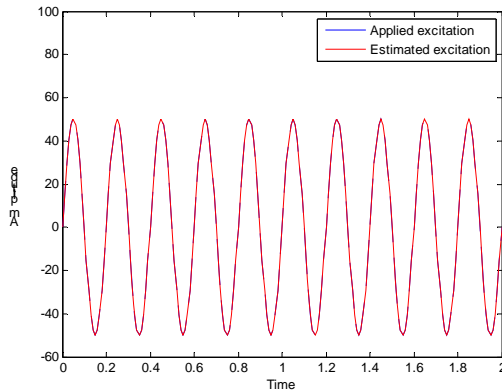


Fig. 3. Results of comparison between applied and estimated harmonic excitation signal

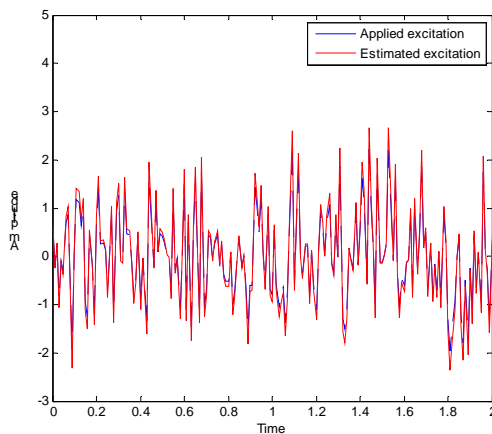


Fig. 4. Results of comparison between applied and estimated random excitation signal

The quantitative results of excitation signal estimation are gathered in Table 1.

Table 1. Results of excitation estimation

Correlation coeff.		Signal fit		Calculation time [s]	
harm.	noise	harm.	noise	harm.	noise
0.999	0.95	99%	92%	165	640

As it can be observed from the above results the method is very accurate for both types of signals. Also it did not required many training data – only one set of time histories for the state space model identification. However its implementation was quite complex and time consuming and the time of calculation was very long. The latter is the biggest drawback of the tested algorithm.

5. FORCE IDENTIFICATION WITH USE OF STATE OBSERVER METHOD

The next method of force identification, which was imported from automatics, uses the state observer with unknown input signal [9]. This type of observer, on the basis of the system responses signals, identifies its states as well as input signals. The method of force identification using such an observer is resistant to measurement noise and may operate in real time. The design of the observer for non-linear objects begins with writing its mathematical model in the form of a state of equations:

$$\begin{aligned} \dot{x}(t) &= Ax(t) + Bu(t) + f((x,u),y) \\ y(t) &= Cx(t) + Du(t) \end{aligned} \quad (3)$$

where: $x(t)$ – vector of object state
 $u(t)$ – vector of desired force
 $y(t)$ – vector of measured outputs
 $f((x,u),y)$ – element introducing non-linearity to the object.

This can be divided into two parts – known and unknown:

$$f((x,u),y) = f_L((x,u),y) + Wf_U((x,u),y) \quad (4)$$

where: $f_L((x,u),y)$ – known non-linear part
 $f_U((x,u),y)$ – unknown non-linear part

The matrices A, B, C, D , and W are constant and have real values. The task consists of designing an observer, which, with the measured system responses, estimates both the state of the object and the forces present at input. Details of the design procedure for this type of observer can be found in [10] and require two assumptions to be met:

Assumption 1:

$f_L((x,u),y)$ must meet the inequality below with the Lipschitz constant:

$$\|f_L(\xi, y) - f_L(\hat{\xi}, y)\| = \gamma \|\xi - \hat{\xi}\|, \wedge y \quad (5)$$

where: $\xi(t) = \begin{bmatrix} x(t) \\ u(t) \end{bmatrix}$

γ - Lipschitz constant – positive real scalar

Assumption 2:

The matrix $[D \ CW]$ has a full column rank. A necessary condition for meeting this assumption is for the number of system outputs to be greater than or equal to the sum of the number of inputs and the size of the non-linear part, which does not meet the Lipschitz condition.

In the tests the authors used the same state space model as in Subsection 4. The state observer implementation was performed with use of the Linear Matrix Inequality Toolbox from the Matlab

package. In Figure 5 the results of comparison between applied and estimated harmonic signal are presented. In Figure 6, the same comparison for random signal is shown.

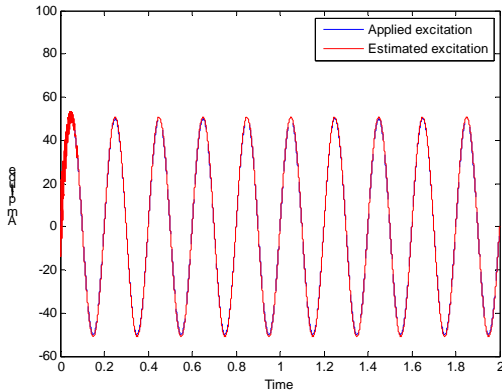


Fig. 5. Results of comparison between applied and estimated harmonic excitation signal

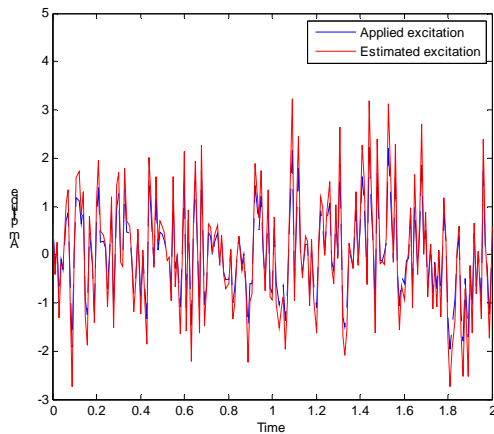


Fig. 6. Results of comparison between applied and estimated random excitation signal

The values of comparison indexes are presented in Table 2.

Table 2. Results of excitation estimation

Correlation coeff.		Signal fit		Calculation time [s]	
harm.	noise	harm.	noise	harm.	noise
0.998	0.713	93%	77%	0.21	0.14

As it can be seen from the results the method is also very accurate. According to the training data its requirements are the same as previously presented QMF method – only one set of time histories. It also worked very fast. However its implementation was very complex and required such a sophisticated tools as LMI toolbox.

6. FORCE IDENTIFICATION WITH USE OF PARAMETRIC MODELS INVERSION

The use of regressive parametric models for the identification of input signals can be seen in automatics. Adaptation of this method for

mechanical systems and force identification can be found in the works [11] and [12]. Its basic stages are: selection of the structure and identification of the regressive parametric model, then inversion of the model and input to the inverse model of the response signal, most often in vibration acceleration form, with the aim of calculating the forces causing the response. The basic problem for solutions is therefore inverting regressive models.

In order to generate responses for an inverse linear dynamic model, it is necessary for it to be proper or strictly proper [13]. A proper object is characterised by having a transmittance with a numerator order lower than the denominator order $nB < nA$, in the strictly proper object, however, the numerator order is equal to the denominator order $nB = nA$. When the numerator order is higher than the denominator order $nB > nA$, the object is physically unrealisable with regard to the required ideal differentiation. Besides this, the object should be linear, stationary and minimum-phase.

Physically realisable inversion for the object described by the continuous model is presented as a combination of the transmittance of the object with its inverse model with an identical structure $H(s) \cdot H_{inv}(s) = 1$. Ideal inversion requires the equality of the inputs $u_0(s)$ and $u(s)$ introducing the standard model $H_w(s)$ which allows the inverse model to be defined according to the dependency:

$$H_{inv}(s) = \frac{H_w(s)}{H(s)} = \frac{u(s)}{y_0(s)} = \frac{a_0 + a_1s + \dots + a_{nA}s^{nA}}{(b_0 + b_1s + \dots + b_{nB}s^{nB})(1 + sT_w)^{(nA-nB)}} \quad (6)$$

where: nA, nB – polynomials order,
 $u(s), y_0(s)$ – estimated input and reference output,
 T_w – time constant,

The scheme of procedures for inverting the model of the object is presented in Figure 7.

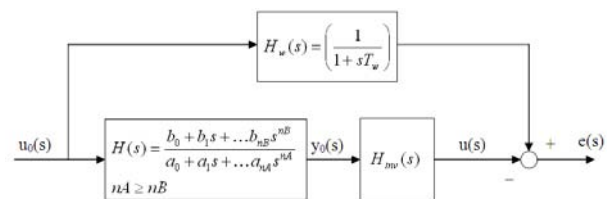


Fig. 7. Scheme of inverting a regressive parametric model of the object

In Figure 7 $e(s)$ designates the error between the reference force $u_0(s)$ multiplied by $H_w(s)$, and the estimated force $u(s)$, $H_{inv}(s)$ is the transmittance of the inverse model of the object.

An excessively large difference between the numerator order nB and the denominator order nA leads to greater inaccuracy of inversion. For large differences in the orders, the accuracy of inversion

falls for increasing frequencies. This results from the possibilities of performing ideal integration (minimal value of T_w). A discrete inverse model is designated as follows:

$$H_{inv}(z) = \frac{H_w(z)}{H(z)} = \frac{u(z)}{y(z)} = \frac{a_0 + a_1z + \dots + a_{nA}z^{nA}}{(b_0 + b_1z + \dots + b_{nB}z^{nB})} \left(\frac{1-c}{z-c} \right)^{(nA-nB)} \quad (7)$$

where: c – constant setting the accuracy of inversion.

for $c = 0$ we gain:

$$H_{inv}(z) = \frac{H_w(z)}{H(z)} = \frac{u(z)}{y(z)} = \frac{a_0 + a_1z + \dots + a_{nA}z^{nA}}{(b_0 + b_1z + \dots + b_{nB}z^{nB})} z^{(nA-nB)} \quad (8)$$

In the case of discrete models, in order to maintain the physical realization of the system, an additional delay z^{-1} exciting causality of the impulse responses of the object is introduced. In other cases, the object would predict the future and the response would form before the force appeared.

In the conducted simulations the authors first identified the regressive parametric model with use of Identification Toolbox. Many different structures of models with different orders of polynomials were tested. In the figure 8 and 9 the harmonic and random signals are compared.

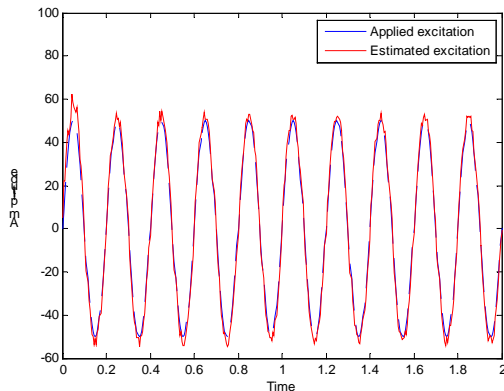


Fig. 8. Results of comparison between applied and estimated harmonic excitation signal

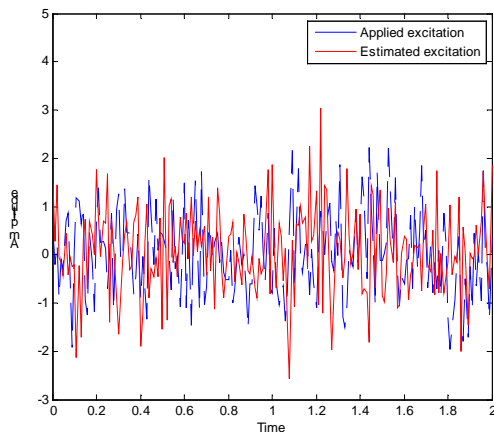


Fig. 9. Results of comparison between applied and estimated random excitation signal

The values of comparison results are placed in Table 3.

Table. 3. Results of excitation estimation

Correlation coeff.		Signal fit		Calculation time [s]	
harm.	noise	harm.	noise	harm.	noise
0.98	0.37	83%	33%	0.35	0.37

The best results for both harmonic and random data were achieved for the ARMAX model. The method worked very fast but the identification accuracy fro random signal was very poor. Also the amount of data required for the model preparation is bigger than in the two previous cases.

7. FORCE IDENTIFICATION WITH USE OF ARTIFICIAL NEURAL NETWORK

Artificial neural networks are constructed from a definite number of basic calculation units known as neurons. These neurons are connected with each other in a series-parallel way. Each of the neurons possesses its own activation function and weight value. A typical network has a structure of layers: the input layer with the number of neurons equal to the number of system inputs, one or a few hidden layers and an output layer. Each layer is built from one or more neurons. Particular types of neural networks differ in the architecture of neurons placement and the flow of information between them, activation functions, methods of learning, etc. and are widely discussed in the literature [14, 15].

The application of artificial neural networks for force identification is described, among others, in the works [16, 17, 18, 19]. Because a machine as a dynamic system may find itself in various phases of loading (run-up, work with full load, without load, run-down etc.), in order to accurately identify the exploitation forces, firstly the state in which the appliance is found should be recognized [31]. On the basis of the value of measured responses or process variables, using the decisive neural network, the load state of the machine is allocated to one of the groups. To do this, it is possible to use a "back-propagation" type network [14, 15] with the same number of input neurons as measured parameters. This process may be realized by a few neural networks in more difficult cases. It should be remembered that one undefined state should be added to the assumed machine work states, which allows qualification errors to be avoided. After performing classification of the loads states of the appliance, neural networks identifying exploitation forces on the basis of measured responses or process variables are constructed. For each load state there is a separate network. Such an approach considerably increases the accuracy of the identifying algorithm.

The universality of artificial neural networks combined with the classification of initial states allows the accurate identification of operational

forces, conducted in real time. The difficulty of using neural networks is based on the lack of an unequivocal recipe for the type and size of networks which should be applied for a given problem.

To identify the forces acting on an object, it was decided to use a neural network with back-propagation of error, the feed-forward type. Input vector to the network was a set of responses of the object to the excitation contained in the output vector. During the trials, there were problems in the identification by the same network the harmonic and stochastic signals, due to their different characters. Therefore, it was decided to use two networks, one for the identification of sinusoidal excitation and the other for noise excitations. The allocation of one of the above networks the simple algorithm decides, on the basis of the number of peaks in a signal Fourier transform. If the number of peaks is more than ten, the signal is fed to the network devoted to the noisy signals. Otherwise, second network is used. In the figures 10 and 11 the harmonic and random signals are compared.

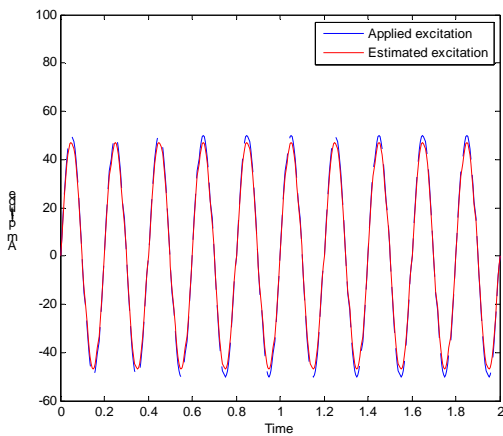


Fig. 10. Results of comparison between applied and estimated harmonic excitation signal

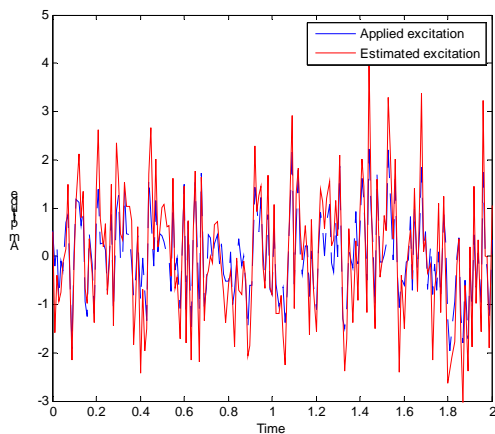


Fig. 11. Results of comparison between applied and estimated random excitation signal

The quantitative results of excitation signal estimation are gathered in Table 4.

Table 4. Results of excitation estimation

Correlation coeff.		Signal fit		Calculation time [s]	
harm.	noise	harm.	noise	harm.	noise
0.999	0.62	89%	57%	0.45	0.47

Application of artificial neural network to the excitation identification for the considered case gave moderate results. It worked fast but the accuracy was worse than the one obtained in SO an QFM methods. Also the amount of training data was the biggest in this case.

8. SUMMARY

In the previous sections four time domain algorithms for excitation identification have been tested. They were verified on the same simulation data. In Table 5 the assessment of the methods efficiency is shown, according to the criteria presented in Section 3.

Table 5. Assessment of excitation estimation algorithms

	SO	ANN	QFM	PMI
Estimation accuracy	1	3	1	4
Time of calculation	1	1	4	1
Training data	2	4	1	3
Complexity of implementation	4	2	3	1
TOTAL	8	10	9	9

The selected evaluation system showed that the method based on state observer seems to be the most versatile. If only the identification accuracy is considered the best choice would be the method based on quality function. When the model of the object is unknown and difficult for identification due to for example nonlinearities then ANN are the only case.

ACKNOWLEDGEMENT

Research funding from the Polish research project 18.18.130.384 (UMO-2011/01/B/ST8/07210) *Teoretyczne podstawy monitorowania stanu technicznego konstrukcji przez rozwiązanie zagadnienia odwrotnego z uwzględnieniem niepewności* is acknowledged by the authors.

REFERENCES

- [1] Balageas D., Fritzen C.-P., Guemes A. (Ed.), "Structural Health Monitoring", ISTE Ltd., London, UK, 2006.
- [2] Uhl T., Mendrok K., „Zastosowanie odwrotnego zadania identyfikacji do wyznaczenia sił obciążających konstrukcje

- mechaniczne*”, Wydawnictwo Instytutu Technologii Eksploatacji – PIB, Radom, 2005.
- [3] Gaeta M., Briolle F., Esparcieux P., “*Blind separation of sources applied to convolutive mixtures in shallow water*”, IEEE SP Workshop on Higher-Order Statistics, Banff, Canada, pp. 340-343, 1997.
- [4] Kompella S. M., Davies P., Bernhard R. J., Ufford D. A., “*A technique to determine the number of incoherent sources contributing to the response of a system*”, Mechanical Systems and Signal Processing, vol. 8 (4), pp. 363–380, 1994.
- [5] Giergiel J., Uhl T., “*Identification of the impact force in mechanical system*”, Archives of Machine Design, tom XXXVI, no. 2-3, 1989.
- [6] Giergiel J., Uhl T., “*Identification of the input impact type forces in mechanical systems*”, The Archives of Transport, vol.1, no. 1, pp. 29-52, 1989.
- [7] Pieczara J., “*Application of genetic algorithms for identification of load vector*”, Machine Dynamics Problems, vol. 29, no. 2, pp. 115–128, 2005.
- [8] Busby H. R., Trujillo D. M., “*Optimal Regularization of an inverse dynamic problem*”, Computers & Structures, vol. 63, no. 2, pp. 243-248, 1997,
- [9] Klinkov M., Fritzen C.-P., „*Online estimation of external loads from dynamic measurements*”, Proceedings of ISMA 2006, Leuven, Belgium, pp. 3957-3968, 2006.
- [10] Ha Q. P., Trinh H., “*State and input simultaneous estimation for a class of nonlinear systems*”, Automatica, vol. 40, pp. 1779–1785, 2004.
- [11] Czop P., Uhl T., “*Load identification methods based on parametric models for mechanical structures*”, Proceedings of the 8th IEEE International Conference on Methods and Models in Automation and Robotics MMAR 2002, Szczecin, vol. 2, pp. 1015-1020, 2002.
- [12] Mendrok K., Kurowski P., Uhl T., “*Operational forces identification from helicopter model in-flight data with the use of inverted regressive parametric models*”, Proceedings of the ASME 2008 International Design Engineering Technical Conferences & Computers and Information in Engineering Conference, New York, USA, 2008.
- [13] Larminat P., Thomas Y., „*Automatyka-układy liniowe*” vol. 2. Identyfikacja, WNT, Warszawa, 1983.
- [14] Norgaard M., Ravn O., Poulsen N. K., Hansen L.K., “*Neural network for modeling and control of dynamic systems*”, Springer-Verlag, London, UK, 2000.
- [15] Tadeusiewicz R., „*Sieci neuronowe*”, Akademska Oficyna Wydawnicza, Warszawa, 1983.
- [16] McCool K. M., Flitter L. A., Haas D. J., “*Development and flight test evaluation of a rotor system load monitoring technology*”, Journal of American Helicopter Society, vol. 45, pp. 19-27, 2000.
- [17] Haas D. J., Milano J., Flitter L., “*Prediction of Helicopter Component Loads Using Neural Networks*”, Journal of the American Helicopter Society, vol. 40, pp. 72-82, 1995.
- [18] Góral G., Bydoń S., Uhl T., „*Intelligent transducers of in-operational loads in construction fatigue monitoring*”, Machine Dynamics Problems, vol. 26, no. 2/3, pp. 73-88, 2002.
- [19] Petko M., Uhl T., “*Smart sensor for operational load measurement*”, Transactions of the Institute of Measurement and Control, vol. 26, no. 2, pp. 99–117, 2004.



**DSc. Eng. Krzysztof
MENDROK**

is a senior researcher in the Department of Robotics and Mechatronics of the AGH University of Science and Technology. He is interested in development and application of various SHM algorithms. He mainly deals with low frequency vibration based methods for damage detection and inverse dynamic problem for excitation identification.

VISION DATA EMPLOYED FOR CRACK DETECTION AND LOCALIZATION

Piotr KOHUT^{1a}, Krzysztof HOLAK^{1b}, Ziemowit DWORAKOWSKI^{1c}, Tadeusz UHL^{1d}

¹AGH University of Science and Technology, Department of Robotics and Mechatronics,
al. A. Mickiewicza 30, 30-059 Krakow, Poland

^{a)} pko@agh.edu.pl; ^{b)} holak@agh.edu.pl; ^{c)} ziemowit.dworakowski@agh.edu.pl, ^{d)} tuhl@agh.edu.pl;

Summary

Nowadays, non-contact measurement systems have found application in the Structural Health Monitoring of civil engineering structures for the detection, localization and assessment of damage. In the field of static deflection measurement, the vision based techniques have become more popular. The deflection curve obtained by image processing and analysis methods can be analyzed in order to detect and localize the change of the curvature, which implies the appearance of a crack. In this paper, the vision based deflection measurement system is discussed. The deflection of beam-like structures is computed by means of digital image correlation. The damage detection and localization is based on the irregularity detection by means of analyzing the deflection curve. A new approach and some selected methods for damage detection and localization will be highlighted and their results obtained in the laboratory setup will be presented and discussed.

Keywords: digital image correlation, image processing, damage detection and localization, wavelet transform, strain energy, deflection curvature analysis.

1. INTRODUCTION

Structural Health Monitoring (SHM) [1, 2] involves the integration of sensors, data transmission, processing and analysis for the detection, localization and assessment of damage within a structure leading to its failure. Damage in SHM is defined as a change in the material properties or the geometry of a structure, which can adversely affect its rigidity and which alters the dynamic and static properties. Generally, SHM methods are divided into two major groups: local and global methods. The latter are applied if a global change in the geometry of a structure can be observed. In practice, the most frequently used methods of damage detection are based on the analysis of variations in dynamic properties caused by the damage [3, 4]. The vibration-based damage identification methods are classified as model-based and non-model-based. The model-based methods identify damage by comparing a theoretical model, usually based on the finite elements, with test data obtained in experimental measurements of the structure [5]. Comparing the updated model with the original one provides information on the damage location and its severity. Non-model-based methods apply signal processing algorithms for the analysis of structures' response signals in time and frequency, as well as time-frequency, domains. Model-based damage detection methods make use of changes in modal parameters between the intact and damaged states of the structure to provide the damage indicators for the localization and assessment of damage. There are many different damage indicators: changes in the natural frequencies [6], changes in the Modal Assurance Criteria (MAC)

across substructures [7], changes in the Coordinate Modal Assurance Criterion (COMAC) [8], changes in modal strain energy [9, 10] and changes in mode shape curvature [11]. However, obtaining dense dynamic data requires high cost devices, such as a laser vibrometer. Moreover, the excitation of large structures can be costly and difficult. The acquisition of static profiles requires much less effort, which makes the damage detection methods based on changes in deflection shapes more attractive for practical use. A lot of damage detection methods based on the analysis of changes in the deflection curve have been developed. The author of [11] described the use of curvature of the deflection in damage detection and localization. The second derivative was obtained by numerical differentiation. A different method of damage detection based on the strain energy of a beam was presented in [12]. This involved a comparison between the strain energy of the reference and damaged states of the structure. In order to avoid the problems associated with noise gain in numerical computation, Hensman [13] proposed the application of Gaussian process in damage detection. The localization of a crack was one of the hyper-parameters of the covariance function. The covariance parameters are optimized based on the measurement data and the damage localization corresponds to the covariance function for which the marginal likelihood of the model is largest. Jang [14] presented a strain damage locating vector (DLV) method combining DLV and static strain measurements. Guo Hui-yong et al. [15] applied a strain energy and evidence theory for damage detection. The evidence theory method was proposed to identify structural damage locations. Then, structural modal strain energy was utilized to

quantify structural damage extents. Chen Xiao-Zhen et al. [16] developed a method of damage identification based on the grey system theory. In his work, the grey relation coefficient of deflection curvature was defined and used to locate damage in the structure. Hui Li [17] et al. proposed a new damage identification method based on fractal dimension (FD). The location of damage in the beam was determined by the fluctuation of the contour of the estimated FD and the extent of the damage was estimated by an FD-based damage index. The author [18] presented the application of roughness measurement as a damage detection tool. The signal is decomposed into two parts: smooth and rough and the damage is localized by analysis of the irregularities of the rough part.

In most of these methods, a densely sampled deflection curve is necessary for the correct damage detection and localization. As the structure becomes more complex, more sensors are needed, which increases the cost of the system installation. Sometimes, it is extremely challenging to attach sensors to a structure because of the environmental conditions or the geometrical constraints. Non-contact vision systems can be a good alternative to contact type transducers. They are easy to use, accurate, low cost and universal tools which can be applied in deformation measurements. Jing [18] et al. presented a use of the computer vision technology to capture the static deformation profile of a structure, and then employ profile analysis methods to detect damages. Staszewski and Patsias [19] presented an application of the wavelet transform for damage detection based on optical measurements. The continuous wavelet transform (CWT) coefficients of both the damaged mode and the approximation function were computed, and thus a reliable damage index could be obtained by taking their difference.

In this paper, the developed vision based method dedicated for in-plane measurement of civil engineering structures' displacement fields is presented. Moreover, the paper introduces a novel damage detection and localization method based on fitting line segments to the displacement field of the beam. The sensitivity of the damage detection algorithm has been tested in a series of lab experiments. The developed method has been compared with a curvature based irregularity detection algorithm.

1.1. Vision based in-plane deflection measurement method

The proposed vision based method [1, 2] of the in-plane deflection measurement consists of the following steps: calibration of the system, image acquisition, and deflection measurement by means of the digital image correlation coefficient. The scale coefficient, which gives information about the length corresponding to one pixel on the image, is obtained by calibration using an object with known geometric

dimensions. In the next step, the reference image and one or more images of the construction under the load are acquired. The photographs can be taken from distinct points in space. The homography mapping H transforms the images in order to remove projective distortions from the image of one, particular, plane of the structure. In the third step, the reference image is divided into intensity patterns. Each of the patterns is matched with the corresponding pattern on the image of the structure under the load by means of the normalized cross correlation coefficient (NCC). The deflection curve is computed as the difference between positions of the equivalent image patches on two images. The last step is scaling the deflection curve using the scale coefficient. The method is schematically shown in Figure 1.

1.2. Image rectification

The homography [18, 19] is a mapping between two sets of points on the plane. If coplanar points' positions are given in homogeneous coordinates, the homography can be represented by a 3-by-3 matrix denoted as H . In the developed measurement system, the homography mapping was introduced for reduction of perspective distortions of an image of one given plane of the construction. The homography matrix H is computed from a set of corresponding points by the DLT algorithm [18]. At least four pairs of coplanar corresponding points are necessary and sufficient to compute the matrix H if no three of them are collinear. In the presence of a noise in real image data, a larger set of corresponding points must be used. The plane of the construction is rectified when all image points are transformed by the homography mapping [1,2].

1.3. Deflection measurement by digital image correlation

The Digital Image Correlation (DIC) method consists of the following three steps: the object's surface preparation; acquisition of the object's image before and after loading, and computation of the displacement field. The construction's surface should have a random gray intensities distribution, which can be a natural texture or artificially made random pattern attached to the structure or painted on it. The basic principle of digital image correlation is matching of the same image path between the two images acquired before and after deformation [19].

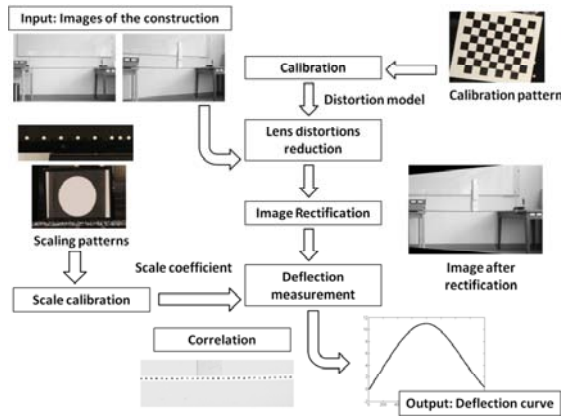


Fig.1. The proposed vision based measurement system of the in-plane deflection of the constructions

In order to compute the displacement of a construction's point, a square or rectangular reference patch of pixels centered at a measurement point is chosen from the reference image and used to match its corresponding location in the deformed image. To evaluate the similarity degree between the reference image path and the search region on the deformed image, the normalized cross-correlation (NCC) is applied. The matching is performed by searching the peak of the correlation function over the search window. The difference in the position of the reference subset center and the deformed image subset center gives the displacement of a point. The NCC coefficient is given by Equation 2 [19].

$$NCC(u,v) = \frac{\sum_{x,y} (f_n(x,y) - \bar{f}_n)(f_d(x-u,y-v) - \bar{f}_d)}{\sqrt{\sum_{x,y} (f_n(x,y) - \bar{f}_n)^2 \sum_{x,y} (f_d(x-u,y-v) - \bar{f}_d)^2}} \quad (1)$$

Where:

$f_n(x,y)$ – an intensity value for a pixel with coordinates (x, y) on the reference image;

\bar{f}_n – mean value of intensities of the pattern on image before deformation;

$f_d(x-u,y-v)$ – intensity value for a pixel with coordinates (x, y) on the image after deformation;

\bar{f}_d – mean value of intensities of the pattern after deformation;

x,y – position of the pattern on reference image;

u,v – displacement of the pattern between two images;

In the process of deflection measurement, the reference image of the unloaded construction is divided into a set of intensity patterns. Each of the patches is matched with a corresponding pixel subset on the image of the loaded structure. The displacement vector is computed as the difference between positions of the pattern on two images. The method performed on each of the points of interest gives a complete course of deflection of the analyzed object. The correlation coefficient computes the position of the pixel as an integer value on the pixel grid. When the sub-pixel methods are introduced [1, 2], the measurement's accuracy

increases up to 0.01-0.1 parts of pixel. An overview of the deflection measurement is presented in Figure 2.

2. CONDITIONS OF THE EXPERIMENT

In order to test the efficiency of the developed diagnostic methods, a series of experiments were performed. Cantilever beams were loaded at a free end with a 0.41 kg mass and damaged by cutting.

Beams with dimensions 40 mm x 60 mm x 4 mm had a random speckle pattern placed on the face side, for vision-based deflection detection by the Digital Image Correlation (DIC) method. In the experiment, the developed software tool “Wiz2D Deflection” was used as software to calculate the deflection curve. At the beginning of each experiment, a number of images were taken which were used for the configuration of the software and which served later as a reference for diagnostic algorithms. Then, a perpendicular cut, 16 mm deep, was introduced to the beam. After each 2 mm deepening 10 images were taken. Deflection curves calculated from the images were averaged and transferred to the diagnostic algorithms. In Figure 2. the restrained beam with optical noise is shown. For the whole experiment 5 beams were used (two cuts in each beam)

In Figure 3, there is a reference image from Wiz2D Deflection with points marked, where deflection was calculated by the DIC method (Correlation windows). The frame of reference is connected to the first correlation window from the left. The images were taken with a Canon EOS 5D MK2 camera with a Canon 24-7-F/2.8L lens (Fig. 3)

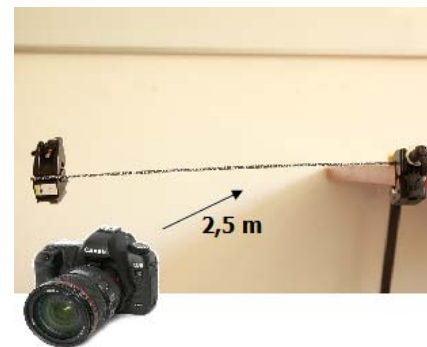


Fig. 2 – Experimental setup

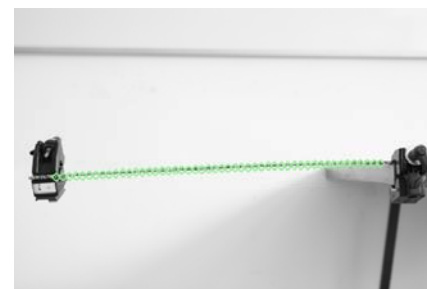


Fig. 3 – Beam with correlation windows

3. DAMAGE DETECTION ALGORITHMS

Wiz2D Deflection calculates the position changes of corresponding points on the reference and measurement (after the introduction of damage) images. Due to the fact that both images were taken under the same load conditions, differences in the calculated deflection curves were caused by the damage introduced.

Two deflection curves were transferred to Matlab software and, after subtraction, the deflection difference curve was used by two independent algorithms, developed by the authors, for damage detection and localization.

3.1. „2nd derivative” - Algorithm based on deflection difference 2nd derivative calculation

At the first stage of the algorithm, filtering of the deflection difference curve is performed, so the sharp changes caused by the measurement noise and resulting large values of the first derivative are eliminated. The smoothing is performed by a 5-element kernel. After filtration, the first derivative of the curve is calculated, the same filtration process is applied, then, calculation of the 2nd derivative and the last smoothing is performed. The maximum value of the obtained curve is treated as the damage indicator and the index of the maximum value is used for damage localization.

In Fig. 4 all stages of the calculations are presented. Efficiency of the presented algorithm is independent of damage localization. However, large measurement noise can lead to errors and false indications of damage. An example of a malfunction of an algorithm is shown in Fig. 5: Noise caused false damage detection. Such errors can be eliminated by adequate setting of the threshold level and control of environment conditions which allows the noise level obtained from the correlation algorithm to be lowered. (Proper lighting, vibration reduction, proper settings of camera).

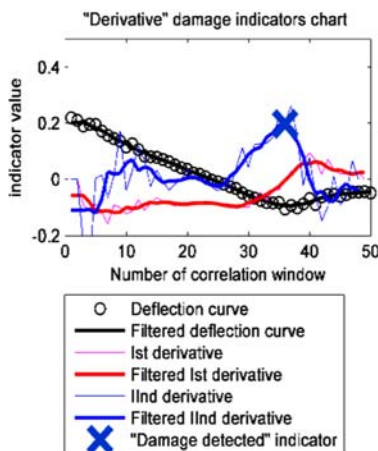


Fig. 4. Stages of 2nd derivative calculation from deflection difference curve

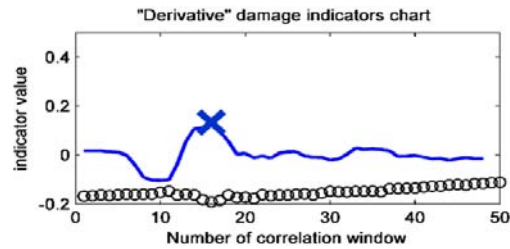


Fig. 5. An example of error caused by high level of noise

3.2. „Line segments” - Method based on geometrical characteristics of the deflection difference curve

Due to the fact that beam load is constant, the only result of damage presence is a break on the deflection curve at the point of damage. The algorithm fits two line segments into the deflection difference curve in such a way that the aggregate matching error is minimal. The index of points between the segments that give the best matching result is the damage localization index. The angle between two segments is the degree of damage indicator. In Fig. 6a, the deflection difference curve is presented with line segments fitted and damage localization marked. The algorithm is resistant to measurement noise, as the fitting of the line segments is performed on a large set of data and scattered breaks in the deflection difference curve do not affect the overall result. However, its drawback is the necessity of limiting the range of damage search in comparison to the “Derivative” method. The algorithm cannot search for damage on the ends of the measurement range, because if the minimal possible length of the line segment is too small, the noise sensitivity sharply increases, as well as the possibility of false damage detection caused by the level of noise at the ends of the measurement range. (See Fig. 6b)

4. RESULTS DISCUSSION

Measurements were taken according to the order described in Section 2. Deflection curves were calculated and used by the diagnostics algorithm. Information concerning the difference of deflection on the end of the measured beam for the maximum depth of cut is essential for the results evaluation. This difference ranges from 0.3 to 0.6 mm (dependent on the position of the cut) which, for the used scale of 0.1360 mm/px results in a position difference in an image between 2.2 to 4.4 pixels.

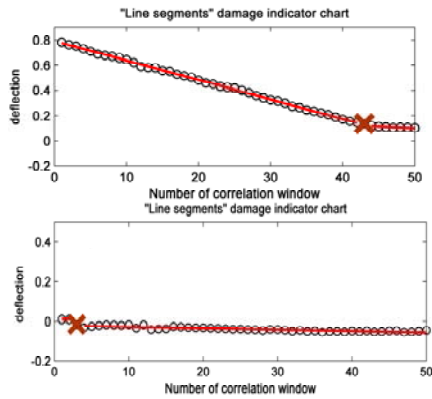


Fig. 6. a) – Deflection difference curve with line segments fitted and detected damage point marked
 b) – False damage detection caused by poorly chosen the minimal line segment length and large noise

Diagnostic algorithms were used for damage detection and localization. The threshold levels were adjusted so the noise would not trigger the detection and to obtain high sensitivity while maintaining a low number of errors. Based upon the location of damage and each correlation window, an index where damage should be detected was computed for each cut. Successful localization was defined as a resulting index at most 3 correlation windows from the expected one. This range was dictated by the observations of algorithm performance: An algorithm which detects the same damage results in indexes from a range of 4 correlation windows.

In Figure 7, the deflection difference curve is shown, as well as the results of the diagnostic algorithms for one cut of different depths. The cut was located at a distance of 430 mm from the left end of the beam, so the correct damage index should appear in 37th correlation window. The damage was detected between 35th and 40th correlation window.

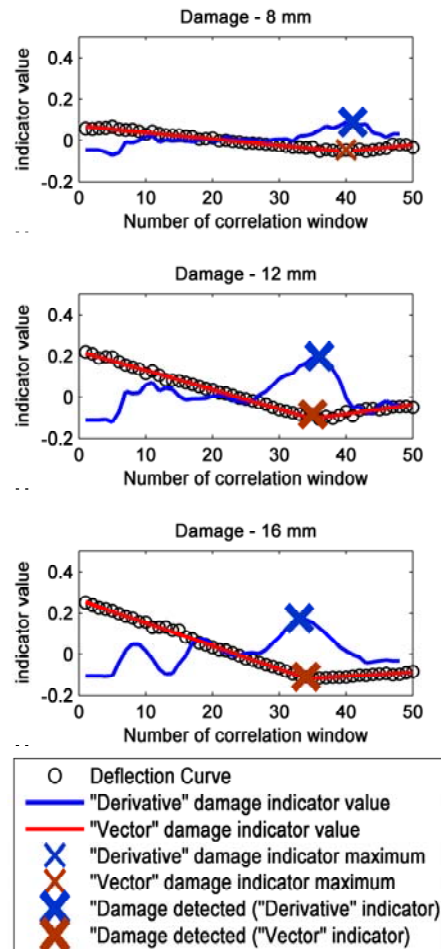
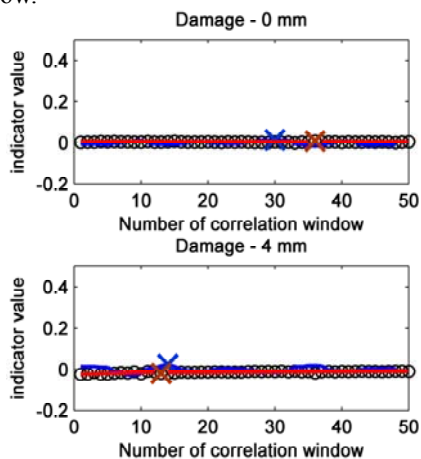


Fig 7. Differences in deflection difference curve caused by the increase of damage; performance of detection algorithms

In Table 1, efficiency of the damage detection and localization as a function of its depth is shown. With the increase in depth, the probability of detection grows. For the maximum depth of the cut (16 mm) the “Line segments” method achieved 100% success. For the given threshold values, no method was able to detect cuts smaller than 6 mm.

In Table 2, efficiency of the damage detection and localization as a function of its location is shown. A significant growth in sensitivity of the method as the location of damage nears the right side of the measurement range is visible. This is caused by the fact that, if the load is constant, the difference in deflection is proportional to the lever arm used and the sensitivity is proportional to the deflection.

Table 1 – Efficiency of damage detection and localization in a function of its depth

Cut depth	Percentage of correct classification		Percentage of errors	
	Derivative	Vector	Derivative	Vector
2mm	0,0	0,0	0,0	0,0
4mm	0,0	0,0	0,0	10,0
6mm	20,0	0,0	10,0	20,0
8mm	10,0	10,0	10,0	0,0
10mm	30,0	10,0	10,0	0,0
12mm	50,0	30,0	10,0	10,0
14mm	70,0	90,0	0,0	0,0

Table 2 – Efficiency of damage detection and localization in a function of its location

Cut position	Quantity of correct classifications		Quantity of errors	
	Correct	Incorrect	Correct	Incorrect
270 mm	3	1	0	0
300 mm	1	2	1	0
330 mm	0	2	2	0
350 mm	2	2	2	0
380 mm	1	2	0	0
400 mm	3	2	0	3
430 mm	4	2	0	0
460 mm	5	5	0	1
480 mm	5	3	0	0

5. CONCLUSIONS

As a result of the conducted experiments, a high sensitivity of damage detection in the developed method was attained. The 16-mm-deep cut was successfully detected in all of the beams used, despite the fact that, for the cuts close to the right side of the measurement range, the deflection difference of the end of the beam was only 0.3 mm. In the field of damage detection as a function of cut depth, the results were satisfactory. For the cuts close to the restrain (on the right side of the measurement range) the number of correct matches reaches 5 out of 8 possible, which means that in some cases cuts of less than 8 mm deep were detected. The efficiency of detection is dependent on the deflection difference between the non-damaged and damaged structure, so it could be increased by applying greater load to the beam. It is also worth noting that both algorithms work independently and have fixed threshold levels. By connecting the two algorithms and lowering the thresholds, if both algorithms suggest damage in the same place the sensitivity may be improved significantly.

6. REFERENCES

- [1] T. Uhl, P. Kohut, K. Holak, *Prototype of the vision system for deflection measurements*. Diagnostyka (4), (2011), 3–11.
- [2] T. Uhl, P. Kohut, K. Holak, K. Krupiński, *Vision based condition assessment of structures*, Journal of Physics, Conference Series, vol. 305 (2011) 1–10.
- [3] P. Kohut, P. Kurowski, *The integration of vision based measurement system and modal analysis for detection and localization of damage Engineering achievements across the global village*, The International Journal of INGENIUM, (2005), 391–398.
- [4] P. Kohut, P. Kurowski, *The integration of vision system and modal analysis for SHM applications Proceedigns*, Of the IMAC-XXIV a conference and exposition on structural dynamics, St.Louis, USA, (2005), 1–8.
- [5] B. Jaishi, W. Rex, *Damage detection by finite element model updating using modal flexibility residual*. Journal of Sound and Vibration 290, (2006), 369–387.
- [6] P. Cawley, R. Adams, *The location of defects in structures from measurements of natural frequencies*. Journal of Strain Analysis 14, (1979), 49–57.
- [7] M. West M, *Illustration of the use of modal assurance criterion to detect structural changes in an orbiter test specimen*, Proceedings of the Air Force Conference on Aircraft Structural Integrity, 1984.
- [8] N. Lieven, D. Ewins, *Spatial correlation of mode shapes, the coordinate modal assurance criterion (COMAC)*, Proceedings of the Sixth International Modal Analysis Conference, (1988), 690–695.
- [9] M. Salehi, S. Ziaei-Rad, *A structural damage detection technique based on modal strain energy*, Proceeding of 17th Annual (International) Conference on Mechanical Engineering ISME2009, 2009.
- [10] H. Guan, V. Karrbhari, *Improved damage detection method based onelement modal strain damage index using sparse measurement*, Journal of Sound and Vibration 309, (2008), 455–494.
- [11] A. K. Pandey, M. Biswas, M. M. Samman, *Damage detection from changes in curvature mode shapes*, Journal of Sound and Vibration 154, (1994), 321–332.
- [12] P. Cornwell, S. W. Doebling, C. R. Farrar, *Application of the strain energy damage detection method to plate-like structures*, Journal of Sound and Vibration, vol. 224, no 2, (1999), 359–374.
- [13] J. Hensman, C. Surace, M. Gherlone, *Detecting mode-shape discontinuities without differentiation - examining a Gaussian process approach*, Journal of Physics: Conference Series 305, (2011), 1–10.
- [14] S. Jang, S. Sim, B. Spencer, *Structural damage detection using static strain data*, Proceedings of the World Forum on Smart Materials and Smart Structures Technology, China, 2007.
- [15] H. J. Guo, Z. Li, *Structural damage detection based on strain energy and evidence theory*. Journal of Applied Mechanics and Materials 48–49, (2011), 1122–1126.
- [16] X. Chen, H. Zhu, C. Chen, *Structural damage identification using test static databased on grey system theory*, Journal of Zhejiang University Science 6(5), (2005), 790–796.
- [17] H. Li, H. Yong, J. O, Y. Bao, *Fractal dimension-based damage detection method for beams with a uniform cross-section*. Computer-Aided Civil and Infrastructure Engineering 26(3), (2011), 190–206.
- [18] S. Jing, X. Xiangjun, W. Jialai, L. Gong, *Beam damage detection using computer vision technology*, Nondestructive Testing and Evaluation, Vol. 25, No 3, (2010), 189–204.
- [19] S. Patsias, W. J. Staszewski, *Damage detection using optical measurements and wavelets*.

Structural Health Monitoring 1(1), (2002), 5–22.

- [20] R. Hartley, A. Zisserman, *Multiple View Geometry in Computer Vision*, Cambridge University Press, 2004.
- [21] Y. Ma, S. Soatto, J. Kosetska , S. Sastry, *An Invitation to 3D Computer Vision*, Springer-Verlag, New York, 2004.



Tadeusz UHL, Prof. is the head of the Department of Robotics and Mechatronics of AGH University of Science and Technology in Cracow. His scientific interests are diagnostics and Structural Health Monitoring of constructions, dynamics of constructions, modal analysis, control systems and mechatronics. He is the author of 16 monographs and over 500 scientific papers.



Piotr KOHUT, Ph.D. is an adjunct professor at the Department of Robotics and Mechatronics of AGH University of Science and Technology in Cracow. His scientific interests focus on mechatronics, vision systems, methods of image processing and analysis as well as 3D measurement techniques.



Krzysztof HOLAK, M.Sc. is Ph.D. student at the Department of Robotics and Mechatronics of AGH University of Science and Technology in Cracow. His works are connected with image processing, analysis and vision measurement systems.



Ziemowit DWORAKOWSKI is a Ph.D student at the Department of Robotics and Mechatronics of AGH University of Science and Technology in Cracow. His research interests include artificial intelligence applied in technical diagnostics, vision systems and mobile robotics.

ISSUES OF DIAGNOSIS FOR A HYBRID ELECTRIC VEHICLE WITH INDEPENDENT FOUR-WHEEL POWER TRANSMISSION SYSTEM

Miłosz MEUS

Katedra Mechatroniki i Edukacji Techniczno-Informatycznej
Uniwersytet Warmińsko-Mazurski w Olsztynie
ul. Słoneczna 46A, 10-710 Olsztyn, tel.: 089 524 51 01, fax: 089 524 51 50
email: miłosz.meus@uwm.edu.pl

Summary

The hybrid electric vehicle with independent four-wheel power transmission system is a promising solution, especially due to fulfilment of requirements for low-level emission of toxic exhaust components, a small fuel consumption and high ride comfort, and also for maximum efficiency of energy conversion. However, these vehicles of the future contain a complicated diagnostic systems.

In a such complex systems is many components related to the strong interactions between them. Therefore, a functionality of the overall system depends primarily on the condition of its individual components. A fault to one of them can reduce the overall performance of the system, and can even lead to an unacceptable loss of its functionality. So the fault diagnosis is crucial.

Keywords: diagnosis, power transmission system, hybrid vehicle.

PROBLEMATYKA DIAGNOSTYKI POJAZDU HYBRYDOWEGO Z AUTONOMICZNYM CZTEROKOŁOWYM UKŁADEM NAPĘDOWYM

Streszczenie

Samochód hybrydowy z autonomicznym czterokołowym systemem napędowym jest obiecującym rozwiązaniem, szczególnie w kontekście spełnienia wymagań co do niskiego poziomu emisji toksycznych składników spalin, małego zużycia paliwa oraz wysokiego komfortu jazdy, a także pod kątem maksymalnej wydajności przekształcania energii. Jednakże te pojazdy przyszłości zawierają skomplikowane do diagnostyki układy.

W takich złożonych układach jest wiele elementów powiązanych silnymi interakcjami. Dlatego też funkcjonalność całego układu zależy przede wszystkim od stanu jego indywidualnych elementów. Uszkodzenie jednego z nich może obniżyć ogólną wydajność układu, a nawet może prowadzić do niedopuszczalnej utraty jego funkcjonalności. Tak więc diagnoza usterek ma tutaj decydujące znaczenie.

Słowa kluczowe: diagnostyka, system napędowy, pojazd hybrydowy.

1. INTRODUCTION

The hybrid electric vehicle (HEV) with independent four-wheel power transmission system is a promising solution, owing to its potentials in reductions of emissions and fuel consumption. This kind of vehicle uses four in-wheel motors to drive four wheels. Torque and driving or braking mode of each wheel can be controlled independently. This way of flexibility actuation, which together with electric motors (with fast and precise torque responses) can enhance the existing vehicle control strategies (traction control system, direct yaw moment control, and other advanced vehicle motion or stability control systems) is really important issue in this field.

In this vehicle the possibility for a fault is higher, especially in-wheel motor or motor driver. This is caused by an increasing of system complexity and number of actuators. Faults of in-wheel motor may

be caused by mechanical failures, overheat of motors, or faults associated with motor drivers. The occurrence of such fault can lead to the situation, when the corrupted wheel may fail to provide the expected torque, and thus jeopardize for the vehicle motion control. Lack of appropriate responses for faults of in-wheel motor or motor driver, may caused deterioration or even instability in the vehicle performance, due to loss of desired torque on a particular wheel. Therefore, the demands on reliability, safety, and fault tolerance for this type of vehicles are substantially elevated.

The main approach to fault diagnosis is the usage of a fault tolerant control system. The objective of this system is to maintain current performances close to the desirable ones and preserve stability conditions in the presence of component faults. Almost all the methods can be categorized into two groups. The first of them is the passive approach. Therein the controller observes the input and output

of the system and based on the measured I/O decides whether a fault has occurred or not. The most of the available methods for fault diagnosis are of this type. The second approach to fault diagnosis is active. Therein the controller generates a test signal which excites the system to decide whether the system represents the normal behavior or the faulty behavior, and if it possible decides which faulty behavior occurs. The test signal should be designed such that it affects the overall system is such a small as it is possible, although enough to make fault diagnosis possible. The advantage of the active approach is in the operating points when the normal system and faulty system represents the same behavior. Under circumstances it is possible to detect faults faster than in passive diagnosis. Active fault diagnosis can also be used to provide initial check in the commissioning phase by generating an appropriate test signal.

Currently in the literature can be found examples of fault diagnosis and fault tolerant control strategies, but mainly adapted for the conventional vehicle. These conventional approaches and methods may not work for the hybrid electric vehicle with independent four-wheel power transmission system. It is known, that the front and rear wheels on the same side of the vehicle have the same effect on the vehicle yaw and longitudinal motion dynamics, when the vehicle is running in a straight line. Some of solutions, which are associated with the actuation redundancy, cause that some of fault tolerant controllers are difficult to implementation on this type of vehicle.

In the hybrid electric vehicle with independent four-wheel power transmission system, when one of in-wheel motors or motor drivers will be damaged, without accommodating control action, the vehicle may not maintain the expected trajectory, because the torque provided by the faulty wheel will be less than expected. An adaptive control based on passive fault tolerant controller, is designed to maintain the vehicle stability and desired motion when an in-wheel motor or motor driver fault happens. Whereas, an active fault diagnosis approach aims to isolate and evaluate the fault under the designed passive fault tolerant controller. Ultimately, control efforts of all in-wheel motors are readjusted based on the diagnosis result to relieve the torque demand on the faulty motor or motor driver for avoiding further damages.

Important is that the vehicle longitudinal speed and yaw rate are controlled to follow references. So, it is assumed, that when a fault happens, the respective control gain will jump to a lower constant value.

The hybrid electric vehicle with independent four-wheel power transmission system is a typical system, in which design of the fault diagnosis is a really complex problem. Also important is the fact, that some motor faults, such as the bearing faults, are difficult to diagnose with only current and voltage sensors. Thus, this paper considers fault

diagnosis and fault tolerant control for the hybrid electric vehicle with independent four-wheel power transmission system, based on a vehicle dynamics. [6, 9, 10, 15, 16]

2. POWER TRANSMISSION SYSTEMS OF THE HYBRID ELECTRIC VEHICLE

The choices of power transmission systems in the hybrid electric vehicle include mainly:

- 1) propulsion mode (such as front-wheel drive, rear-wheel drive, or four-wheel drive),
- 2) number of electric motors in a vehicle,
- 3) drive approach, for instance, indirect or direct drive,
- 4) number of transmission gear levels.

Therefore, the possible power transmission systems in the hybrid electric vehicle have some configurations.

Important is a fact, that output characteristics of electric motors are different from this of an internal combustion engine (figure 1). Typically, the electric motor eliminates the necessity for an engine to be idle while at a stop, it is allowed to produce large torque at low speed, and it offers a wide range of speed variations. It may be possible to develop lighter, more compact, more efficient systems by taking advantages of characteristics of electric motors.

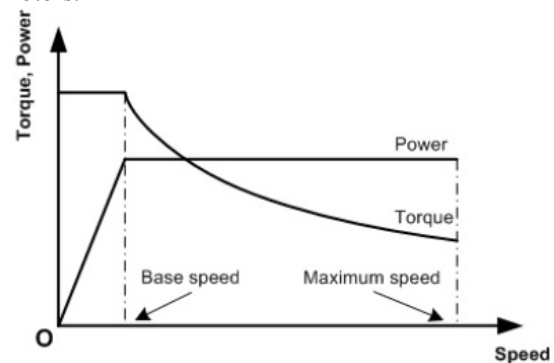


Figure 1. Output characteristics of electric motor drives in the hybrid electric vehicle.

The most promising solution for hybrid electric vehicle is the usage of the independent four-wheel power transmission system (figure 2).

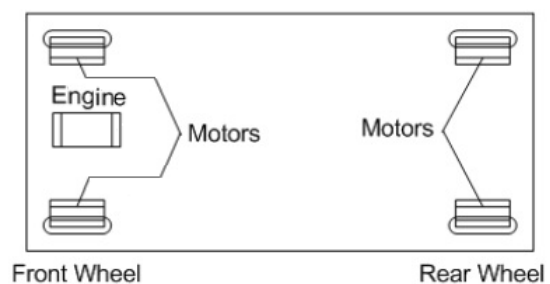


Figure 2. The independent four-wheel power transmission system.

This kind of power transmission system takes up more compact dimensions and reduces power

transmission losses. At the same time, the engine, electric motors and the reduction gear must be reduced in size and weight. The power transmission system, which requires electric motors, are light and develop a large torque.

The internal combustion engine in this system has the task of batteries recharge, when it is necessary.

To fully take advantages of the wide range of output characteristics and small electric motors size arising from high maximum speed for electric motor drives, the power transmission system with the single level reduction gear is the good choice. [7, 8, 12, 13, 14, 17]

3. ANALYSIS OF THE VEHICLE DYNAMICS

Because, as was assumed, that the vehicle dynamics is a basis to fault diagnosis and fault tolerant control for the hybrid electric vehicle with independent four-wheel power transmission system, so at first considerations should be focused on the construct of equations, which describe the vehicle motion.

In the mechanical sense a moving car is a multi-mass dynamic object with multiple degrees of freedom. Four wheel vehicle, in the simplest approach, consists of a body and four wheels, and thus in a considerable simplification it can be considered as a system composed of 5 mass, which are combined by kinematic constraints through weightless suspension system via springs, dampers, etc., which allow their mutual movement. Each of these five mass is treated as a rigid body about six degrees of freedom. The physical model of vehicle, despite the simplification, is characterized by 30 degrees of freedom, what in the mathematical model involves 30 coupled with each differential equations. However, in reality, the greater number of vehicle elements performs the specified movements. Thus, for a more accurate mathematical recognition of a vehicle motion, it should be assume a model, whose the number of degrees of freedom is more than 30. However, an excessive number of coupled equations impedes recognition and analysis of the basic dynamic vehicle properties. Therefore, to know laws governing of vehicle motion, and its basic dynamic properties, is necessary to adopt certain simplifying assumptions.

To get a vehicle model about three degrees of freedom, it should be ignored the pitch and roll motion. A schematic diagram of a vehicle model is presented in Figure 3.

At this figure 3 are marked respectively:

- V_x - longitudinal speed,
- V_y - lateral speed,
- $\dot{\Psi}$ - yaw rate,
- δ - front wheel steering angle,
- m - mass of the vehicle,
- I_z - yaw inertia,
- M - total moment generated by tire forces at all four wheels.

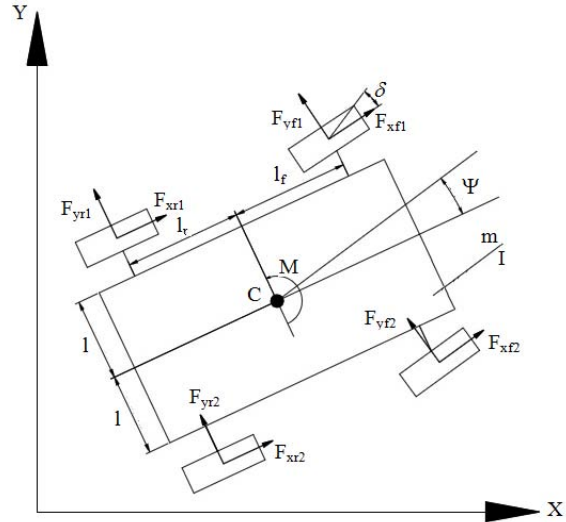


Figure 3. A schematic diagram of a vehicle model.

Based on the figure 3, equations that describe the vehicle motion can be expressed by matrix equation:

$$\begin{bmatrix} \dot{V}_x \\ \dot{V}_y \\ \dot{\Psi} \end{bmatrix} = \begin{bmatrix} V_y \cdot \dot{\Psi} & -\frac{c_x}{m} \cdot V_x^2 & \frac{1}{m} \cdot F_X & 0 & 0 \\ 0 & -V_x \cdot \dot{\Psi} & 0 & \frac{1}{m} \cdot F_Y & 0 \\ 0 & 0 & 0 & 0 & \frac{1}{I} \cdot M \end{bmatrix}, (1)$$

where c_x is an aerodynamic drag, however F_X and F_Y are total forces generated by tire forces at all four wheels.

This (1) equation can be written shorter:

$$\dot{X} = f(X) + A_x \cdot F_x + A_y \cdot F_y, (2)$$

where A_x and A_y are auxiliary matrices, F_x and F_y are matrices of longitudinal and lateral forces operating on tire.

The auxiliary matrix A_x is:

$$A_x = G \cdot \begin{bmatrix} \cos\delta & \cos\delta & 1 & 1 \\ \sin\delta & \sin\delta & 0 & 0 \\ l_f \cdot \sin\delta - l_r \cdot \cos\delta & l_f \cdot \sin\delta + l_r \cdot \cos\delta & -1 & 1 \end{bmatrix}, (3)$$

where $G = \text{diag}(g_{f1}, g_{f2}, g_{r1}, g_{r2})$. However, the auxiliary matrix A_y is:

$$A_y = G \cdot \begin{bmatrix} -\sin\delta & -\sin\delta & 0 & 0 \\ \cos\delta & \cos\delta & 1 & 1 \\ l_f \cdot \cos\delta + l_r \cdot \sin\delta & l_f \cdot \cos\delta - l_r \cdot \sin\delta & -l_r & -l_f \end{bmatrix}. (4)$$

If dynamics of the vehicle is lower than dynamics of in-wheel motor, then dynamics of the motor driver and in-wheel motor can be ignored. The next important assumption is, that the each pair of in-wheel motor and motor driver are treated as an unit. Then this unit can be described by a gain control g_i , which is defined as:

$$g_i = \frac{T_i}{s_i}, (5)$$

where i indicates the specific wheel (f1, f2, r1, r2), T_i is the torque of the in-wheel motor and s_i is the torque control signal to the motor driver.

Summarizing, if a fault happens, that the corresponding gain control will be reduced.

The rotational dynamics of each wheel is represented by formula:

$$I_w \cdot \dot{\omega}_i = g_i \cdot s_i - r_{err} \cdot F_{xi}, \quad (6)$$

where ω_i is the wheel longitudinal rotational speed, R_{err} is the tire effective rolling radius, and I_w is the wheel moment of inertia. The $\dot{\omega}_i$ can be estimated in real-time by using a special filter.

Based on above considerations, the vehicle model can be written as:

$$\dot{X} = f(X) + \frac{A_x}{r_{err}} \cdot G \cdot S + A_y \cdot F_y - \frac{I}{r_{err}} \cdot \Omega, \quad (7)$$

where:

$$S = [s_{f1}, s_{f2}, s_{r1}, s_{r2}]^T,$$

$$\Omega = [\dot{\omega}_{f1}, \dot{\omega}_{f2}, \dot{\omega}_{r1}, \dot{\omega}_{r2}]^T.$$

At this point, two cases may be considered. The first is situation, when the vehicle is running in a straight line. Then the vehicle model is the same as in (7) equation, except that the front wheel steering angle is 0. The second is, when the vehicle is turning. Then the vehicle longitudinal speed and yaw rate are controlled to follow references. So in the vehicle model a component associated with the vehicle lateral speed is omitted, and also the front wheel steering angle is higher than 0. However, in this article considerations will be mainly focused on the situation, when the vehicle is running in a straight line. [1, 2, 3, 4, 5]

4. THE DIAGNOSTIC METHOD

At first an attention will concentrate on passive fault tolerant diagnosis. However, before the diagnostic model for this way of diagnosis will be discussed, should be made some simplifying assumptions.

If two control signals at the same side of the vehicle are identical, then some used functions to the description of the vehicle motion, can be minimized. It follows therefore, that for the left side of the vehicle the torque control signal to the motor driver can be written as a one factor – s_l (analogous for the right side of the vehicle – s_r).

For the left side of the vehicle, the required total torque is defined as:

$$T_l = s_{f1} \cdot g_{f1} + s_{r1} \cdot g_{r1}. \quad (8)$$

Analogous for the right side of the vehicle, the required total torque can be written as:

$$T_r = s_{f2} \cdot g_{f2} + s_{r2} \cdot g_{r2}. \quad (9)$$

Of the foregoing considerations follows, that two wheels on the same side of the vehicle have the same effect on the vehicle dynamics. For the left side of the vehicle:

$$g_l = g_{f1} + g_{r1}. \quad (10)$$

Analogous for the right side of the vehicle:

$$g_r = g_{f2} + g_{r2}. \quad (11)$$

When a fault happens, the actual value of g_l or g_r will be unknown as g_i is unknown due to the fault. An adaptive controller does not need the accurate value of g_l or g_r . Here appears the concept to use the passive fault control for stabilizing the faulty vehicle. As the vehicle trajectory is mostly determined by its longitudinal speed and yaw rate, only these two states are controlled to follow references.

The diagnostic method will be based on the stability analysis method developed by Lyapunov. At first is required to elaboration the Lyapunov function. Here is proposed:

$$V = \frac{(V_{rx} - V_x)^2 + (\Psi_r - \Psi)^2 + (g_l - \hat{g}_l)^2 + (g_r - \hat{g}_r)^2}{2}, \quad (12)$$

where V_{rx} are the longitudinal speed reference, Ψ_r are the yaw rate reference, and \hat{g}_l , \hat{g}_r are the estimations of g_l and g_r . The Lyapunov method uses a derivative of this function. In the next step is necessary to specify control equations for s_l and s_r with tunable parameters L_1 and L_2 higher than 0. After all these actions, the derivative of the Lyapunov function can be written as:

$$\dot{V} = -L_1 \cdot e_{rx}^2 - L_2 \cdot e_{\Psi}^2, \quad (13)$$

where $e_{rx} = V_{rx} - V_x$, and $e_{\Psi} = \Psi_r - \Psi$. This function is lower or equal to 0, which means that the actual longitudinal speed and yaw rate can follow their references.

In order to guarantee the control signals are bounded, a projection method is used to modify the adaption equations. Based on the control gain definition, one can see that \hat{g}_l and \hat{g}_r should be bounded as:

$$\begin{aligned} 0 < \varepsilon \leq \hat{g}_l \leq 2 \cdot g_{\max} \\ 0 < \varepsilon \leq \hat{g}_r \leq 2 \cdot g_{\max} \end{aligned}, \quad (14)$$

where ε is a small positive constant and g_{\max} is the maximal gain control of a single motor. Note that if only one motor is in fault, ε will equal to the single motor minimal control gain g_{\min} .

This passive fault tolerant controller is not an ideal, because the torque demand on the faulty wheel is not specifically reduced.

Here, should be defined a control function. This function for four in-wheel motors can be written as:

$$CF = \sum_i c_i \cdot s_i^2, \quad (15)$$

where c_i is the correction factor for each of wheels. With the assumption, that four wheels are the same, is possible to write the correction factor for each of the wheels as a one factor ($c = c_{f1} = c_{f2} = c_{r1} = c_{r2}$). It follows, that better is to actively adjust the correction factor of the faulty motor in the control function to discourage use of the faulty motor.

From the foregoing follows, that two wheels on the same side have the same effect on the vehicle speed or yaw rate. So, an active fault diagnosis method is intended to locate the faulty wheel and estimate its gain control to better allocate control efforts.

So, now an attention will concentrate on the active fault diagnosis. Suppose, that the passive fault tolerant controller for the vehicle, which function properly, can give a control signal s_0 , what can maintain the vehicle in the desired trajectory. For the left side of this vehicle, which is running in a straight line, can be written equation:

$$s_l \cdot (g_{fl} + g_{rl}) = s_{0l} \cdot (g_{0fl} + g_{0rl}). \quad (16)$$

Analogous for the right side of the vehicle:

$$s_r \cdot (g_{fr} + g_{rr}) = s_{0r} \cdot (g_{0fr} + g_{0rr}). \quad (17)$$

If $g_i \neq g_{0i}$, what means, that the fault happens to a wheel. If $s_j = s_{0j}$ (j indicating the left or right side), what determines a condition, when no fault happens. However, if $s_j \neq s_{0j}$, then it means, that the fault happens. From the foregoing follows, that for two wheels on the faulty side, gains control (g_{fu} and g_{ru}) of this motors, satisfy:

$$g_{fu} + g_{ru} = \frac{(g_{0fu} + g_{0ru}) \cdot s_{0f}}{s_f}, \quad (18)$$

where s_f is the control signal for motors on the faulty side after the fault happens. Next, from the foregoing follows, that in this equation are two new and unknown parameters, g_{fu} and g_{ru} , what means the actual gain control of the faulty wheel cannot be solved from its alone. Therefore, an another equation should be used to calculate this two gains control on the faulty side. The gain control of the motor can be virtually changed by multiplying a positive value (α) to the control signal. After introduced this additional fault, (18) equation can be written as:

$$\alpha \cdot g_{fu} + g_{ru} = \frac{(g_{0fu} + g_{0ru}) \cdot s_{0f_c}}{s_{f_c}}, \quad (19)$$

where s_{f_c} is the control signal of the motor on the faulty side after the introduction of this virtual fault. Based on these two equations (18 and 19) the actual gain control can be solved for two gains control (g_{fu} and g_{ru}) for two motors on the faulty side, and the estimated gain control will be different from the nominal value. Important is a fact, that the fault tolerant controller can follow the vehicle references even this additional virtual fault is introduced. Also this virtual fault should be used only, when the passive fault tolerant controller have reached all states of the vehicle references.

Alluding to the control function for two wheels on the faulty side:

$$CF = c_e \cdot s_e^2 + c_f \cdot s_f^2, \quad (20)$$

where s_e is the control signal for efficient motor on this side, s_f is the control signal for faulty motor on this side, c_e and c_f are the corresponding weighting factors for this two motors. However the desired total torque of motor from this side is:

$$T_d = s_e \cdot g_e + s_f \cdot g_f. \quad (21)$$

By using the Lagrange multiplier method, the control function can be minimized, if:

$$\frac{s_e}{s_f} = \frac{c_f \cdot g_e}{c_e \cdot g_f}. \quad (22)$$

Definition of the correction factor for the faulty wheel can be written as:

$$c_f = \frac{c_e \cdot g_e}{g_f}. \quad (23)$$

Finally, can be written:

$$\frac{s_e}{s_f} = \frac{g_e^2}{g_f^2}. \quad (24)$$

From the foregoing follows, that the correction factors do not change, when the fault do not occur. However, if the fault occurs, the gain control of the faulty wheel decreases and c_f will increase. If the loss of the gain control is large, the associated component will be more heavily weighted. And when $c_f \rightarrow \infty$, then the actual gain control of the faulty wheel goes to 0, which means that the faulty wheel will not be used. The estimated gain control of faulty wheel will be used as g_f in (24) equation. [9, 10, 15, 16]

5. CONCLUSION

After performing an analysis of created diagnostic model, it turned out, that the estimated gain control of the faulty wheel is very close to the actual value. Based on the estimated gain control of the fault wheel, the correction factor for the fault wheel in the control function must be readjusted to better allocate control efforts. Moreover, two wheels on the efficient side always provided the same torque, no matter whether there was a fault or not on the other side. The efficient motor on the faulty side increased the torque, as the passive fault tolerant controller increased more control effort to the faulty side to compensate the tracking error caused by the faulty motor.

In the case, when the same control signals are still sent to two motors on the faulty side and also gains control of these motors have became the same, due to the virtual fault introduced to the efficient motor, then these motors started providing the same torque.

When the active diagnosis period has been finished, then the efficient motor on the efficient side has began to provide the most of the torque, which are required for this side, as the control efforts are redistributed according to the change of the correction factor in the control function.

The effectiveness of this controller is significant, because the controlled vehicle can follow well to the reference of the velocity and yaw rate, while the uncontrolled vehicle failed to follow references, because the faulty wheel failed to provide the required torque.

A passive fault tolerant controller is designed to maintain the vehicle stability and desired performance when a fault happens. An active fault diagnosis approach is proposed to isolate and evaluate the fault under the designed passive fault tolerant controller. Based on an active fault detection mechanism for the in-wheel motor or motor driver,

the control efforts among wheels can be redistributed to minimize the control function considering the fault.

REFERENCES

- [1] Prochowski L., *Mechanika ruchu*, Wydanie 1, Warszawa, WKŁ, 2005.
- [2] Siłka W., *Teoria ruchu samochodu*, Skrypt uczelniany nr 110, Wyższa Szkoła Inżynierska w Opolu, Opole, 1987.
- [3] Struski J., *Quasi – statyczne modelowanie sterowności samochodu*, Monografia 144, Politechnik Krakowska, Kraków, 1993.
- [4] Romaniszyn K. M., *Badanie i modelowanie dynamiki układów napędowych samochodów*, Monografia 232, Politechnik Krakowska, Kraków, 1998.
- [5] Mitschke M., *Dynamika samochodu, Tom 1: Napęd i hamowanie*, tłumaczył Reński A., Syta S., Warszawa, WKŁ, 1987.
- [6] Tabatabaeipour S., Ravn A. P., Bak T., Izadi-Zamanabadi R., *Active Fault Diagnosis of Linear Hybrid Systems*, 7th IFAC Symposium on Fault Detection, Supervision and Safety of Technical Processes, Barcelona, Spain, 2009.
- [7] BOSCH, *Napędy hybrydowe, ogniwa paliwowe i paliwa alternatywne*, praca zbiorowa, tłumaczył Brzeżański M., Juda Z., Warszawa, WKŁ, 2010.
- [8] Szumanowski A. *Fundamentals of hybrid vehicle drives*, Institute for Terotechnology, Warsaw, Radom, 2000.
- [9] Blanke M., Kinnaert M., Lunze J., Staroswiecki M., *Diagnosis and Fault-Tolerant Control*, Springer, 2006.
- [10] Wallmark O., Harnefors L., Carlson O., *Control Algorithms for a Fault-Tolerant PMSM Drive*, IEEE Trans. on Industrial Electronics, 2007.
- [11] Merkisz J., Mazurek S., *Pokładowe systemy diagnostyczne pojazdów samochodowych*, Warszawa, WKŁ, 2007.
- [12] Miller J., *Propulsion Systems for Hybrid Vehicles*, IEE Trans. on Industrial Electronics 2004.
- [13] Ocioszyński J. Michałowski K., *Pojazdy samochodowe o napędzie elektrycznym i hybrydowym*. Warszawa, WKŁ, 1989.
- [14] Bramson E., Grabowiecki K., Jaworowski B., Krasucki J., Rostkowski A., Szumanowski A., Tomczyk J., *Układy napędowe z akumulacją energii*, pod redakcją Szumanowskiego A., Warszawa, PAN, 1990.
- [15] Muenchhof, M., Beck, M. and Isermann, M., *Fault-tolerant actuators and drives—Structures, fault detection principles and applications*, Annual Reviews in Control, 2009.
- [16] Stoustrup J., *An observer parameterization approach to active fault diagnosis with applications to a drag racing vehicle*, 7th IFAC

Symposium on Fault Detection, Supervision and Safety of Technical Processes, Barcelona, Spain, 2009.

- [17] Rahman K. M., Patel N. R., Ward T. G., Nagashima J. M., Federico Caricchi F., Crescimbeni F., *Application of direct-drive wheel motor for fuel cell electric and hybrid electric vehicle propulsion system*, IEE Trans. on Industry Applications, 2006.



mgr inż. **Miłosz MEUS** (ur. 1985), absolwent Wojskowej Akademii Technicznej w Warszawie (2009) – Wydział Mechatroniki, Kierunek Mechatronika, specjalność Komputerowe Wspomaganie w Mechatronice. Obecnie pracuje w Katedrze Mechatroniki i Edukacji

Techniczno – Informatycznej na Wydziale Nauk Technicznych Uniwersytetu Warmińsko – Mazurskiego w Olsztynie. Zajmuje się problematyką związaną z wykorzystaniem:

- 1) potencjału energetycznego z biogazu,
- 2) szeregowego napędu hybrydowego w pojazdach.

MARINE DIESEL ENGINES TURBOCHARGERS DIAGNOSTIC METHODS

Tomasz LUS

Polish Naval Academy, Institute of Ship Construction and Maintenance
ul. Śmidowicza 69, 81-103 Gdynia, t.lus@amw.gdynia.pl

Summary

Vibration and acoustic signals generated by turbochargers need different signal processing methods to be effective and faultless in turbochargers diagnostics. Diagnostic methods which based on vibration and acoustic signals analysis are sensitive on engine load and speed changes. Methods presented in this paper based on vibration and acoustic signals processing in time and frequency domain. Using this methods checking technical condition of the turbochargers and its rotors and bearings without stopping the engine and dismantling it is possible.

Keywords: Marine diesel engine, turbocharger, diagnostics, vibration.

METODY DIAGNOZOWANIA TURBOSPREŻAREK SILNIKÓW OKRĘTOWYCH

Streszczenie

Sygnaly drganiowe i akustyczne generowane przez turbosprężarki wymagają stosowania różnych metod obróbki, aby być efektywnymi i niezawodnymi w ich diagnozowaniu. Metody diagnostyczne bazujące na sygnałach drganiowych i akustycznych są wrażliwe na zmiany prędkości obrotowej i obciążenia silnika. Metody przedstawione w referacie bazują na przetwarzaniu sygnałów akustycznych i drganiowych w dziedzinie czasu i częstotliwości. Używając tych metod sprawdzanie stanu technicznego turbosprężarek, ich wirników i łożysk bez zatrzymywania i demontażu silnika jest możliwe.

Słowa kluczowe: okrętowe silniki spalinowe, turbosprężarka, diagnozowanie, drgania.

INTRODUCTION

Most of marine diesel engines are turbocharged. Turbochargers also caused significant number of engine malfunctions especially when engine is fueled by heavy fuel oil. Conventional maintenance methods for engine turbochargers depend on bearings clearances checks between rotor shaft and bearing housing. Some parts of the turbocharger have to be checked on the special stands. Heavy fuel oil not burnt to the end and severe engine working conditions (long time idling) led to several typical turbocharger malfunctions and damages of it in some cases.

Typical vibro-acoustic diagnostic methods base on the analysis of acoustic and vibration signals amplitude in time or frequency domain [1,6]. It is known that engine load and speed changes disturb observed turbocharger parameters. Acoustic signal analysis method presented in this paper based on sound intensity level analysis and is rather not convenient for turbocharger diagnostic in real operation conditions because of other sound sources and sound reflection effects presence in small engine room compartments.

Much more convenient and popular diagnostic methods for turbochargers are methods connected with vibration signals amplitude analysis in time and frequency domain[5]. Results of some tests carried out on engine stands in Polish Naval Academy

laboratory using these methods are presented in this paper.

1. OBJECTS OF INVESTIGATIONS –THE WSK–HOLSET 4MD TURBOCHARGER AND NAPIER C–045/C TURBOCHARGER

The basic aim of investigations were attempt to achieve acoustic and vibration characteristic of the high-speed marine diesel engines and its turbochargers and check which signal (acoustic or vibration) and which signal processing method could be better to use for turbocharger on-line diagnostic systems [2,4,5].

There were two objects of investigations. The first object of investigation was high-speed marine diesel engine WOLA type 57HGAA (Engine no. 1) with its turbocharging system. The second was SULZER engine type 6AL20/24 (Engine no. 2) with its turbocharger both installed in Polish Naval Academy laboratory in Gdynia-Oksywie.

The main data of these engines and turbochargers are presented in the table no. 1. Measuring systems configuration and places where acoustic and vibration sensors were installed are shown on figures number 1, number 2 and number 3.

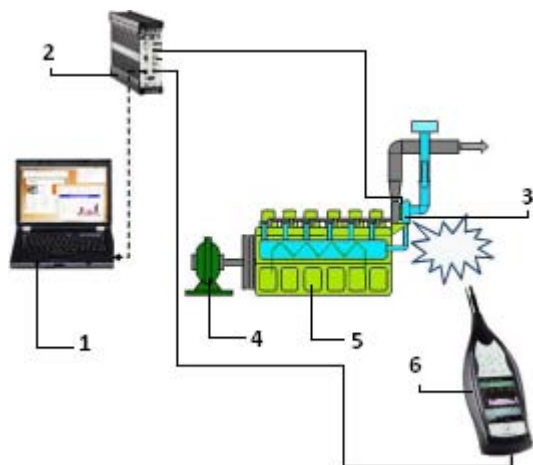


Fig. 1. Acoustic and vibration parameters measuring system configuration on stands of WOLA 57H6Aa and SULZER 6AL20/24 type high-speed diesel engines
 1 – laptop, 2 - Brüel & Kjær PULSE system, 3 – turbocharger, 4 – hydraulic brake, 5 – diesel engine, 6 - Brüel & Kjær 2250 analyser

Both tested engines were high-speed, 4-stroke marine diesel engine types with six-cylinder in line, turbocharged with direct fuel injection. WOLA engine could be loaded by two hydraulic brakes HWZ-3 type up to 254 kW at 1500 rpm and SULZER engine could be loaded by one Froude' DPY6D type hydraulic brake up to 420 kW at 750 rpm. During the tests WOLA engine was loaded up to 155 kW at 1500 rpm. SULZER engine was loaded up to 420 kW and 750 rpm.

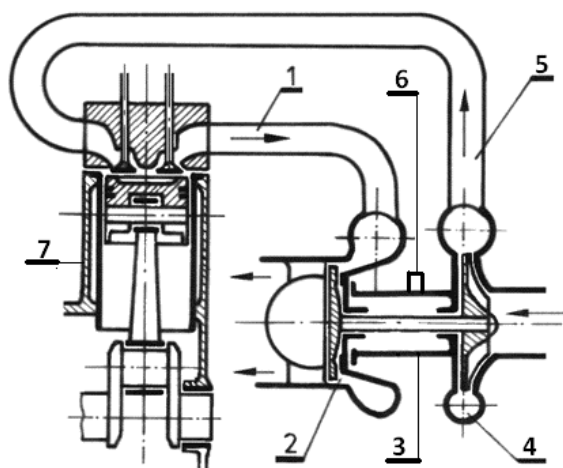


Fig. 2. Turbocharged diesel engine sketch with vibration sensor place
 1 – engine exhaust canal, 2 – turbine, 3 – turbocharger bearing housing, 4 – compressor, 5 – engine intake duct, 6 – vibration sensor, 7 – diesel engine

Tab. 1. Basic data of the high-speed diesel engines type WOLA 57H6Aa and SULZER 6AL20/24

Engine type	WOLA Henschel 57H6Aa	SULZER 6AL20/24
Turbocharger type	WSK–Holset 4MD	Napier C–045/C
No. of cylinders / Configuration	$i=6 / ,, L''$	$i=6 / ,, L''$
Nominal output at 1500 rpm/750 rpm	$P_n = 155 \text{ kW}$	$P_n = 420 \text{ kW}$
Cylinder bore	$D = 135 \text{ mm}$	$D = 200 \text{ mm}$
Piston stroke	$S = 155 \text{ mm}$	$S = 240 \text{ mm}$
Compression ratio	$\epsilon = 14,0$	$\epsilon = 12,7$
Total displacement volume	$V_{ss} = 13,3 \text{ dm}^3$	$V_{ss} = 45,2 \text{ dm}^3$
Mean piston speed	$c_{sr} = 8,26 \text{ m/s}$	$c_{sr} = 6 \text{ m/s}$
Firing order	1-5-3-6-2-4	1-4-2-6-3-5
Effective specific fuel consumption	$g_e = 231 \text{ g/kWh}$	$g_e = 212 \text{ g/kWh}$
Number of valves per cylinder	$z = 4$	$z = 4$
Fuel injection pressure	$p_w = 19,4 \text{ MPa}$	$p_w = 24,5 \text{ MPa}$

Measuring system and vibro-acoustic apparatuses based on Brüel & Kjær PULSE system and 2250 analyzer [3]. The 1/2" B&K microphone type 4189 was used together with 3185D vibration sensor. Parallel to B&K measuring system SVAN 946A vibration analyzer was used as a second set of equipment to verify if such not very expensive system could be also used in every day diesel engine diagnostics (but only in vibration signals analyzing).



Fig. 3. Napier C-045/C type turbocharger with vibration sensor mounted on the bearing housing and 2250 B&K analyzer

2. RESULTS OF ACOUSTIC INVESTIGATIONS

Brüel & Kjær PULSE system with 2250 analyzer and microphone type 4189 was used for acoustic measurements. Microphone on tripod was located in 1 meter distance from turbocharger and on the same level as the turbocharger was. Position of the microphone was parallel and perpendicular to turbocharger rotor.

Measurements were made for both engines and with whole engines load and turbochargers speed ranges. Some non-destructive malfunctions were simulated on turbochargers to check if it is possible to assess some kinds of malfunctions on the changes in acoustic parameters values.

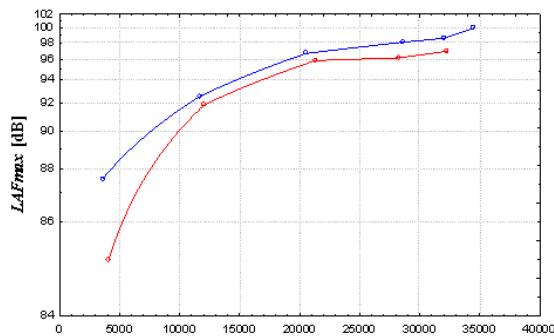


Fig. 4. Sound intensity level versus turbocharger rpm in two different technical conditions – engine no. 1 – blue (lower) – turbocharger in proper technical condition, - red (upper) – air filter and silencer removed from the turbocharger

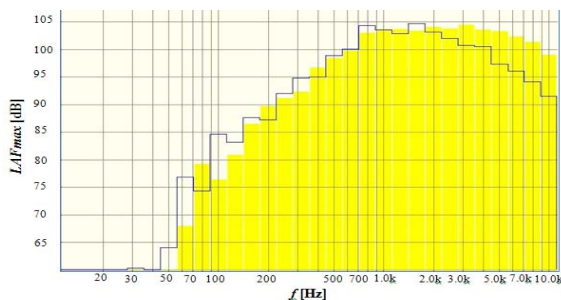


Fig. 5. Acoustic spectrum of turbocharger in octave mode for two different technical conditions – engine no. 1
 yellow – spectrum after air filter and silencer removed from the turbocharger

In the fig. 4 and fig. 6 two sound intensity levels of engine no. 1 and engine no. 2 turbochargers versus turbocharger speed in two different technical conditions are shown. Blue (lower) line shows sound intensity level L_{AFmax} [dB] for turbocharger in good technical conditions – without any visible malfunctions. Red (upper) line shows sound intensity level measured on turbochargers with removed air filters and silencers. The difference between two curves is not significant (taking into account that it is logarithmic scale).

Acoustic spectrum of these same two signals on both engines in octave frequency bands are

presented in the fig. 5 and fig. 7. It is seen that higher frequencies are amplified and lower frequencies are a little bit smaller because of taking off the air filter and silencer from the turbocharger. But also even using for acoustic signal processing frequency analysis it is not easy to avoid influence of other sound sources and sound reflection effects in laboratory and in engine room compartment on the ship which could strongly disturb acoustic parameters measuring process.

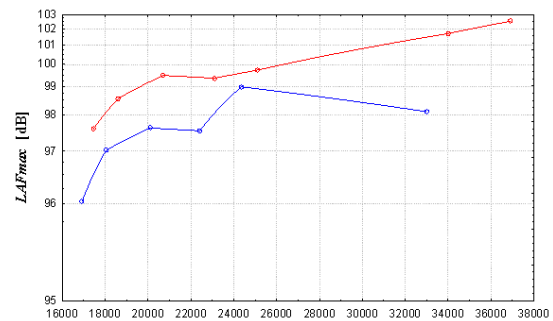


Fig. 6. Sound intensity level of turbocharger in two different technical conditions versus turbocharger rpm – engine no. 2
 – blue (lower) – turbocharger in proper technical condition, - red (upper) – air filter and silencer removed from the turbocharger

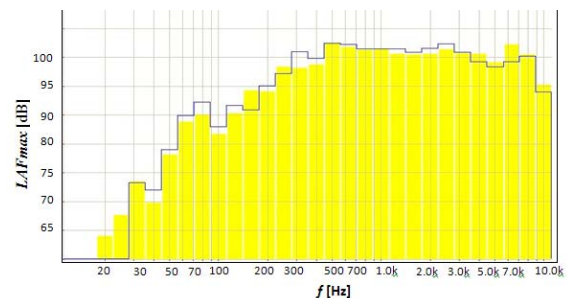


Fig. 7. Acoustic spectrum of turbocharger in octave mode for two different technical conditions – engine number 2
 yellow – spectrum after air filter and silencer removed from the turbocharger

From these reasons acoustic methods are not so popular in turbocharger diagnostics but of course they are used by (OEM) manufactures in official certification. Vibrations signals measured on housing of the turbocharger are also disturbed by engine crankshaft and pistons operation but there are reliable methods in vibration signal processing to separate these disturbances [1, 5]. Measuring the vibration signals one should have awareness how important is place and method of vibration sensor mounting on the tested machine. To present these phenomenon in the fig. 8 the acoustic signal spectrum of the turbocharger and its environment and for the same turbocharger in the fig. 9 vibration signal spectrum in frequency range from 0 kHz to 4 kHz are presented. The vibration sensor was

mounted on the turbocharger casing by magnetic holder which was the reason to cut-off higher signal frequencies over 1,5 kHz – fig.9. In examples presented in the next paragraph vibration sensors were mounted on the turbocharger casing using screw holder. Other method which could be used in ship environment without losses in signal spectrum is method with glue mounted sensors.

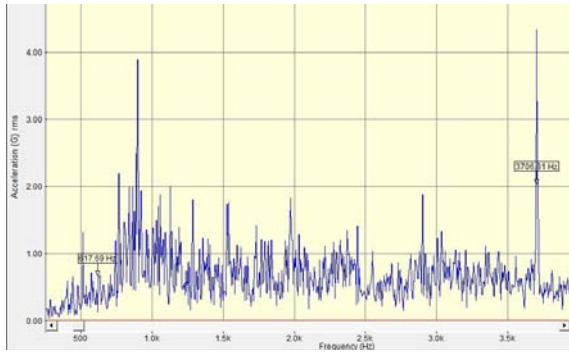


Fig.8. Acoustic signal spectrum of the turbocharger in frequency range from 0 kHz to 4 kHz – engine no. 1



Fig.9. Vibration signal spectrum of the turbocharger in frequency range from 0 kHz to 4 kHz – magnetic sensor holder – engine no. 1

According to technical specifications of turbochargers manufacturers values of the vibration level on bearing casing are the one of the most important diagnostic parameters.

3. RESULTS OF VIBRATION SIGNALS INVESTIGATIONS –THE NAPIER C–045/C TURBOCHARGER

During tests several turbochargers type Napier C-045/C were tested on the same stand in Polish Naval Academy laboratory. If it was possible Sulzer engine type 6AL20/24 was loaded up to nominal output at nominal speed 750 rpm. In situations when technical conditions of tested turbochargers were very bad and carrying tests could endanger the engine and turbocharger operation tests were stopped and turbochargers were sent to workshop for repair.

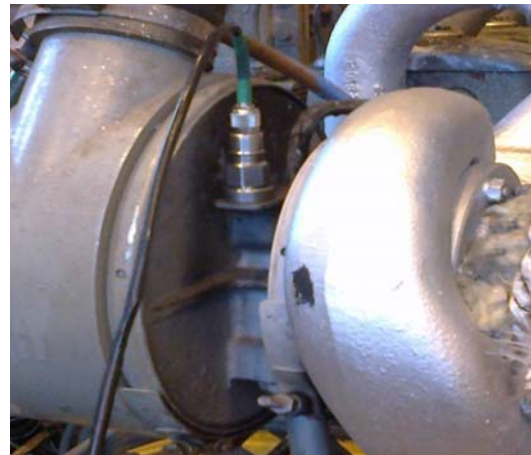


Fig. 10. WSK–Holset 4MD type turbocharger with vibration sensor mounted on the bearing housing – engine no. 1

After repairs tests were carried out again. Vibration sensor was mounted on the turbocharger bearing housing using screw bolt as it seen in figure 11. Some chosen results from these tests are presented in this paragraph on figures from number 12 to number 16. In the figure number 12 tests results of three turbochargers are presented. At the axis of abscissae the turbocharger speed in rpm and at the axis of ordinates the value of vibration acceleration amplitude of first harmonic in [g] scale are presented.



Fig. 11. Napier C–045/C type turbocharger with vibration sensor mounted on the bearing housing – engine no. 2

Vibration acceleration amplitudes of I harmonic of two turbochargers (blue and violet line) have such a value that is acceptable. Third turbocharger at first test had very high value of amplitude (red line) which enforced to stopped test and sent the turbocharger to workshop to repair. After repair third turbocharger was tested again and this time results (green line) were in acceptable by manufacturer regulations zone.

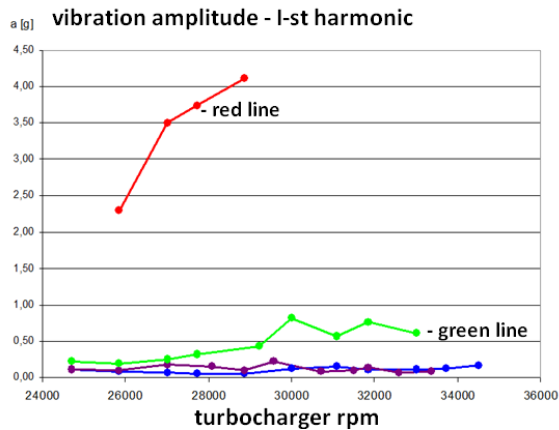


Fig. 12. Vibration acceleration amplitude of first harmonic for three turbochargers – engine no. 2 blue and violet line - turbochargers in good technical condition, red and green line – turbocharger in bad technical condition (red) and after repair (green)

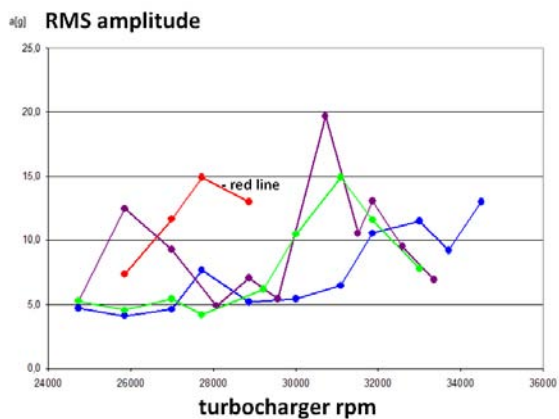


Fig. 13. RMS amplitudes for three turbochargers – engine no. 2 red line – turbocharger in bad technical condition, blue, violet and green – turbochargers in good technical conditions

Very popular measuring indicator in vibro-acoustic measurements – RMS – (Figure 13) is not such effective and clear tool for diagnostics as I-st harmonic as it is seen in figure 13. In RMS mode values of vibrations amplitudes are very similar and not such recognizable as it is for I-st harmonic mode.

In some situations for example when there is probability that compressor or turbine rotor's blades are damaged higher groups of harmonics equivalent numbers of rotors blades could be better indicators. In the figure number 14 the amplitude of 13-th harmonic vibrations (equivalent of turbine blades number) and in the figure number 15 the 15-th harmonic (equivalent of compressor blades number) are presented. As it is seen for these the same three turbochargers – three in good technical conditions and one in bad technical condition – vibration method which using blades harmonic is not effective for technical condition assessment for malfunctions

occurred in this case – unbalanced turbocharger rotor.

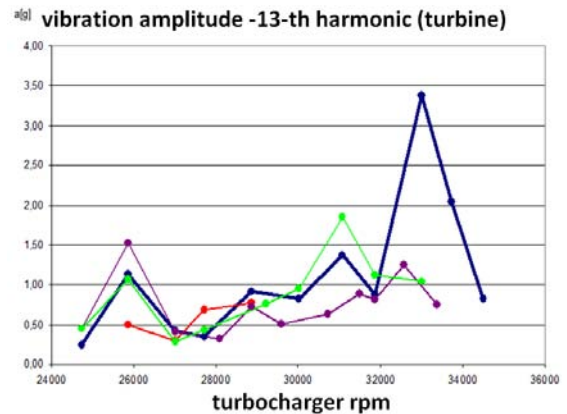


Fig. 14. Value of 13-th harmonic vibrations of accelerations amplitude equivalent of turbine blades number – engine no. 2

For such malfunction the best tool for turbocharger test is the I-st harmonic of vibrations accelerations amplitude signal measurement in whole turbocharger speed range or at list in whole engine output range.

During the research done in PNA connected with turbochargers technical conditions assessment several turbochargers were tested. In the figure no. 16 one of chosen results of these tests are presented. The I-st harmonic of vibrations acceleration amplitude for twelve turbochargers tested on the same diesel engine stand varies from less than 0,50 [g] to more than 2,5 [g]. Only turbochargers with this parameter value below 1[g] were accepted by classification societies to use on ships and in stationary power plants.

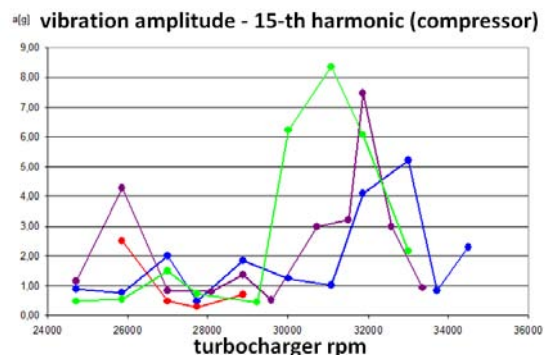


Fig. 15. Value of 15-th harmonic vibrations of accelerations amplitude equivalent of compressor blades number – engine no. 2

Much more reliable in operation are off course these turbochargers which are in lower region of acceptable vibrations amplitude zone.

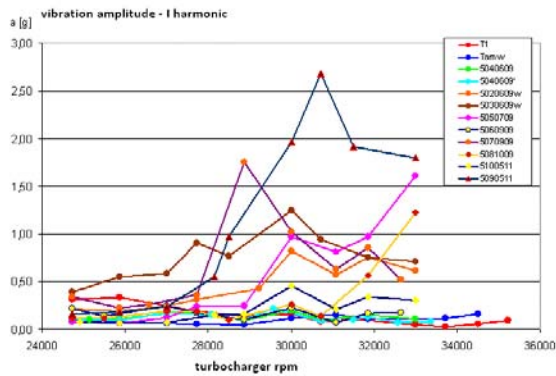


Fig. 16. Vibrations acceleration amplitude – I-th harmonic measured on turbocharger bearing casing versus turbocharger rpm – twelve turbochargers in different technical conditions tested on the same marine diesel engine stand – engine no. 2

4. CONCLUSIONS

Diesel engines technical condition assessment is a very complex process. Some of the malfunctions and troubleshooting in diesel engine installations are generated by turbochargers. There are some tools available in signal analysis which gives opportunity to trace changes in signal patterns in real time online monitoring systems. Acoustic signals processing methods which are attractive by their simplicity are not efficient in real turbocharged engines conditions assessing especially on board the ship in very narrow engine compartments. In this respect vibration signals processing methods seems to be much more effective. There are still many research works [8] to find out much more convenient diagnostic tools for rotating machinery. Presented vibration diagnostic methods gives opportunity to change the old engine maintenance philosophy connected with turbochargers maintenance process. It is possible using on-line vibration monitoring systems to go from scheduled to condition based turbochargers maintenance without fear about real operating engine conditions.

REFERENCES

[1] Batko W., Dąbrowski Z., *Nowoczesne metody badania procesów wibroakustycznych*, Wydawnictwo i Zakład Poligrafii Instytutu Technologii Eksploatacji – PIB, Radom 2006 (In Polish language).
 [2] Bengtsson M., *Condition Based Maintenance System Technology – Where is Development Heading?*, Euromaintenance 2004 – Proceedings of the 17th European Maintenance Congress, 11th – 13th of May, 2004, AMS (Spanish Maintenance Society), Barcelona, Spain, B-19.580-2004
 [3] Brüel & Kjær., *Machine Diagnostics Toolbox Industrial Solutions*, 2006.

[4] Klockars, T., Eykerman, A., Mayr, I., *Making the most of perfect maintenance timing, in detail*, Wärtsilä Technical Journal, 01.2010, pp. 57-60, Finland 2010.
 [5] Krzyworzeka P., *Wspomaganie synchroniczne w diagnozowaniu maszyn* Biblioteka Problemów Eksploatacyjnych Wydawnictwo Instytutu Technologii Eksploatacji, Radom, 2004 (In Polish language).
 [6] Kurowski W., *Podstawy diagnostyki systemów technicznych Metodologia i Metodyka* Biblioteka Problemów Eksploatacyjnych Wydawnictwo Instytutu Technologii Eksploatacji Warszawa – Płock 2008 (In Polish language).
 [7] Madej H., *Diagnozowanie uszkodzeń mechanicznych w silnikach spalinowych maskowanych przez elektroniczne urządzenia sterujące*, Wydawnictwo Naukowe Instytutu Technologii Eksploatacji – PIB, Radom 2009 (In Polish language).
 [8] Wang w., Chen J., Wu Z., *The application of a correlation dimension in large rotating machinery fault diagnosis*, Proceedings of the Institution of Mechanical Engineers, Part C: Journal of Mechanical Engineering Science IMechE, Shanghai 2000.

Kmdr dr inż. **Tomasz LUS**
 Akademia Marynarki
 Wojennej w Gdyni, Wydział
 Mechaniczno-Elektryczny,
 Instytut Budowy i Eksploatacji
 Okrętów.
 Navy Cap. Tomasz LUS,
 Mech. Eng., Ph. D.
 Polish Naval Academy in
 Gdynia, Mechanic-Electric
 Faculty, Institute of Ship
 Construction and
 Maintenance.



DYNAMIC PROGRAMMING OF FULL CONDITIONAL PROGRAM FOR DIAGNOSING

Paweł SZCZEPAŃSKI

paszczep@neostrada.pl

Summary

The approach the idea of full conditional program for diagnosing is the aim of article as well as the adaptation for his needs the dynamic programming according to Bellman's principle of optimality. This was made in reference to serial connection four electric lines.

Key words: dynamic programming, full conditional program for diagnosing.

PROGRAMOWANIE DYNAMICZNE PEŁNEGO WARUNKOWEGO PROGRAMU DIAGNOZOWANIA

Streszczenie

Celem artykułu jest przybliżenie idei pełnego warunkowego programu diagnozowania oraz adaptacji dla jego potrzeb programowania dynamicznego według zasady optymalności Bellmana. Uczyniono to w odniesieniu do szeregowego połączenia czterech przewodów elektrycznych.

Słowa kluczowe: programowanie dynamiczne, warunkowy program diagnozowania.

1. WPROWADZENIE

O prawdziwym kunszcie diagnozowania obiektu przesądza efektywne wykorzystanie wyników dostępnych sprawdzeń, których wykonanie w optymalnej kolejności gwarantuje uzyskanie pełnej i wiarygodnej diagnozy drogą poniesienia minimalnego kosztu. Można także powiedzieć, że diagnozowanie to powinno być tak zaprogramowane, aby przy jego manualnej realizacji zagwarantować wykonawcy minimalny wysiłek. Obecnie, przy masowym zastępowaniu wykonawcy komputerem, często nie dostrzega się tego aspektu (patrz metody słownikowe). Prawdopodobnie mniema się, że komputer się przecież nie męczy i może wykonać wszystkie te sprawdzenia nie zważając na jakąkolwiek ich kolejność. Niestety, bliższa analiza tego zjawiska wykazała, że często prowadzi to do znacznego spadku wiarygodności diagnozy i na dodatek – wykonania sprawdzeń w liczbie poważnie przekraczającej niezbędne minimum. - Warto zauważyć, że diagnozowanie może skończyć się przecież już po jednym sprawdzeniu. O takim stanie rzeczy decyduje jednak struktura połączeń elementów.

Sekret efektywnego wykorzystania wyników sprawdzeń tkwi w realizacji **pełnego warunkowego programu diagnozowania**. Diagnozowanie to należy do najbardziej naturalnych metod pozyskiwania wiedzy o stanie niezawodnościowym obiektu. Nie ma w nim podziału na rozpoznanie i lokalizowanie niezdatności. Nieistotne są także rozważania na temat uszkodzeń pojedynczych i wielokrotnych. Istotna jest natomiast analiza właściwości pełnego

zbioru rozróżnialnych stanów niezawodnościowych wraz z właściwościami probabilistycznymi jego poszczególnych elementów.

2. IDEA PEŁNEGO WARUNKOWEGO PROGRAMU DIAGNOZOWANIA

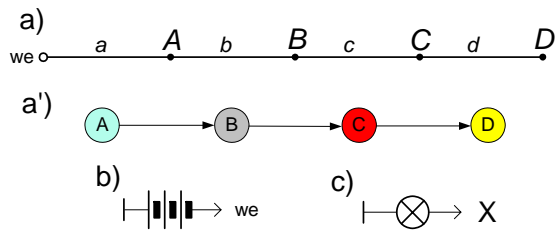
Dla realizacji **pełnego warunkowego programu diagnozowania** przyjmuje się, poza pełną wiarygodnością wyników sprawdzeń, że:

po pierwsze - element obiektu uważany jest za niezdatny jeżeli wszystkie jego sygnały wejściowe są dopuszczalne, a sygnał wyjściowy – niedopuszczalny, i

po drugie - chociażby jeden niedopuszczalny sygnał wejściowy elementu prowadzi do powstania na jego wyjściu sygnału niedopuszczalnego.

Przykładem zasadności użycia tych założeń mogą być wszystkie obiekty techniczne. Tu opracowaniu diagnostycznemu poddane zostało szeregowe połączenie czterech przewodów, którego schemat wraz z digrafem i przyrządami sprawdzeń przedstawiono na rys. 1. Punkty: *A*, *B*, *C* i *D* oznaczają nie tylko wyjścia poszczególnych przewodów, ale także i – w zależności od kontekstu - je same, sprawdzenia i koszty tych sprawdzeń. Małymi literami: *a*, *b*, *c* i *d* oznaczono prawdopodobieństwa zdatności przewodów.

Wszystkie (możliwe dla tej struktury) programy diagnozowania przedstawiono na rys. 2. Liczebność programów - równa 14 - jest czwartą liczbą **ciągu Catalana** [1]. – Dla pięciu elementów, piąta liczba tego ciągu jest równa 42, a dla sześciu – już 132.

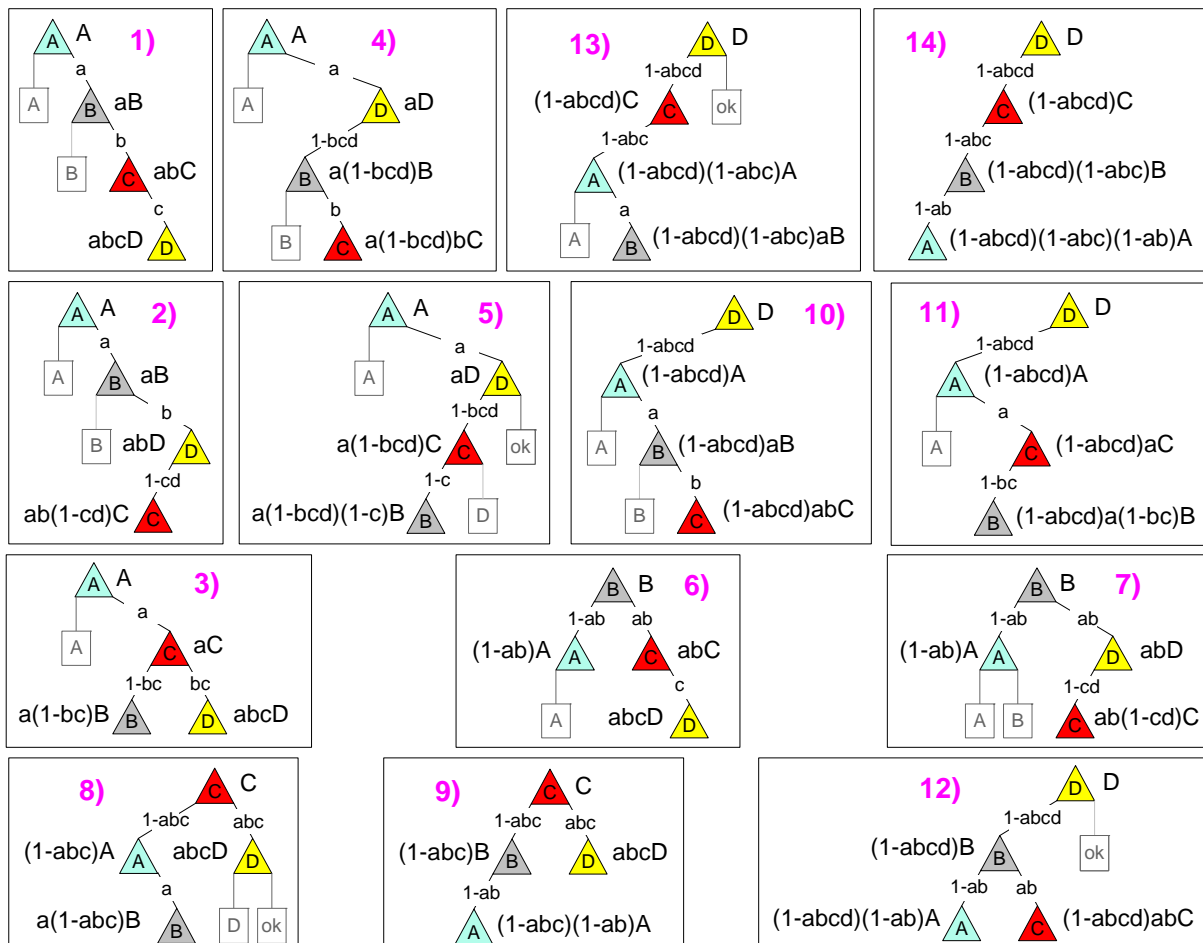


Rys. 1. Obiekt diagnozowania – szeregowe połączenie czterech przewodów (a) wraz z jego modelem (digrafem) (b) i przyrządami sprawdzeń (c, d)

Konsekwencją wykonania dowolnego sprawdzenia jest eliminacja jakiejś części obiektu z dalszych badań – elementów, które znajdują się „przed” lub „za” sprawdzeniem jeśli ma ono odpowiednio: pozytywny lub negatywny wynik. Warunkowy program diagnozowania kończy się z chwilą braku wyboru następnego sprawdzenia.

Prawdopodobieństwo pozytywnego wyniku sprawdzenia jest iloczynem prawdopodobieństw zdatności przewodów, które ono obejmuje. Każdorazowo uwzględnia się tu wspomniany efekt eliminacji. Prawdopodobieństwo negatywnego wyniku sprawdzenia jest dopełnieniem do jedności tego pierwszego. Oba te prawdopodobieństwa, tam gdzie było to istotne, zamieszczono na gałęziach wychodzących z trójkątów, z których każda prawa gałąź oznacza pozytywny, natomiast lewa – negatywny wynik danego sprawdzenia.

Choć na rys. 2, wprowadzono prostokątami diagnozy, to z uwagi na temat niniejszego artykułu, nie mają one istotnego znaczenia. Tam, gdzie należało zmniejszyć gabaryty rysunku usunięto je całkowicie lub zasłonięto je oczekiwanym kosztem pokonania danego sprawdzenia. Każdorazowo porządek diagnoz z lewej strony ku prawej nie zmienia się i jest następujący: **A, B, C, D, ok**, gdzie „ok” oznacza stan zdatności obiektu – w tym przypadku szeregowego połączenia czterech przewodów.



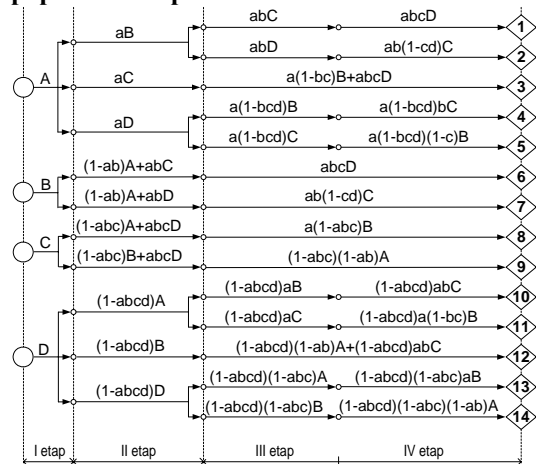
Rys. 2. Wszystkie pełne warunkowe programy diagnozowania szeregowego połączenia czterech przewodów, gdzie trójkątami i prostokątami oznaczono odpowiednio sprawdzenia i diagnozy, natomiast lewymi i prawymi gałęziami wychodzącymi z trójkątów – negatywne i pozytywne wyniki sprawdzeń; na gałęziach i obok trójkątów przedstawiono odpowiednio prawdopodobieństwa pozyskania wyników i oczekiwane koszty pokonania sprawdzeń

3. IDEA PROGRAMOWANIA DYNAMICZNEGO

Idea programowania dynamicznego, zgodnie z zasadą optymalności Bellmana [2], jest dość szeroko prezentowana w literaturze przedmiotu. Mimo swojej wiekowości, nadal cieszy się niesłabnącym zainteresowaniem. Tu w znacznym stopniu będzie ona zgodna z prekursorską pracą Tadeusza Rozwadowskiego z 1974 r. pt.: „Diagnostyka techniczna obiektów złożonych”. Zasadnicza różnica polega na wyeliminowaniu błędnego użycia metody bayesowskiej [3], polegającego na lokalizacji tylko i wyłącznie uszkodzeń pojedynczych za przyjęciem założenia o szeregowej strukturze niezawodnościowej obiektu.

Rysunek 3. przedstawia zbiorcze zestawienie oczekiwanych kosztów pokonania poszczególnych etapów diagnozowania według programów przedstawionych na rys. 2.

Oczekiwany koszt pokonania danego etapu jest równy sumie kosztów sprawdzeń na tym etapie pomnożonych przez iloczyny prawdopodobieństw pozyskania wyników poprzednich sprawdzeń.



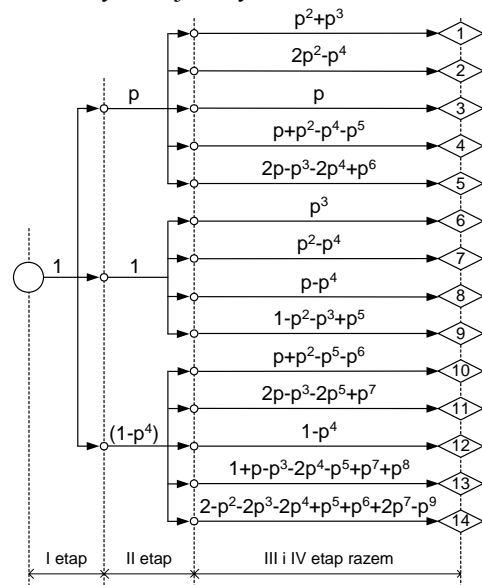
Rys. 3. Zbiorcze zestawienie właściwości poszczególnych programów diagnozowania, przedstawionych na rys. 2.

Układ rysunku jest zgodny z tradycyjną metodą przedstawiania problemu optymalizacyjnego. Lewa pionowa linia uosabia linię startu, natomiast prawa – linię mety. Między jedną, a drugą linią istnieją drogi podzielone na etapy, z których każdy charakteryzowany jest określonym kosztem pokonania. Problem znalezienia „najtańszej drogi” – zgodnie z zasadą optymalności Bellmana – rozpoczyna się od porównania kosztów ostatniego etapu.

Z uwagi na dość liczne możliwości wzajemnych relacji między kosztami sprawdzeń i prawdopodobieństwami niezdatności czterech przewodów, postanowiono, aby analizie porównawczej były poddane programy, w których wartości: A, B, C i D były jednakowe i równe 1 , a wartości: a, b, c i d – też jednakowe lecz równe p . Ponieważ nie wszystkie programy mają jednakową

liczebność etapów, tam gdzie było to niezbędne (patrz dwa pierwsze wiersze na rys. 2.) zsumowano koszty czwartego z trzecim etapem.

Po dokonanych modyfikacjach rysunek 3. przeobrażony zostaje w rysunek 4.

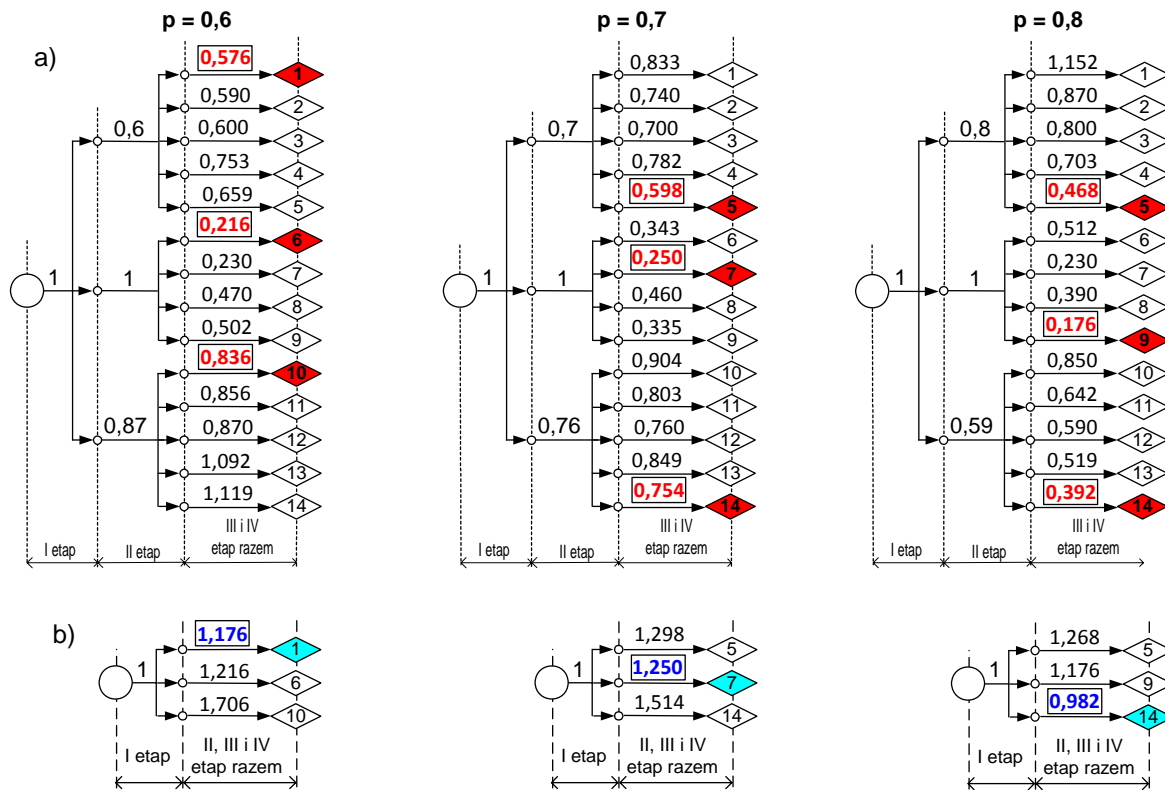


Rys. 4. Modyfikacja rys. 3. po ujednorodnieniu kosztów sprawdzeń, zrównaniu prawdopodobieństw zdatności przewodów oraz zsumowaniu kosztu III z IV etapem

Na rysunku 5.a i b przedstawiono dwustopniowe procesy wyborów najlepszych programów diagnozowania dla trzech prawdopodobieństw p o wartościach: $0,6, 0,7$ i $0,8$. Rozpoczęto od porównania sumarycznych kosztów IV z III etapem, (a), a skończono na porównaniu sumarycznych kosztów IV z III i z II etapem (b). Porównanie sum wszystkich kosztów poszczególnych etapów stało się bezzasadne, gdyż do już uzyskanych należałoby dodać wartość stałą równą 1 . Dokonana selekcja wyłoniła odpowiednio programy o numerach: $1, 7, i 14$. (patrz rys. 2.).

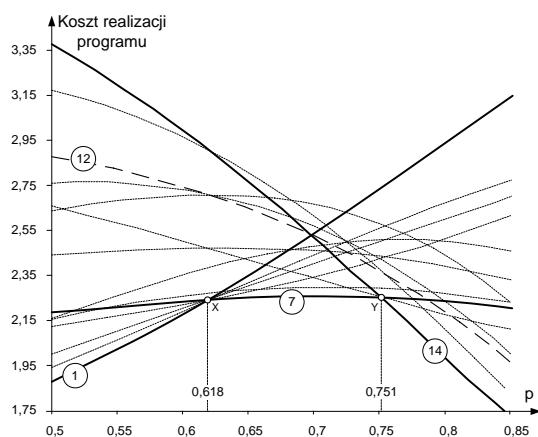
4. WNIOSKI

Przedstawiona metoda służy wyłonieniu optymalnego pełnego warunkowego programu diagnozowania. Choć wymaga ona wielu żmudnych obliczeń i porównań bez wątpienia jej ostateczny wynik zasługuje na miano pewnego. Przyjęte tu, dla jej zobrazowania, szeregowo połączenie czterech przewodów wprawdzie nie należy do w pełni reprezentatywnych to jednak uzyskane w związku z nim rezultaty mogą mieć przełożenie na obiekty o dowolnej złożoności. Przy prawdopodobieństwach zdatności elementów mniejszych od $0,618$ (punktu złotego podziału) bezwzględnie należy badać obiekt od jego elementów wejściowych ku wyjściowym. Gdy natomiast elementy charakteryzuje niezawodność bliska jedności – odwrotnie – od elementów wyjściowych ku wejściowym.



Rys. 5. Dwustopniowa selekcja: a) i b) najtańszych (optymalnych) realizacji pełnych warunkowych programów diagnostowania dla wartości prawdopodobieństw zdatności przewodów równych odpowiednio: 0,6, 0,7 i 0,8

Rys. 6. przedstawia zmienności kosztów realizacji poszczególnych programów diagnostowania. Koszt realizacji pojedynczego programu jest równy sumie kosztów realizacji jego etapów. Optymalne programy wyróżniono liniami ciągłymi pogrubionymi. Dla porównania, linią przerywaną wyróżniono program 12, zwany **programem podziału poławkowego**.



Rys. 6. Zmienności kosztów realizacji programów diagnostowania czterech szeregowo połączonych przewodów

LITERATURA

- [1] Koshy T. *Catalan Numbers with Applications*, Oxford University Press, 2008.
- [2] Bellman R. *On the Theory of Dynamic Programming*, Proceeding of the National Academy of Sciences (USA), 1952.
- [3] Szczepański P. *Erroneous use of Bayes' theorem in technical diagnostic*, Diagnostyka 57/2011, str. 47-54.



Dr inż. **Paweł Szczepański**. Absolwent Technikum Radiowego im. M. Kasprzaka w Warszawie. W latach 1976-1981 studia w WAT na Wydziale Mechatroniki. Specjalność: eksploatacja urządzeń radioelektronicznych. Rok 1990 - obrona rozprawy doktorskiej nt.: „Diagnozowanie złożonych obiektów technicznych z uszkodzeniami wielokrotnymi”. W latach 1983 – 2009 pracownik naukowo - dydaktyczny WAT. Obecnie emeryt. Dorobek naukowy obejmuje ponad 55 publikacji w tym dwa skrypty. Zrzeszony w PTDT i w PNTTE.

THE POSSIBILITY OF USING MULTIVALUED EVALUATION OF RESIDUALS IN THE DIAGNOSTICS OF MARINE DIESEL ENGINE

Kazimierz WITKOWSKI

Gdynia Maritime University, Faculty of Marine Engineering
Morska Street 83, 81-225 Gdynia, Poland, fax: +48 81 6210211, e-mail: wika@am.gdynia.pl

Summary

This paper describes the possibility and the advisability of using multivalued evaluation of residuals in marine diesel engine diagnostics. All considerations relate to triple-valued evaluation (-1; 0; +1) based on two examples of FIS (Fault Isolation System). The first one refers to a diagnostic matrix of a turbocharging system, the second one refers to a matrix of on the injection system. FIS examples are based on the results of research conducted a real object – a Sulzer's four-stroke, medium speed marine diesel engine.

Keywords: diagnostics, marine diesel engine, diagnostic matrix, multivalued evaluation of residuals.

MOŻLIWOŚĆ WYKORZYSTANIA W DIAGNOSTYCE OKRĘTOWYCH SILNIKÓW WYSOKOPRĘŻNYCH WIELOWARTOŚCIOWEJ OCENY RESIDUÓW

Streszczenie

W referacie przedstawiono możliwość i celowość wykorzystywania w diagnostyce okrętowych silników wysokoprężnych wielowartościowej oceny residuów. Rozważania odniesiono do trójwartościowej ich oceny (-1, 0, +1) w oparciu o dwa przykłady FIS (Fault Isolation System). Pierwszy dotyczy macierzy diagnostycznej turbosprężarkowego układu doładowania, a drugi macierzy dla układu wtryskowego. Przykłady FIS powstały w oparciu o wyniki badań obiektu rzeczywistego – czterosuwowego, średnioobrotowego wysokoprężnego silnika okrętowego firmy Sulzer.

Słowa kluczowe: diagnostyka, silnik okrętowy, macierze diagnostyczne, wielowartościowa ocena residuów.

1. INTRODUCTION

Modern marine diesel engines are characterized by a complex and complicated construction and high levels of thermal and mechanical loads. Overlap is also specific working conditions, the impact of aggressive of combustion of heavy fuel oil (residual) and a number of other factors, which together can lead to a number of faults. Although the engine continues to perform its basic function working, that are serviceable, but no worse after the failure of technical-operational property. If the faults is not diagnosed in time, it can lead to failure to discontinue operation of the vessel, which together lead to serious economic depreciation.

Implementation of the diagnosis to operation of marine engines give a chance for early detection of possible a and effectively avoid serious and costly consequences of failure.

The success and widespread use of diagnostics systems and devices for marine engines depends to a large extent on the perfection of diagnostic algorithms.

High efficiency is characterized primarily based on the diagnosis of parametric algorithms built on actual experimental research.

Creating algorithms and diagnostic programs should seek to obtain a good distinguishability of faults, which ensures and clarity of diagnosis.

2. CREATE DIAGNOSTIC SYSTEM

The diagnostic system a very important stage of our work is to understand the relationship between respective faults and the values of diagnostic signals.

This information may be come from modeling studies. There are analytical models, neural and fuzzy [3]. They are also used to actual experimental research. They can carry out the passive or active experiment. Passive experiment is time consuming, because very often you use the active experiment. Individual faults are then simulated as faithfully as possible. The course of active experiment can be significantly reduced by selecting the diagnosis of major motor functional nodes, and they often resulting faults. For this purpose, use of statistical data and knowledge from experts, talking about the frequency of occurrence of faults and linking a particular fault disability with a potential threat to the correct operation of the engine.

So this is an action to decompose the object and diagnosis in decentralized structures. Correctness

and effectiveness of such actions was confirmed in the work of many authors, including [1, 2].

On the significant advantages of a decentralized approach to solve the diagnostic complex technical object is the possibility of the occurrence of an assumption of single failure in particular systems object. The simplifies considerably the diagnosis algorithm, and the stage of collecting data obtained through active experiment, significantly shortens the course of the experiment and its costs.

Made actively experiment with simulated faults allows you to built a diagnostic matrix and then the algorithm and diagnostic program.

3. RESEARCH

Test object was a ship's diesel engine SULZER AL25/30 (Fig.1) the following basic specification:

- power of a cylinder [kW] 136,
- number of cylinder [-] 3,
- rotational speed [r/min] 750,
- mean effective pressure [MPa] 1,575,
- compression ratio [-] 13,
- specific fuel consumption [g/kWh] 204,
- turbocharged – turbocharger BBC VTR160N,
- load an electrical generator.

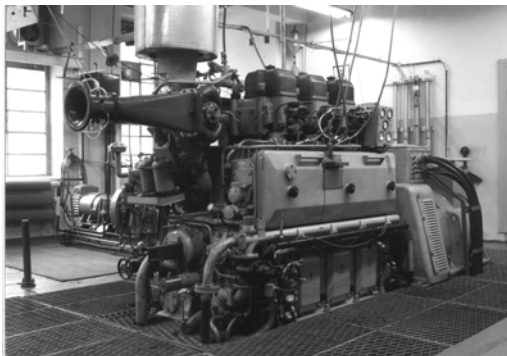


Fig. 1. Test object – diesel engine SULZER A25/30

The marine diesel engine is technically complex object. Therefore, in accordance with previous considerations must be made of its decomposition. To avoid an arbitrary division, adopted the following procedure. Collected statistics data on the frequency of specific faults and data on their potential negative impact on the process of working. This allowed the diagnosis to select appropriate motor functional nodes and in them the most common faults [4, 5].

Eventually selected for the diagnosis of components are: turbocharging system and engine fuel injection system.

To their diagnosis, select the appropriate set of diagnostic parameters according to the following basic criteria:

- information value, the amount of information about technical condition of the object, witch contains a parameter.

- accuracy of location of fault and therefore the closest possible relationship with one specific structure parameter,
- availability and ease of measurements of parameter.

The selection of suitable components and fir each of them the right set of diagnostic parameters allowed testing marine diesel engine, based on the active experiment.

Simulations were performed, with big accuracy obtain a faithful reproduction of the actual faults occurring during the life of the engine [6].

Our results indicated helped minimize the multiplicity of diagnostic parameters based on:

- calculated sensitivity of each of them to change the engine condition,
- statistical analysis of measurements results.

The concept of sensitivity defines the following relationship:

$$K = \frac{\Delta_D}{\Delta_C} \quad (1)$$

where:

- K – sensitive diagnostic parameter,
- Δ_D – relative deviation of the diagnostic parameter,
- Δ_C – relative deviation of the stricture parameter,
- relative deviation of the diagnostic parameter Δ_D :

$$\Delta_D = \frac{\Delta D}{D} \quad (2)$$

where:

- ΔD – deviation of the diagnostics parameter for the unserviceable engine,
- D – diagnostic parameter value for technically serviceable engine,
- relative deviation of the stricture parameter Δ_C :

$$\Delta_C = \frac{\Delta C}{C} \quad (3)$$

where:

- ΔC – deviation of the stricture parameter at a given fault,
- C – structure parameter value for technically serviceable engine.

Ultimately to the turbocharger system diagnosis selected the following parameters:

- air pressure charging p_d ,
- air mass flow trough the compressor \dot{m}_s ,
- pressure drop over the filter Δp_f ,
- rotational speed of the turbocharger n_{TS} ,
- exhaust gas temperature T_g ,

and for the diagnosis of fuel injection system:

- maximum cylinder pressure p_{max} ,
- maximum injection pressure $p_{max inj.}$,
- mean indicated pressure p_i ,
- air pressure charging p_d ,
- exhaust gas temperature T_g .

Based on the obtained experimental data was possible to build a Fault Diagnostic System (FIS), examples of which are shown in figure 2 and 3.

S/F	f ₁	f ₂	f ₃	f ₄
s ₁	0	+1	+1	+1
s ₂	0	-1	+1	-1
s ₃	-1	-1	+1	-1
s ₄	-1	-1	+1	-1
s ₅	0	-1	-1	+1

Fig.2. FIS injection system marine diesel engine

s₁ – air pressure charging,
 s₂ – exhaust gas temperature of the cylinder,
 s₃ – maximum cylinder pressure,
 s₄ – mean indicated pressure,
 s₅ – maximum injection pressure,
 f₁ – drop injector opening pressure,
 f₂ – non-leakproof injection pump (precise pair),
 f₃ – wear the spray holes,
 f₄ – carbonization the spray holes (plugging spray holes).

FIS describes the relationship between fault and diagnostic signals and an adaptation of the information system for fault location purposes. Adaption of trivalent residuals assessment of the facilitate distinguish all faults. But we can not authoritatively say that the diagnosis had to extend for a further faults (previously unrecognized), leaving the overall number of diagnostic signals (s), whether this fault could be identified.

Then would increase the set of diagnostic signals, by applying to them the right choice of criteria which were mentioned earlier.

4. SUMMARY

For the technically complex objects, objects decomposition and decentralized diagnosis, assuming a single fault, enables good location of fault.

Making the right choice of diagnostics parameters is one of the most important factors determining the proper operation of the diagnostic algorithm prepared.

For the technically complex objects, a possible large number of diagnostic parameters is also important to minimize the number of diagnostic parameters, as done for diagnostic algorithm was relatively simple but well-recognized faults.

The above-mentioned objectives can be achieved by introducing the concept of diagnostic sensitivity parameter. Greatly facilitates this, making

the selection of diagnostic parameters appropriate decisions. Unfortunately, sometimes difficulty to access and measure the diagnostic parameter may be the reason for withdrawal from using in diagnostic algorithm of good, sensitive diagnostically parameter.

S/F	f ₁	f ₂	f ₃
s ₁	-1	-1	+1
s ₂	+1	-1	-1
s ₃	-1	-1	-1
s ₄	-1	-1	-1
s ₅	+1	0	0
s ₆	+1	+1	+1

Fig.3. FIS turbocharger system marine diesel engine

s₁ – air pressure charging,
 s₂ – rotational speed of the turbocharger,
 s₃ – air mass flow through the compressor,
 s₄ – air mass flow through the cylinder,
 s₅ – pressure drop over the filter,
 s₆ – exhaust gas temperature of the cylinder,
 f₁ – pollution of the air filter,
 f₂ – pollution of the air compressor,
 f₃ – pollution of the air cooler.

REFERENCES

- [1] Kościelny J. M. *Diagnostics of Processes in Decentralized Structures*. Archives of Control Sciences, 1998, Vol, 7, No3/4, pp.181-202.
- [2] Kościelny J. M. *Diagnostyka procesów w strukturach zdecentralizowanych*. DPP'2001, Łągow, 2001r., s.355-358.
- [3] Kościelny J. M. *Bezwarunkowa i warunkowa rozróżnialność uszkodzeń przy wielowartościowej ocenie residuów*, VI Konferencja Naukowo-Techniczna, DPP, Władysławowo, 2003 r., s.55-60.
- [4] Witkowski K. *Komputerowa metoda diagnozowania silnika okrętowego z wykorzystaniem teorii rozpoznawania obrazów*, IV Konferencja Naukowo-Techniczna, DPP, Kazimierz, 1999r., s. 249-252.
- [5] Witkowski K. *Wykorzystanie komputerowego programu diagnostycznego do racjonalnego planowania bieżących prac remontowych na*

- przykładzie silnika okrętowego*, IV Konferencja Naukowo-Techniczna, DPP, Łągów Lubuski, 2001 r., 483-486.
- [6] Witkowski K. *Wybór i minimalizacja liczby parametrów diagnostycznych złożonych obiektów technicznych*, VI Konferencja Naukowo-Techniczna, DPP, Władysławowo, 2003 r., s. 85-88.



Kazimierz WITKOWSKI, Ph.D, graduated from Gdynia Maritime Academy, Faculty of Marine Engineering. His research interests include exploitation and diagnostics marine diesel engine.

APPLICATION OF NUMERICAL ANALYSIS IN DYNAMIC STATE DIAGNOSIS OF THE MACHINE WITH A SHOCK CHARACTER OF OPERATION

Janusz ZACHWIEJA

University of Technology and Life Sciences in Bydgoszcz, Faculty of Mechanical Engineering, Bydgoszcz

Summary

Numerical analysis is a basic tool for the engineer. Over the years many methods have been developed which turned out to be more or less universal in applications. In the approach to the problem of machine vibration damping based on the machine model, many approximate calculation methods must be used or combined so as to benefit from their advantages and eliminate possible weak points. The hybrid method, developed as a combination of a deformable finite elements method and the dynamics of multi-link systems, was used in the study as one of the tools for vibrating screen's dynamic state diagnostic. The exemplary application of numerical modelling to the issue of multidirectional optimization of an effective machine vibration isolation at the design stage is presented.

Keywords: numerical methods, diagnostics, resonance frequency, structure vibrations, vibration isolation

ANALIZA NUMERYCZNA W DIAGNOZOWANIU STANU DYNAMICZNEGO MASZYN O UDAROWYM CHARAKTERZE PRACY

Streszczenie

Analiza numeryczna stanowi podstawowe narzędzie inżyniera. Na przestrzeni lat powstało wiele metod, które okazały się w zastosowaniach mniej lub bardziej uniwersalne. Podejście do zagadnienie tłumienia drgań maszyny w oparciu o jej model wymaga stosowania wielu metod obliczeń przybliżonych lub ich łączenia w sposób umożliwiający wykorzystanie zalet każdej z nich oraz wyeliminowanie ewentualnych wad. Metoda hybrydowa powstała z połączenia metody odkształcalnych elementów skończonych i dynamiki układów wieloczłonowych została wykorzystana w pracy jako jedno z narzędzi diagnozowania stanu dynamicznego przesiewacza wibracyjnego. Pokazany został przykład zastosowania modelowania numerycznego do zagadnienie wielokierunkowej optymalizacji przy opracowaniu skutecznej wibroizolacji maszyny.

Słowa kluczowe: model numeryczny, diagnozowanie, częstotliwość rezonansowa, drgania konstrukcji, wibroizolacja

1. INTRODUCTION

In case of a machine with the impact type of operation, the diagnostics of dynamic state is much more difficult than a similar analysis for equipment and devices in which vibrations occur as the undesirable factor associated with their operation. In case of facilities like mills, sieves and shaker conveyors, vibrations of working elements constitute a principle of their operation [1, 2].

A shaking sieve consists of a working part which vibrates with a speed as high as $100 \text{ mm}\cdot\text{s}^{-1}$; the travel is even of several millimetres, and the supporting structure is permanently fixed to the foundation. Therefore, the vibrations of this part of machine structure should be as low as possible. Thus, we are facing a situation in which one of machine elements vibrates and these vibrations cannot be avoided by eliminating their origin [3].

High positive forces acting on the working elements are favourable for the examination of their resonance characteristics. On the other hand, if the dynamic state of the machine is incorrect, possible structural changes must be implemented with great

caution; otherwise they may cause dangerous effects to the surroundings [4, 5].

2. VIBRATION CHARACTER EXAMINATION FOR VIBRATING SCREEN

The sieve, which is the main part of the screen, has a mass of several tonnes and the instantaneous value of its absolute acceleration reaches $30\text{-}40 \text{ m}\cdot\text{s}^{-2}$. In such circumstances the force applied by such mass to the supporting structure exceeds the value of 100 kN.

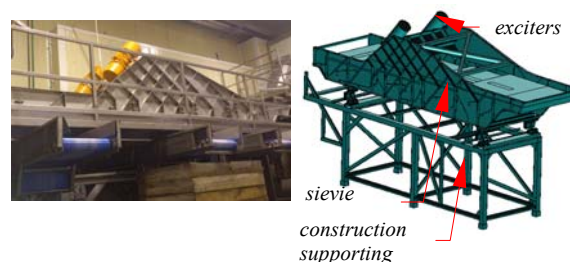


Fig. 1. ROSTA vibrating screen produced: a) general view, b) structural diagram

In case of screens the sieve vibration frequency is particularly important. This frequency may reach the value between ten and twenty Hz, significantly higher than for mills or eccentric hammers with a large mass of the connecting rod/beater system. The inertial force resulting from the sieve acceleration and mass transfers to the sieve supporting structure. With properly selected vibration isolators the forces transferred to supports are less than the positive input value, nevertheless they can also reach a significant level. This leads to the formation of cracks and breaks in the sieve supporting structure and causes subsidence of foundations. Both the foundation and the sieve supporting structure resting on it should be properly designed to ensure sufficient strength of elements and, moreover, they should be feature vibration-damping properties.

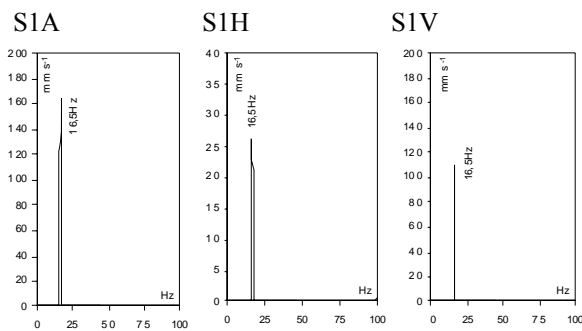


Fig. 2. Amplitude-frequency curves for the vibration speed of the sieve in the following directions: longitudinal (A), transversal (B), and vertical (C) with respect to the machine axis

The amplitude-frequency curves for vibration speed of the front part of the sieve in the direction of the raw material movement are presented on the graphs (Fig. 2).

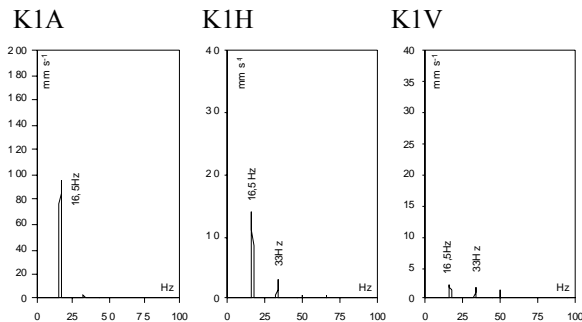


Fig. 3. Amplitude-frequency curves for the vibration speed of the screen structure in the following directions: longitudinal (A), transversal (B), and vertical (C) with respect to the machine axis

The vibration speed amplitude in the direction of the screen axis reaches the value of $100 \text{ mm}\cdot\text{s}^{-1}$. In the direction perpendicular to the sieve axis the vibration speeds are also high, reaching the level of $15 \text{ mm}\cdot\text{s}^{-1}$ in the front part and up to $20 \text{ mm}\cdot\text{s}^{-1}$ in the rear part. Much smaller values for vibration speed amplitude were measured in the vertical direction. This is

understandable, because the structure shows the least deformation in this direction.

The highest sieve vibration speeds are to be found in the direction perpendicular to its axis ($\sim 160 \text{ mm}\cdot\text{s}^{-1}$), however vibration speed amplitudes in the vertical direction reach similar values. This results from the design of vibration isolators used in the vibrating screen.

The resonance frequencies were determined using the short-time Fourier transformation of the vibration speed vs. time curves determined during machine coasting. The measurements were taken in three directions, in the points situated in the front and rear part of the sieve.

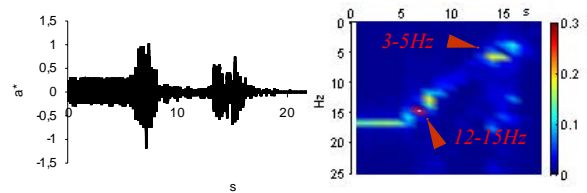


Fig. 4. Time waveforms and short-time Fourier transform of the acceleration of structural vibrations during sieve coasting

The shape of the transform presented in Fig. 4 suggests unfavourable distribution of frequency ranges in which free vibrations of the structure are excited. Free vibrations occur within the range of 3-5 Hz and 12-15 Hz. While the lower frequency vibrations unfavourably affect the structure life during machine start-up and coasting phases, the higher frequency range is located near the shaker excitation frequency.

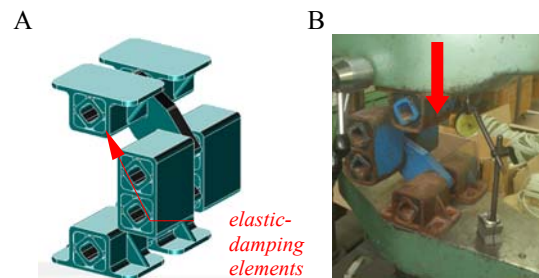


Fig. 5. Design of ROSTA vibration isolator (A) and its static characteristic curve determination method (B)

The sieve part of the vibrating screen rests on the vibration isolators manufactured by Spanish ROSTA (Fig. 5). They are isolators with plastic inserts used as the elastic-damping elements. Their design allows deflection in both vertical and horizontal directions.

Table 1. Features of the vibration isolator type AB 50 TWIN

Load [N]	Free vibrations frequency [Hz]	Horizontal rigidity [N mm ⁻¹]	Vertical rigidity [N mm ⁻¹]
5,000 – 12,000	2.1 – 2.4	170	340

The rigidity values of this vibration isolator are shown in Table 1. The manufacturer guarantees its correct operation under the load within the range of 5.000 – 12.000 N.

A very important parameter characterizing the vibration isolator is its free vibrations frequency. This parameter should be understood as the resonant frequency of the system composed of the vibration isolator itself and the loading mass ensuring the static deflection value recommended for this type of a vibration isolator [6].

For the ratio of the excitation frequency to the free vibrations frequency the value of mistuning factor is:

$$\varepsilon = \frac{\omega}{\omega_0} = \frac{16.5 \cdot 2\pi}{2.4 \cdot 2\pi} = 6.8 > \sqrt{2} \quad (1)$$

Therefore the criterion of correct isolation is met.

In order to verify the data published by ROSTA, the characteristic curve of the vibration isolator's horizontal rigidity was determined. The determination method is shown in Fig. 5. Based on the measurement results of deformation as a function of applied force, it was possible to determine the curves presented in Fig. 6.

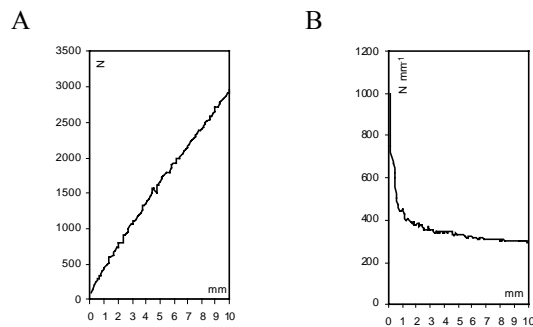


Fig. 6. Static characteristic curves for the vibration isolator: (A) force-deformation, (B) rigidity-deformation

The graph clearly shows the linear relationship between the isolator deflection and the loading force, therefore a wide range of deflection exists for which the rigidity values vary only within a narrow range of values.

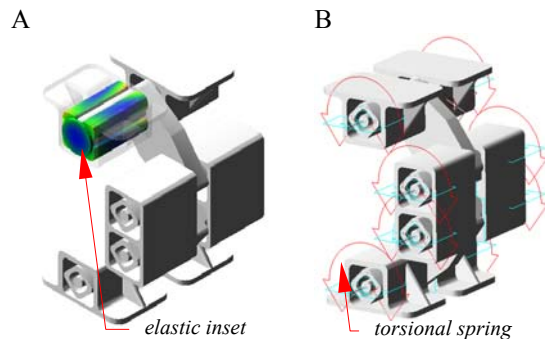


Fig. 7. Models of vibration isolator: with an elastic insert (A), and with elastic-damping elements (B)

The modelling of vibration isolator with elastic inserts made of highly deformable plastic (Fig. 7A) is a quite complicated task, because the interactions

between the insert and the surfaces of the nest are of contact nature [7]. For the purpose of correct representation of these interactions the values of parameters valid in the contact zone, first of all the rigidity, must be known. Consideration of the contact nature of interactions, even in the rigid body – deformable body system, significantly extends the duration of calculations. Therefore, for the purpose of numerical analysis the vibrating isolator model was assumed composed of rigid solids and elastic-damping elements in the form of torsion springs with the rigidity factor of 3.3 N·mm·deg⁻¹ (Fig. 7B).

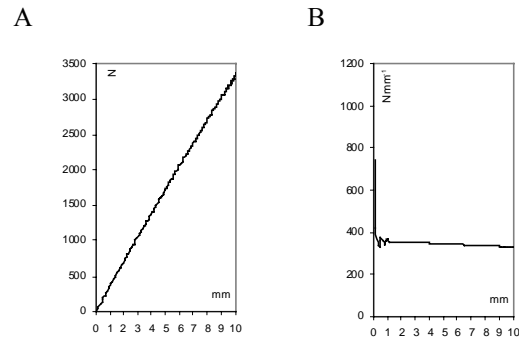


Fig. 8. Static characteristic curves for the vibration isolator: (A) -force-deformation, (B) - rigidity-deformation

The static characteristics for the vibration isolator model with assumed rigidity of springs is close to static characteristics determined for the examined isolator. It can be seen in Fig. 8(A) and, first of all, in Fig. 8(B).

In the numerical analysis the vibration isolator was statically loaded with the force of 8 750 N equal to the fraction of sieve weight acting on each of the four supporting elements. The assumed value of the dynamic load was 32 000 N, which corresponds to the shaker excitation force.

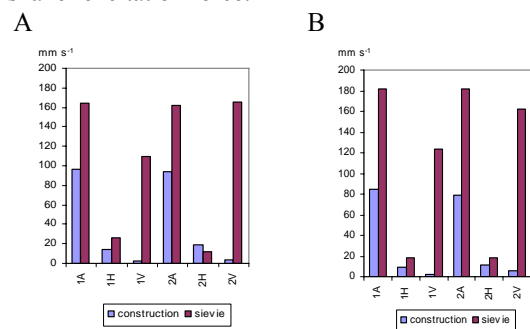


Fig. 9. Sieve and supporting structure vibration speed amplitudes: (A) for the real object, (B) for the model

The efficiency of the vibration isolator in the aspect of vibration damping can be determined based on the ratio of the sieve and the support vibration speeds. The figures 9(A) and 9(B) show respectively the amplitudes of the sieve vibration speed (brown bar) and the supporting structure (blue bar) for the vibrating sieve and its numerical representation. Based on these figures, the conclusion may be drawn

that responses of both systems on identical excitation are almost the same. This is a substantial confirmation of compliance between the dynamical features of the model and a real object. In each case, the ratio of sieve and support vibration velocity is less than one for both horizontal and vertical vibration direction.

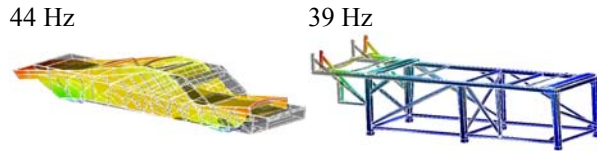


Fig. 10. First forms and free vibration frequencies for the sieve and supporting structure

In designing the model for numerical calculations, the following rules were observed:

- The sieving part of the vibrating screen constitutes a rigid structure. It can be concluded from the natural vibration frequency (Fig. 10). The free vibration frequencies of the sieve and the supporting structure do not differ dramatically because the sieve mass is much greater than the mass of the supporting structure.
- The sieve, as the rigid element, affects the screen dynamics through its inertia only.
- The sieve is connected with a compliant part, i.e. the frame, through elastic-damping elements, i.e. vibration isolators.

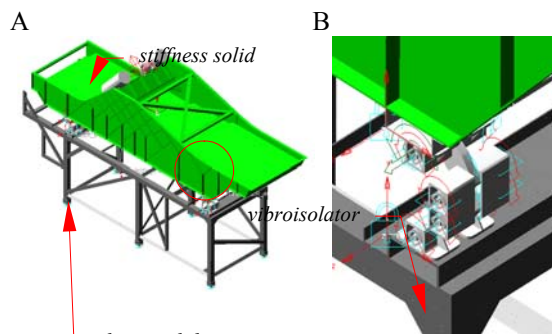


Fig. 11. The hybrid model of vibrating screen (A) and the connection of a rigid solid with a deformable solid by the elastic-damping element in the hybrid model (B)

Such an arrangement is shown in Fig. 11 and is very well suited to modelling by using the method of multi-body systems (MSD - *multibody system dynamics*) [8, 9].

The model built for the purpose of numerical analysis consists of a rigid solid corresponding to the sieve with respect to the mass and moments of inertia. The supporting structure consists of solid elements in the form of profiles divided into deformable finite elements. Such a combination of the multi-mass dynamics method with the method of deformable finite elements leads to the hybrid model having this advantage that it allows to determine system's response to excitation, along with determination of stresses, for the elements subjected to the analysis

only. Consequently, the calculation duration is much shorter. In the model of the vibrating screen the previous model of vibration isolator was used.

Fig. 12 shows two basic frequencies and corresponding forms of free vibrations of the vibrating screen. Since these frequencies are both lower than the excitation frequency, they are distinctly visible on the short-time Fourier transform (STFT). The results obtained are consistent with the results of object's examinations, during which free vibrations were found with the frequency of 3 – 5 Hz (as compared to 4.9 Hz occurring in the model) and 12 - 15 Hz (14.7 Hz in the model). The next calculated free vibration frequency is 22.2 Hz. Since it exceeds the excitation frequency by almost 6 Hz, is not visible on the vibration spectrum even with small damping occurring in the system.

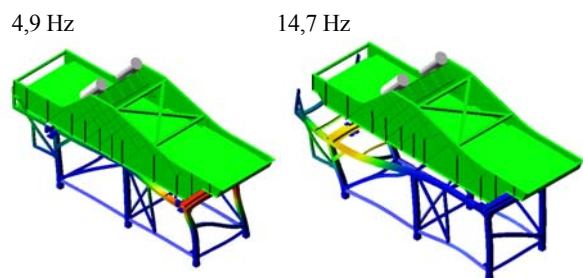


Fig. 12. Basic frequencies and corresponding forms of free vibrations of the vibrating screen

The character of system vibrations determined for the model is similar to the character of the real object's vibrations.

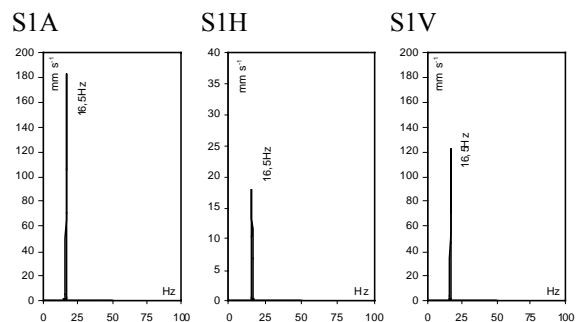


Fig. 13. Amplitude-frequency characteristics for vibration speed in the model of sieve

This conclusion can be drawn by comparing speed spectra presented in Figure 2 & 3 with amplitude-frequency characteristics shown in Figures 13 & 14.

Having the model verified, we can consider the modification of supporting structure in such a way that the vibration level is reduced while the required parameters of sieve vibration are maintained. An exemplary solution is shown in Fig. 15.

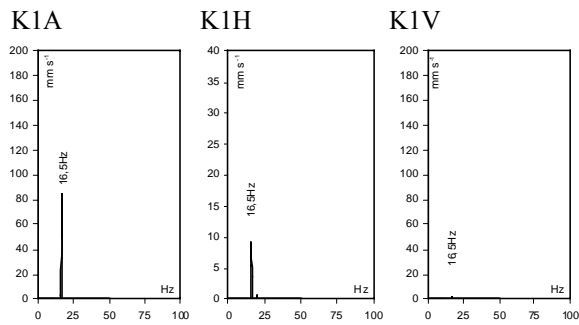


Fig. 14. Amplitude-frequency characteristics for vibration speed in the model of the vibrating screen supporting structure

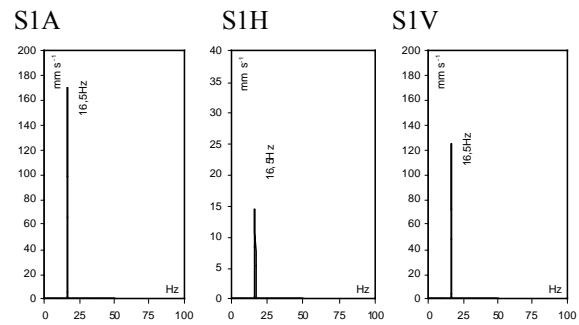


Fig. 17. Amplitude-frequency characteristics for the vibration speed of the sieve part of the vibrating screen after modification of the sieve supporting structure

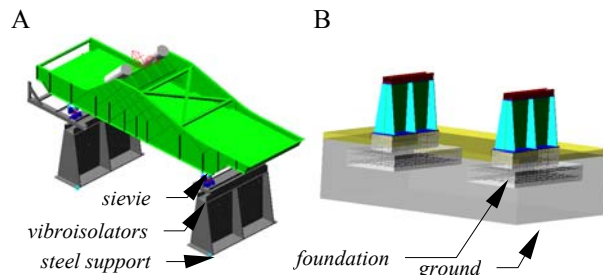


Fig. 15. The solution of sieve support in which the results of system vibrations numerical analysis are taken into account:
 A – supports and sieve, B – supports and foundation

Admittedly, in this solution the resonance frequency is lower than excitation frequency and during machine start-up and coasting the amplitude of vibrations will be high, but this effect cannot be eliminated due to the requirements specified for vibration isolators.

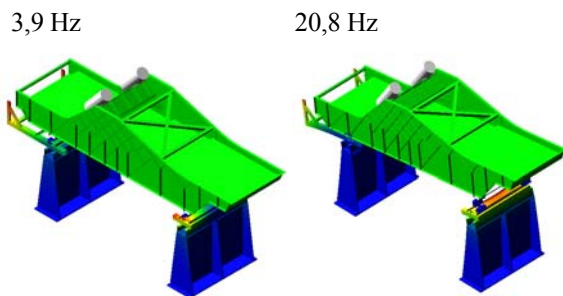


Fig. 16. Forms and the lowest frequencies of free vibrations of the vibrating screen following foundation design modification

Based on the analysis of vibration forms it can be seen that at the resonance frequency of 3.9 Hz the vibrations of the sieve will occur rather than vibrations of the supporting structure and the foundation. The next free vibrations frequency is 20.8 Hz and, being higher than the excitation frequency (16.5 Hz), it does not create a risk for the lifetime of the screen's supporting structure.

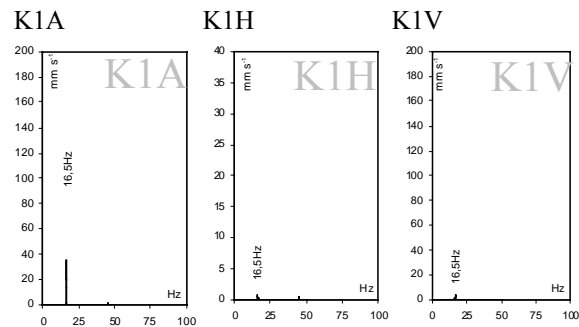


Fig. 18. Amplitude-frequency characteristics for vibration speed of modified sieve supporting structure

From the structure durability point of view, the foundation mass and strength are important. Stresses occurring in both foundation blocks and steel members of the supporting structure can be determined numerically based on the model.

Table 2. Loads exerted on the vibrating screen support

Item	Load type	Load value, N	
		total	per support
1	Vibrating screen mass	36,297	18,149
2	Shaker force, vertical	128,000	64,000
3	Shaker force, horizontal	128,000	64,000
4	Steel support mass	29,640	14,820
5	Foundation & reinforcement mass	227,920	11,3960

Table 2 presents the loads acting on the supports, i.e. sieve weight, force exerted on the sieve by shakers, support weight, and foundation weight. For these loads the values of deformations and stresses occurring in the cross-sections of the supports and the foundations, and also in the ground should be determined.

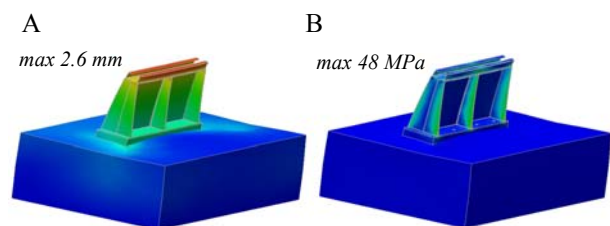


Fig. 19. The value and character of deformation of the support (A); and stress distribution in steel part and ground (B)

As it follows from calculations, the maximum deformation of the metal part of the support should not exceed the value of 2.6 mm, whereas the maximum reduced stress will occur in cross-sections of the support plate reinforcing elements and it will reach the value of 48 MPa. These results are satisfactory in the aspect of support strength. The stresses in the foundation concrete blocks are small.

3. CONCLUSIONS

It was the purpose of this study to demonstrate the usefulness of numerical methods to determination of dynamic properties of the examined system based on its numerical model. In order to obtain reliable results, the representation used for this purpose should be very close, if not identical, to the real object with respect to basic properties like mass, rigidity and damping. The most difficult issue is to make a reliable estimation of two last quantities. As it was pointed out, such an estimation is not necessary for each member of a system which was constructed as the model of the analysed machine. The examined case of two massive members, i.e. the sieve and the sieve supporting structure, joined together by elastic-damping elements is a good example of application of the hybrid method for machine dynamic state analysis. The sieve itself, with its strength properties and vibration eigenforms which are not essential for the problem, is modelled as a rigid solid. The situation is different in case of the sieve supporting structure which, similar to the foundation or ground, may not be treated as a rigid structure. The dynamic properties of such a model should be specified on the basis of real object examination results. The structure mass is usually known with sufficient accuracy. The rigidity of the system can be assumed based on the determined resonance characteristics. The most difficult problem results from the insufficient knowledge of damping in the system [10]. Such damping can be determined based on the response of the system to a specified excitation.

The problem of structure vibration damping can be approached differently than presented in this study, i.e. by using a pure experimental method. However, such a method has one obvious disadvantage, namely the suitability of a given solution can be evaluated only when the solution is fully implemented. Regrettably, it can turn out that the problem is not eliminated at all. If the concept is verified at the earlier stage based on the model, the risk associated with such "hit and hope" method is eliminated, because already the shape of amplitude-frequency characteristics of vibration speed for the model of the vibrating screen with modified supporting structure indicates that the modification of the vibrating screen mounting structure, basically consisting in making it more rigid, will cause dramatic reduction of vibrations of these machine elements which are required to ensure the smallest vibration amplitudes while maintaining high amplitudes of sieve

oscillations, necessary for correct segregation of individual fractions of the material being sieved.

REFERENCES

- [1] Chmielewski T., Zembaty Z., *Podstawy dynamiki budowli*, Arkady, Warszawa, 1998.
- [2] Borkowski W., Konopka S., Prochowski L., *Dynamika maszyn roboczych*, WNT, Warszawa, 1996.
- [3] Zachwieja J., Gołębiowska I., *Efektywność wybranych metod ochrony przeciwdrganiowej konstrukcji wsporczej separatorów*, Budownictwo Ogólne, Wydawnictwa UTP, pp. 119-126, 2009.
- [4] Zachwieja J., Gołębiowska I., *Damping building vibrations excited by surface wave propagating in the ground*. Journal of Polish CIMAC, 7(3), 2012, s. 373-381.
- [5] Praca zbiorowa, *Wspomaganie konstruowania układów redukcji drgań i hałasu*, WNT, Warszawa, 2001.
- [6] Zachwieja J., *The role of vibroisolators in damping an radial fan's vibrations*, Diagnostyka, 44, pp. 113-118, 2007.
- [7] Zachwieja J., Łyczywek T., 2011, *Wpływ niewspółosiowości wałów na charakter drgań wirnika sztywnego*, Industrial Monitor, 4(2), s. 62-69.
- [8] Praca zbiorowa, *Metoda elementów skończonych w mechanice konstrukcji*, Arkady, Warszawa, 1994.
- [9] Shabana A., *Dynamics of multibody systems*, Cambridge University Press, Edinburg, 1998.
- [10] Zachwieja J., Holka H., 2011, *The effectiveness of rigid rotor balance with resonant extortion of the system with small damping*, Journal of Polish CIMAC, 6(1), s. 211-219.



dr inż. **Janusz ZACHWIEJA** is the Assistant Professor in the Department of Applied Mechanics at the University of Technology and Life Sciences in Bydgoszcz (Poland). His scientific interests include dynamics of mechanical systems and fluid mechanics.



Wspomnienie o prof. Januszu Gardulskim

Prof. dr hab. inż.
Janusz Gardulski,
wieloletni nauczyciel
akademicki z Wydzia-
łu Transportu Polite-
chniki Śląskiej, zmarł

w Katowicach 30 sierpnia 2012 roku w wieku 70 lat. Mimo postępującej choroby niemal do końca życia starał się aktywnie uczestniczyć w życiu uczelni, z którą był związany ponad pół wieku, od ukończenia szkoły średniej (LO im. Marii Konopnickiej w Katowicach) i rozpoczęcia studiów w 1960 roku.

Janusz Gardulski urodził się 7 czerwca 1942 roku w Radomsku. W 1965 roku ukończył studia na Wydziale Mechaniczno-Energetycznym Politechniki Śląskiej (mechanika, specjalność ciepłe maszyny tłokowe) i podjął pracę na Wydziale Górniczym Politechniki Śląskiej. Stopień doktora nauk technicznych uzyskał w 1971 roku na podstawie pracy „Przyczyny hałasowania przekładni zębatych” wykonanej pod kierunkiem prof. Ludwika Müllera na Wydziale Górniczym. W 1975 przeniósł się do Instytutu Transportu i Komunikacji przekształconego później w Wydział Transportu. Był jednym z organizatorów kierunku studiów transport na Politechnice Śląskiej. Stopień doktora habilitowanego uzyskał w 1999 roku na Wydziale Samochodów i Maszyn Roboczych Politechniki Warszawskiej na podstawie monografii „Simulation studies of mechanical systems with non-linear parameters of structure for operating and construction needs”. W 2001 roku został po raz pierwszy mianowany na stanowisko profesora nadzwyczajnego. Nominację profesorską z rąk prezydenta RP otrzymał we wrześniu 2011 roku.

Pracując na stanowiskach od stażysty przez asystenta, starszego asystenta, adiunkta do profesora nadzwyczajnego, pełnił różne funkcje organizacyjne, m.in. był zastępcą dyrektora Instytutu Transportu w latach 2001–2002 i prodziekanem ds. studenckich na Wydziale Transportu w kadencji 2002–2005.

W pracy naukowej zajmował się problematyką układów napędowych, budową i eksploatacją maszyn, a zwłaszcza dynamiką i diagnostyką wibroakustyczną maszyn i pojazdów (m.in. przekładni zębatych dużych mocy, amortyzatorów i zawieszęń) oraz minimalizacją hałasu i drgań.

W dorobku naukowym i dydaktycznym prof. Gardulskiego jest ponad 120 publikacji, promotorstwo kilku doktoratów i ponad 170 dyplomów magisterskich i inżynierskich. Wykonywał kilkadziesiąt prac naukowo-badawczych, których wyniki zostały wdrożone w przemyśle, kierował projektami badawczymi wykonywanymi na zlecenie Komitetu Badań Naukowych lub Ministerstwa Nauki i Szkolnictwa Wyższego.

Znaczne są osiągnięcia Profesora w zakresie integracji środowiska naukowego w kraju. Był głównym organizatorem kilkudziesięciu ogólnopolskich konferencji naukowych na temat diagnostyki maszyn i kilkunastu konferencji na temat badań przekładni zębatych, był członkiem komitetów naukowych wielu konferencji. Duże znaczenie Profesor przykładał do rozwoju kadry młodych nauczycieli akademickich oraz kadr inżynierskich. Zainicjował i przez dekadę organizował studenckie sesje naukowe na Wydziale Transportu. Był członkiem założycielem Zespołu Diagnostyki Maszyn przy Sekcji Podstaw Eksploatacji Komitetu Budowy Maszyn Polskiej Akademii Nauk, a przez kilka kadencji członkiem zarządu Polskiego Towarzystwa Diagnostyki Technicznej oraz członkiem Komisji Transportu Oddziału Polskiej Akademii Nauk w Katowicach. Jako rzeczoznawca techniki samochodowej i ruchu drogowego PZMot wykonał ponad 1000 ekspertyz i wyszkolił wielu rzeczoznawców. Prowadził dla studentów zajęcia przede wszystkim z podstaw techniki pomiarowej, metrologii, podstaw konstrukcji maszyn i rysunku technicznego. Tworzył od podstaw bazę dydaktyczno-naukową laboratoriów metrologii, techniki pomiarowej i wibroakustyki.

Prof. Janusz Gardulski był laureatem licznych nagród za osiągnięcia dydaktyczne, organizacyjne lub naukowe, był wyróżniany odznaczeniami uczelnianymi, resortowymi i państwowymi, m.in. odznaką Zasłużonemu dla Politechniki Śląskiej, Złotym Krzyżem Zasługi, Medalem Komisji Edukacji Narodowej.

Osiągnięcia Profesora Janusza Gardulskiego w zakresie badań, kształcenia kadry naukowej i inżynierów były znaczne i doceniane przez środowisko akademickie. W pamięci współpracowników, studentów i licznie zgromadzonych na Jego pogrzebie przedstawicieli uczelni w kraju pozostaje On jako Osoba życzliwa, lubiana i powszechnie szanowana. Uroczystości pogrzebowe odbyły się 7 września 2012 r. na cmentarzu przy ul. Sienkiewicza w Katowicach.

Obszar zainteresowania czasopisma to:

- ogólna teoria diagnostyki technicznej
- eksperymentalne badania diagnostyczne procesów i obiektów technicznych;
- modele analityczne, symptomowe, symulacyjne obiektów technicznych;
- algorytmy, metody i urządzenia diagnozowania, prognozowania i genezowania stanów obiektów technicznych;
- metody detekcji, lokalizacji i identyfikacji uszkodzeń obiektów technicznych;
- sztuczna inteligencja w diagnostyce: sieci neuronowe, systemy rozmyte, algorytmy genetyczne, systemy ekspertowe;
- diagnostyka energetyczna systemów technicznych;
- diagnostyka systemów mechatronicznych i antropotechnicznych;
- diagnostyka procesów przemysłowych;
- diagnostyczne systemy utrzymania ruchu maszyn;
- ekonomiczne aspekty zastosowania diagnostyki technicznej;
- analiza i przetwarzanie sygnałów.

Wszystkie opublikowane artykuły uzyskały pozytywne recenzje wykonane przez niezależnych recenzentów.

Redaktorzy działowi:

dr hab. inż. Tomasz BARSZCZ
prof. dr hab. inż. Wojciech CHOLEWA
prof. dr hab. Wojciech MOCZULSKI
prof. dr hab. inż. Stanisław RADKOWSKI
prof. dr hab. inż. Wiesław TRAMPCZYŃSKI
prof. dr hab. inż. Tadeusz UHL

Topics discussed in the journal:

- General theory of the technical diagnostics,
- Experimental diagnostic research of processes, objects and systems,
- Analytical, symptom and simulation models of technical objects,
- Algorithms, methods and devices for diagnosing, prognosis and genesis of condition of technical objects,
- Methods for detection, localization and identification of damages of technical objects,
- Artificial intelligence in diagnostics, neural nets, fuzzy systems, genetic algorithms, expert systems,
- Power energy diagnostics of technical systems,
- Diagnostics of mechatronic and antropotechnic systems,
- Diagnostics of industrial processes,
- Diagnostic systems of machine maintenance,
- Economic aspects of technical diagnostics,
- Analysis and signal processing.

All the published papers were reviewed positively by the independent reviewers.

Kopia wszystkich artykułów opublikowanych w tym numerze dostępna jest na stronie www.diagnostyka.net.pl

Druk:

Centrum Graficzne „GRYF”, ul. Pieniężnego 13/2, 10-003 Olsztyn, tel. / fax: 89-527-24-30

Oprawa:

Zakład Poligraficzny, UWM Olsztyn, ul. Heweliusza 3, 10-724 Olsztyn
tel. 89-523-45-06, fax: 89-523-47-37

Cena 25 zł (w tym 23% VAT)

Wszystkie opublikowane w czasopiśmie artykuły uzyskały pozytywne recenzje, wykonane przez niezależnych recenzentów.

Redakcja zastrzega sobie prawo korekty nadesłanych artykułów.

Kolejność umieszczenia prac w czasopiśmie zależy od terminu ich nadesłania i otrzymania ostatecznej, pozytywnej recenzji.

Wytyczne do publikowania w DIAGNOSTYCE można znaleźć na stronie internetowej:

<http://www.diagnostyka.net.pl>

Redakcja informuje, że istnieje możliwość zamieszczania w DIAGNOSTYCE ogłoszeń i reklam.

Jednocześnie prosimy czytelników o nadsyłanie uwag i propozycji dotyczących formy i treści naszego czasopisma.

Zachęcamy również wszystkich do czynnego udziału w jego kształtowaniu poprzez nadsyłanie własnych opracowań związanych z problematyką diagnostyki technicznej. Zwracamy się z prośbą o nadsyłanie informacji o wydanych własnych pracach nt. diagnostyki technicznej oraz innych pracach wartych przeczytania, dostępnych zarówno w kraju jak i zagranicą.